Characterizing the *in vivo* functions of Cyfip1 in the development of cardiovascular, hematopoietic, and nervous systems by precise targeted genome editing in zebrafish

by

Pongrat Jaisil

A thesis submitted to the graduate faculty

in partial fulfillment of the requirements for the degree of

MASTER OF SCIENCE

Major: Neuroscience

Program of Study Committee:
Baoyu Chen, Co-major Professor
Jeffrey Essner, Co-major Professor
Maura McGrail

The student author, whose presentation of the scholarship herein was approved by the program of study committee, is solely responsible for the content of this thesis. The Graduate College will ensure this thesis is globally accessible and will not permit alterations after a degree is conferred.

Iowa State University

Ames, Iowa

2022

DEDICATION

I dedicate my thesis to my beloved parents, Nawarat Jaisil and Prasit Jaisil, my brother, Ratanasit Jaisil, nae sarang Dae-Gyu Jang, all my family members, and my little furry loves. None of these accomplishments would have been possible without their precious and unconditional love and support.

TABLE OF CONTENTS

Page

ACKNOWLEDGMENTS

I would like to acknowledge my major professors, Dr. Baoyu Chen and Dr. Jeffrey Essner, for their kind mentorship, consistent and valuable support and guidance, and patience throughout my graduate studies and research. I am greatly grateful for their kindness in accepting me and giving me an invaluable opportunity to be a student in their labs and teaching me so patiently to learn an immeasurable number of new aspects of science and to become a good scientist. I would also like to thank another committee member, Dr. Maura McGrail, for her kind support, guidance, and input, as well as her inspiring and beautiful works.

Additionally, I would like to thank the Chen lab friends, the Essner-McGrail lab members, and the Jeffery lab friends of my former mentor, for their kind support and assistance. Also, I would like to thank all my dear friends and colleagues, both in my hometown and here in Ames, who have been very supportive and caring.

Lastly, I would like to acknowledge Khon Kaen University Scholarship for this invaluable opportunity to study abroad in the United States, along with the staff in my hometown university, the staff in the department of Biochemistry, Biophysics, and Molecular Biology (BBMB), and the department of Genetics, Development, and Cell Biology (GDCB), as well as those in the Graduate College and the International Students and Scholars Office (ISSO), for their kind assistance and advice regarding my study here in the Iowa State University, making it a memorable experience in my life.

CHAPTER 1. GENERAL INTRODUCTION

Literature Review

Actin and Its Biological Functions

Actin is the most abundant protein and is highly conserved in most eukaryotic cells. The actin cytoskeleton is a complex network of polarized actin filaments in which its reorganization is involved in various essential cellular processes, ranging from supporting cell shape integrity and cell shape alteration, cell proliferation, cell migration, cell adhesion and fusion, endocytosis, vesicle trafficking, chromatin remodeling, DNA repair and regulation of transcription[1–13]. Tight regulation of actin rearrangement is especially critical during early development and is required to maintain the normal functions of cells, organs, biological systems, and whole living organisms. Dysregulation of actin remodeling contributes to various diseases, including cardiovascular diseases, neurological disorders, cancer, immune deficiency, and hematopoietic disorders[14–18]. For example, mutation-induced actin malfunctioning can cause cardiomyopathies[19,20]. Deletion of actin in mice is lethal, in which the actin-depleted mice died within 2 weeks after birth[21]. Additionally, defective actin polymerization mediated by knockdown of WAVE2 (Wiskott-Aldrich syndrome protein family verprolin-homologous protein2), a key protein associated with promoting actin polymerization, resulted in impaired early mobilization and proliferation of mouse hematopoietic stem cells in bone marrow[18]. Moreover, altered synaptic development and morphology, presumably resulting from dysregulation of actin dynamics, has been demonstrated in a mouse model for Fragile X syndrome[22]. Also, changes in the rate of actin polymerization have been identified in familial Parkinson's disease-associated mutation of α-synuclein[23]. Altogether, this evidence strongly

emphasizes the essential role of actin cytoskeleton dynamics in establishing and maintaining normal physiological functions of several biological processes.

Regulation of Dynamic Actin Remodeling

In cells, there are two forms of actin cytoskeleton: monomeric, or globular actin (G-actin), and polymeric, or filamentous actin (F-actin). The dynamic actin remodeling between the two forms of actin is a coordinated process critical for several essential cellular activities and is tightly and spatiotemporally controlled by a number of signaling, scaffolding, and actin-binding proteins (ABPs)[24,25]. In response to extracellular signals, diverse ABPs regulate various processes of actin assembly, which in turn generate the actin cytoskeleton dynamics. These processes range from actin filament nucleation, filament branching, filament elongation, severing of pre-existing filaments to generate new barbed ends, filament barbed- and pointed-end capping to restrict polymerization, filament bundling and crosslinking, and actin monomer sequestration or depolymerization[3,4,26]. This regulation by ABPs is often mediated by Rho family GTPases, particularly Rho, Rac, and Cdc42[27]. Several potential Rho-family effector proteins have been identified, including the Wiskott-Aldrich syndrome protein (WASP) family, formins, and IRSp53[28–30]. Among these proteins, the major regulator of dynamic actin remodeling is the ubiquitous cellular WASP-family protein, which composes of WASP, N-WASP (neural-WASP), WAVE (Wiskott-Aldrich syndrome protein family verprolin-homologous protein), WASH (Wiskott-Aldrich syndrome protein and SCAR homologous protein), WHAMM (WASP homolog-associated protein with actin, membranes and microtubules), JMY (junction-mediating and -regulatory protein), and WHIMP (WAVE homology in membrane protrusions). One of the most fascinating proteins governing actin dynamics is the WAVE protein, which functions as

actin nucleation promoting factor (NPF) of the actin-related protein 2/3 complex (Arp2/3 complex)[31,32]. Intriguingly, rather than standing alone in the cytoplasm, the WAVE protein exists in a cytosolic heteropentameric protein complex called the WAVE regulatory complex (WRC). The WRC is basally auto-inhibited and well-regulated by intramolecular interaction between its own subunits[33–35,38]. The WRC can be activated by its ubiquitous regulator Rac1 GTPases and can be recruited and localized to the cell membrane by diverse specific ligands[34–42]. Rac1 binding to the WRC culminates in allosteric conformational change of the WRC from the inhibited state to the active form. Once activated and membrane-localized, the WRC then triggers the Arp2/3 complex to promote actin nucleation and branching from the pre-existing actin filaments[32]. This results in force-generating branched F-actin network at the cell leading edge of a migrating cell, which eventually gives rise to many essential cellular processes, such as membrane protrusion, lamellipodia formation, cellular process extension, cell adhesion, cell fusion, synapse formation, cell motility, and cell migration (Figure 1).

The WAVE Regulatory Complex (WRC) and Its Regulation

The WAVE regulatory complex (WRC) is the major regulator of Arp2/3 complex-mediated actin remodeling. In nature, this 400-kDa complex exists in a basally auto-inhibited heteropentameric protein assembly consisting of five conserved protein subunits: Cyfip (cytoplasmic FMR1-interacting protein), Nap (Nck-associated protein), Abi (Abelson-interacting protein), HSPC300 (hematopoietic stem progenitor cell 300), and WAVE (Wiskott-Aldrich syndrome protein family verprolin-homologous protein)[33–35].

Central to functions of the WRC is the regulation of the complex by its activation[35]. The basally auto-inhibited WRC is tightly regulated by intramolecular interaction of the specific site

on the Cyfip subunit with highly conserved carboxy-terminus of the WAVE protein called WCA (WH2 (WASP homology 2), central, acidic) domain[33–35,38]. The WRC can be primarily activated by its ubiquitous regulator Rac1 GTPases[36–41] and is recruited to the plasma membrane by various specific ligands containing a short peptide motif named WIRS (WRC interacting receptor sequence) (Figure 1). These ligands range from phospholipids, transmembrane receptor proteins, and kinases[42–50]. Rac1 binding to the WRC, which takes place on the specific binding sites of the Cyfip subunit, causes allosterically conformational change of the complex, liberating the Cyfip1-bound WCA domain[33–35,38]. The release of this WCA tail ultimately triggers Arp2/3-mediated actin nucleation and branching from the pre-existing actin filament, forming a branched F-actin network underneath cell leading edge (Figure 1). Interestingly, the signaling pathways for both the WRC activation by Rac1 binding leading to the WCA release, and the WRC recruitment, converge on Cyfip subunit of the complex[35,37,42] (Figure 1). This makes the Cyfip one of the most fascinating protein subunits to be further explored to investigate the functions of the WRC through its activation and recruitment signaling pathways converging on the Cyfip, not only in biochemistry, but also in cells and biological and physiological systems.

Cyfip and Its Biological Functions

Cyfip protein is encoded by a *cyfip* gene, which is highly conserved during evolution[51]. In addition to serving as an integral component of the WRC, Cyfip has also been reported to regulate post-synaptic mRNA translation by acting as a non-canonical translation initiation factor 4E binding protein (4E-BP), and by repressing the expression of specific fragile X mental retardation protein (FMRP) mRNA targets[51–53]. However, whether or not the role of Cyfip in

RNA metabolism through its interaction with FMRP and/or other RNA-binding proteins really exists *in vivo* is still unclear.

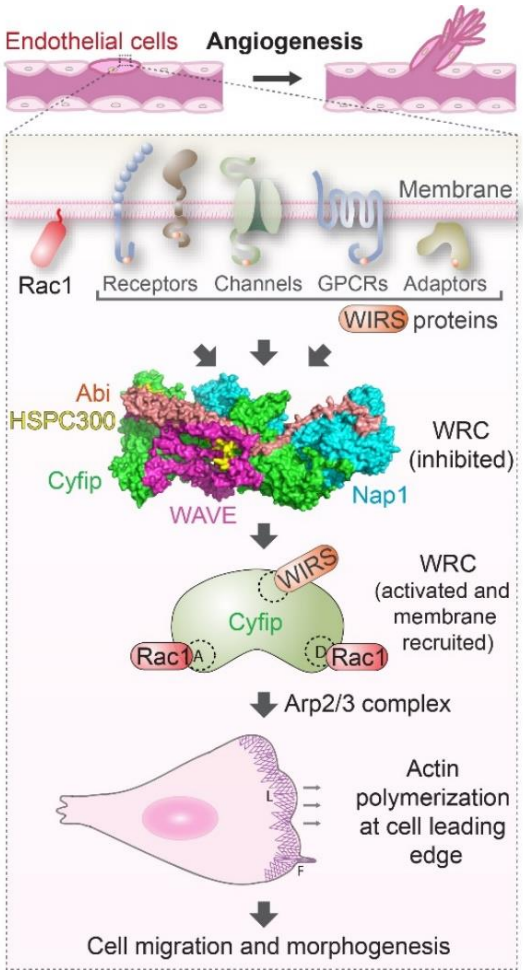

Figure 1. Schematic showing various membrane proteins signal through Cyfip subunit of the WRC to drive actin assembly, as well as cell migration and morphogenesis. This diagram uses the context of endothelial cell migration during angiogenesis as an example. In angiogenic sprouting endothelial cells, the auto-inhibited WRC can be activated by Rac1 GTPases, as well as membrane-recruited by several other WIRS-containing membrane proteins, including membrane receptors, membrane channels, G-protein-coupled receptors (GPCRs), and adaptor proteins. Both signaling pathways converge on Cyfip subunit through 3 distinct binding sites: one WIRS binding pocket, and two Rac1 binding sites (named approximate (A) and distant (D) sites). Once the WRC is activated and membrane-recruited, it can then trigger the Arp2/3 complex to promote actin nucleation, branching, and polymerization underneath cell membrane at the cell leading edge of a migrating cell. This results in membrane protrusions including lamellipodia (L) and filopodia (F) at the front edge of motile tip and stalk cells, which eventually give rise to sprouting, migration, and morphogenesis of the angiogenic endothelial cells, and, therefore, angiogenesis. The structural model of basally inhibited state of the WRC is also shown here to represent

all five protein subunits comprising the whole complex, including Abi (peach), HSPC300 (yellow), Cyfip (green), WAVE (magenta), and Nap1 (cyan).

In vertebrates, there are two isoforms of Cyfip protein: Cyfip1 and Cyfip2. These two Cyfip proteins are highly conserved among vertebrates, in which human CYFIP1 shares 98.7% and 93% amino acid sequence identity with their mouse and zebrafish orthologues, respectively. While human CYFIP2 shares 99.9% and 98% protein sequence identity with their mouse and zebrafish orthologues, respectively[51,54]. Additionally, there has been shown high sequence homology between Cyfip1 and Cyfip2 proteins within each species. For instance, 88% amino acid sequence identity between human CYFIP1 and CYFIP2, and, similarly, 86% between the two zebrafish Cyfip isoforms[51,54]. Intriguingly, despite this high sequence homology between Cyfip1 and Cyfip2, there has been several studies indicating differential expression patterns and cell-type-expression of the two Cyfip proteins within the neural tissue, as well as the different clinical features of individuals with *CYFIP1* and *CYFIP2* variants[55–58]. This suggests non-redundant and distinct functions of the two Cyfip isoforms.

There is a limited understanding of the physiological functions of the Cyfip subunit of the WRC *in vivo*. For instance, a few studies have shown that the *Drosophila* Cyfip, which has only one isoform, is specifically expressed in the nervous system and controls axon growth, axon branching and pathfinding, synaptogenesis, as well as specific aspects of eye morphogenesis, through Arp2/3-mediated actin reorganization[51,59]. In addition, a few studies in mouse neuronal cells have shown that Cyfip1 and Cyfip2 are enriched at inhibitory synapses in which altered Cyfip1 level can impact inhibitory synaptic structure and function, and that Cyfip1 also plays a critical role in neuronal spine morphogenesis by promoting protein translation and actin

polymerization[52,60]. Some *in vivo* studies have been conducted to investigate functions of Cyfip2 in particular. They have found that Cyfip2 is required for axon-axon interactions, filopodial dynamics and optic tract sorting, as well as for actin dynamics during retinal lamination and axon pathfinding in zebrafish retinotectal system[54,55]. Additionally, Cyfip2 has been shown to be a novel regulator of the innate acoustic startle threshold, in which loss of Cyfip2 in zebrafish larvae specifically enhances spiral fiber neuron activity[61]. There have been some attempts to study the effects of *cyfip1* and *cyfip2* deletion in mice, however, either *cyfip1* or *cyfip2* loss-of-function mutants are early embryonically lethal, posing challenges to study physiological roles of Cyfip proteins in a mouse model. These results also indicate that these two *cyfip* genes cannot compensate for each other *in vivo* and thus strongly suggest that Cyfip1 and Cyfip2 have distinct functions *in vivo*[56]. However, the detailed mechanisms underlying their differences remain unclear, and very little is known about the *in vivo* physiological functions of Cyfip1. Lack of this knowledge has hindered the understanding of the physiological roles of Cyfip1 involving WRC signaling-mediated actin remodeling in various biological systems, as well as understanding the functional differences from its isoform, Cyfip2. In addition, key to studying a molecular mechanism in animals is to obtain a stable mutant line and a strong, quantifiable phenotype for the gene of interest, which have not been pursued in those aforementioned studies for Cyfip1. Altogether, this emphasizes the critical need for establishing a stable line of *cyfip1* knockout animal model to investigate *in vivo* physiological functions of Cyfip1 in various biological systems, as well as the molecular mechanisms behind them.

Zebrafish as an Animal Model for Research

Animal study is a critical step to comprehension of the underlying biochemical and biological mechanisms in health and disease, as well as any alterations resulted from an intervention to these processes in the whole complex organism. Therefore, *in vivo* model organisms are of importance for biological, genetic, developmental, and biomedical research, as the *in vivo* study can provide a ground foundation for translational research in the future.

Zebrafish (Danio rerio) is a small tropical fresh-water fish in the minnow family (Cyprinidae) with a few horizontal dark blue/black stripes on each side of the body and is approximately 3-4 cm. in length in adult stage. It was first introduced as a vertebrate model for research on genetics and development in the 1970s by a scientist named George Streisinger at the University of Oregon[62]. For the past decades, zebrafish has quickly become a significant vertebrate model organism and widely used as an experimental system for various research areas besides developmental genetics[63–65], for example, gene editing[66], regenerative medicine[67–70], as well as biomedical sciences and medical research, including physiology[69,71–73], toxicology[74–76], disease modeling; such as kidney and cardiovascular diseases, neurological and neurodegenerative diseases, psychiatric disorders, muscular dystrophies and congenital myopathy, bone metabolic and pathogenic disorders , cancer, immunological and infectious diseases, and diabetes and obesity[70–73,76–92]; and drug development, particularly pre-clinical studies[72,80,82,93–97].

There are several reasons that zebrafish is more advantageous over other types of vertebrate animal models, such as mouse, rat, or rabbit. Firstly, zebrafish has short generation time, about 2-3 months on average, and can be bred relatively more easily and can reproduce frequently (averagely every week), with high fecundity; approximately 100-200 eggs per mating

pair. This allows for robust and high throughput experiments, for example, drug screening and phenotypic analysis[72,74–76,80,82,93,97]. Secondly, the zebrafish embryo grows and develops incredibly fast as much in a day as a human embryo in a month[98]. These advantages can greatly increase sample size within considerably less amount of time, providing scientists faster progression in their research along with more accurate statistical analysis. Thirdly, zebrafish embryos and larvae are fertilized and develop externally, as well as are transparent[98]. These advantages allow for an ease of genetic manipulation or pharmacological treatment, observation, and data collection with non-invasive techniques. For example, high-resolution confocal imaging and video capturing of phenotypes of internal organs or tissue and cellular structures (particularly fluorescent labeling ones) in a living animal is straightforward, especially during very early stage of development. Fourthly, zebrafish genome is completely sequenced and annotated[98]. Despite of being non-mammalian vertebrate, zebrafish genes are highly conserved to human orthologous genes, in which it shares 71% of genes with human, including *cyfip* genes, and more than 84% of human genetic disease-causing genes are present in zebrafish genome[99]. Moreover, it shares many cellular biological mechanisms, developmental processes, and major organs, in common with all other vertebrates including humans[94,100,101]. For instance, zebrafish has a closed cardiovascular system and a cardiac cycle that is highly comparable with human cardiovascular physiology. Furthermore, many well-characterized transgenic and mutant strains are readily available[102–105]. Therefore, zebrafish can very well serve as a human disease model organism which can be used to resemble various human diseases and study the pathogenesis and molecular mechanisms behind them. Lastly, compared with other experimental vertebrates, zebrafish is relatively more cost-effective regarding housing, maintaining, and breeding. Taken together, these strongly suggest zebrafish as a very powerful and effective vertebrate animal

model organism for research, which can be applicable for many different areas of study. It is well-suited for research relating to modeling human development and genetic functions, especially those that can cause multiple human genetic diseases.

Actin and the Development of Cardiovascular System, the Emergence and Early Development of Hematopoietic Stem and Progenitor Cells, and the Development of Spinal Motor Nervous System in Zebrafish

General concept of actin and cell migration and functions

Cell migration is an evolutionarily conserved, intricate process of all complex organisms that allows for spatial and temporal movement, relocation, and organization of a single cell or specialized groups of cells into a precise location, to form, develop, and preserve normal functions of tissues and organs throughout the development, as well as to maintain homeostasis and promote tissue regeneration and repair[106,107]. This process is fundamental yet critically essential to ultimately drive morphogenesis, as well as to maintain homeostasis and normal physiological functions of several biological systems and immunological defense mechanisms. For example, neural cell migration gives rise to the organization and formation of the nervous system. Moreover, cell migration also allows the immune cells to mobilize through tissues and reach at the injured site to facilitate the wound healing process[108].

Eukaryotic cell migration requires an intricate mechanism of membrane extension at the front edge and retraction at the rear, which is controlled by coordinated dynamic cytoskeleton rearrangement. While migrating, cells extend membrane protrusions at their leading edge and form lamellipodia and filopodia, which are generated by actin cytoskeleton remodeling. A key component that initiates cell migration is lamellipodia, a thin, sheet-like membrane protrusions containing enriched polarized array of actin filament networks underneath the cell membrane,

which is a characteristic feature of the membrane leading edge of motile cells, such as endothelial cells, neurons, immune cells, and epithelial cells[109,110]. This dynamic actin assembly at the cell periphery generates major mechanical driving forces that promote directional membrane protrusions and result in lamellipodial growth at the cell leading edge[3,6,109–116], and, consequently, cell migration.

Lamellipodia at the cell leading edge consists primarily of branched F-actin network beneath the cell membrane. The formation and organization of this branched F-actin network is initiated by a major Y-branching actin nucleator, the Arp2/3 complex. Despite of being inefficient actin nucleator by itself, the Arp2/3 complex can be activated by its binding to the NPFs. The NPFs activate the Arp2/3 complex by using its WCA domain, which is composed of WH2 domain(s) that binds actin monomer(s), a central connector region, and an acidic peptide, that altogether bind the Arp2/3 complex[26]. One of the key NPFs and actin remodeling regulators governing Arp2/3-mediated F-actin branching is the WRC[32]. Once the basally auto-inhibited WRC is activated by binding to its specific ligands at the binding sites on the Cyfip subunit, an allosteric conformational change of the complex is induced and turns it to an active state[33–35,38]. The activated WRC with its released WCA tail is then membrane-recruited to localize at the cell leading edge, and capable of triggering Arp2/3-mediated actin nucleation and branching[31,32,109]. At the cell leading edge, the liberated WCA tail recruits the Arp2/3 complex and promotes actin nucleation by interactions of the connector and acidic regions of the WCA domain with multiple subunits of the Arp2/3 complex, resulting in significant conformational change of the Arp2/3 complex that; 1) facilitate its binding to the side of the pre-existing actin filament at an approximate angle of 70 degrees; 2) primes it for nucleation by mimicking of Arp2 and Arp3 to the first two subunits of the nascent actin filament, which also incorporate with an actin

monomer brought by the WH2 domain of the WCA, and all together serve as an actin nucleus seed that actively generates branched F-actin[117]. After activating the Arp2/3 complex, the WCA domain of the WRC will then dissociate from the complex and facilitate multiple additional cycles of actin nucleation and branching at membrane periphery. Overall, together with complementary functions of other supporting ABPs, adhesive molecules, other associated cytoskeletons, as well as the dynamic treadmilling between incorporation of ATP-bound G-actin at the barbed (or plus) end and dissociation of ADP-bound G-actin at the pointed (or minus) end, allowing for recycling pool of G- and F-actin at the membrane periphery, this results in extensive, mechanically force-generating branched F-actin polymerization and organization at the cell leading edge that gives rise to lamellipodial protrusion, cellular process extension, cell morphological change, and ultimately directed cell migration and morphogenesis[2,109,110,118,119].

The development of zebrafish cardiovascular system: Cardiac development, vascular morphogenesis, and tubulogenesis

Cardiovascular development requires coordinated migration of endothelial cells. For instance, during angiogenesis, endothelial cells lining the preexisting vessels must transform into a motile, sprouting state and migrate to the surrounding tissue[120]. This process requires faithful remodeling of the actin cytoskeleton under the guidance of membrane signals. During vertebrate embryonic development, the heart is the first organ of the cardiovascular system that forms and functions[102]. During gastrulation and early somite stages of zebrafish embryo, the atrial and ventricular cardiac progenitor cells (for endocardium and myocardium), which are located bilaterally in the lateral marginal zone, migrate dorsally towards the midline in the anterior lateral plate mesoderm (ALPM), where they receive essential signals to induce their cardiogenic

differentiation[121]. During mid- and late-somite stages, cardiogenic differentiation and heart morphogenesis take place simultaneously. Cardiogenic differentiation is initiated first in the specified ventricle myocardial cells by the expression of cardiac myosins at the 12-somite stage (15 hours post fertilization; hpf), followed by continuous cardiogenic differentiation of the specified atrial cardiomyocytes, giving rise to the myocardial tissue expansion into more lateral regions of the ALPM. The fused bilateral heart field at the midline in a later stage then form a cardiac disc with the endocardial cells, ventricular cardiomyocytes, and atrial cardiomyocytes, lining from the center to the outermost layer of the disc, respectively. The cardiac disc is next transformed to a nascent cardiac tube, in which the endocardium lines the inner layer of the tube. At 28 hpf, the linear heart tube is formed with the arterial and venous poles, in which the pacemaker is also generated within the inner curvature of the atrium near the venous pole where coordinated, sequential heart contractions begin[122]. At 36 hpf, cardiac tube looping is generated, with the ventricle displacing towards the midline, and continues the process to form an S-shaped loop. An epicardial layer is then developed to cover the myocardium. Additionally, the pacemaker is formed within the inner curvature of the atrium near the venous pole. In zebrafish heart, the atrioventricular (AV) valves also begin to develop from 36 hpf by a process called endocardial transdifferentiation, in which the endocardial cushions become enlarged and differentiate into AV valve leaflets extending into the ventricular lumen by 105 hpf[123,124]. At 48-72 hpf during the linear heart tube and looping stage, the epicardium, an outermost cellular layer covering the outside of the myocardium, begins to develop from a group of extracardiac cells called pro-epicardium and spread over the myocardial surface of the looped heart[125,126].

Together, this suggests the essentiality of tightly spatiotemporal control of each step of the cardiogenic development in order to maintain normal cardiac morphogenesis and

functioning. Any dysregulation of these processes can lead to pathological cardiovascular disorders, for example, congenital AV valve and septum defects, and cardiomyopathies, which are diseases primarily affecting the myocardium[127]. The two most prevalent types are dilated cardiomyopathy (DCM) and hypertrophic cardiomyopathy (HCM). Human DCM is characterized by enlargement of one or both ventricles of the heart, along with reduced myocardial contractility, while HCM is thickening of the myocardium in one or both ventricles in an absence of other diseases causing myocardial hypertrophy, such as high blood pressure. HCM and DCM are considered to be multifactorial disorders with relatively strong genetic influence. DCM is associated with mutations in genes encoding cytoskeletal or contractile proteins, for instance, *chap* (cytoskeletal heart-enriched actin-associated protein) which encodes Z-disc protein, and *silent-heart/tnnt2* which encodes cardiac troponin T[128–130].

In parallel with the heart development, the vascular morphogenesis also takes place via two distinct mechanisms, called vasculogenesis and angiogenesis. Vasculogenesis is a biological process by which a formation of a primary vascular network occurs, while angiogenesis is a process by which new blood vessels are generated from preexisting ones. During the vascular morphogenesis, vasculogenesis begins first, in a blood flow-independent manner[131], establishing the dorsal aorta (DA) and the posterior cardinal vein (PCV), followed by angiogenesis to create further fine blood vessels, ultimately forming a complete functional circulatory loop[132–134] (Figure 2). In early vascular development, free angioblast progenitor cells derived from the lateral plate mesoderm (LPM) migrate to the midline and differentiate to endothelial cells (ECs), establishing the first two major blood vessels[134–136]. This migration of angioblast progenitors takes place in two different phases. The first angioblast migration occurs at the 14-17 somite stage (16-17.5 hpf) and gives rise to an arrival and aggregation of the progenitors at the midline,

creating the primitive non-lumenized arterial cord which in turn becomes the DA (Figure 2). Next, the second phase establishes the primitive unhollowed venous cord which finally turns to the PCV, with the caudal vein (CV) located in the caudal part of the PCV beginning from the end of the yolk extension[137]. The DA subsequently becomes lumenized at around 23 hpf, while the PCV becomes hollowed when the full circulatory loop is completed at around 28 hpf[136], allowing the blood cells to flow through the vascular lumen creating a functional blood circulation (Figure 2).

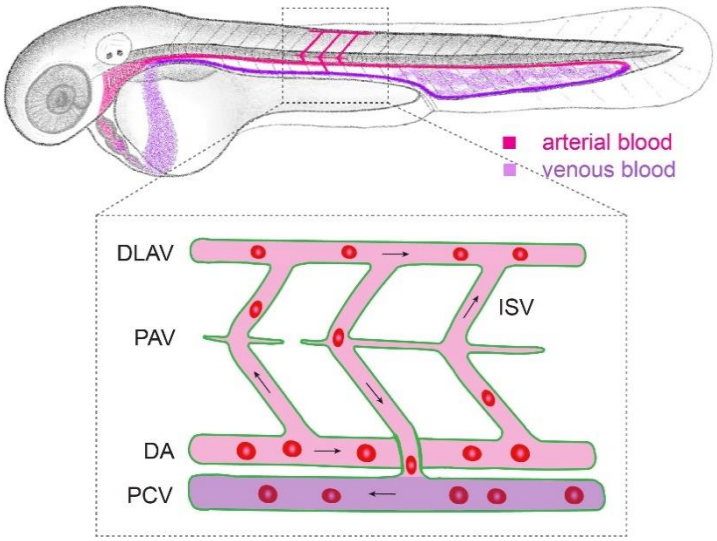

Figure 2. Schematic illustration showing the complete cardiovascular system in developing zebrafish embryo at 3 dpf. The diagram focuses only on the main blood vessels in trunk area (lateral view), as indicated in the dotted box. Arterial and venous blood circulation are represented in pink and purple color, respectively, with red blood cells circulating inside. The direction of blood flow is indicated by the arrows. DLAV: dorsal longitudinal anastomotic vessel, PAV: parachordal vessels, DA: dorsal aorta, PCV: posterior cardinal vein, ISV: intersegmental vessel.

Shortly after that, sprouting angiogenesis takes place, establishing the secondary vascular network. Sprouting angiogenesis is a biological process that guides two distinctive groups of ECs, tip cells and stalk cells, to grow during the vascular development. Tip cells are the ECs

resided at the distal part of the sprouts, extending long filopodia and leading the migratory path of the growing sprouts. The stalk cells are found behind the tip cells, proliferating, migrating following the tip cell lead, and maintaining the vascular lumen structure[138]. Dependent of blood flow and pressure[139], angiogenic sprouting of the secondary arterial and venous blood vessels arises from the pre-existing vessels, in two distinct stages[140]. During the first angiogenic phase, the endothelial tip cells initiate sprouting from the dorsal wall of the DA to form intersegmental arteries (aISVs) at around 22 hpf[131,140] (Figure 2). These newly formed aISV sprouts then start to migrate dorsally to make connections by anastomosis with their adjacent aISVs, eventually forming the dorsal longitudinal anastomotic vessel (DLAV) by 28-30 hpf[140] (Figure 2). During the second angiogenic phase, the tip cells begin to sprout from the PCV and CV at around 32 hpf[140] and, by 54 hpf, anastomose with the neighboring aISVs, forming intersegmental veins (vISVs)[141,142]. The newly formed aISVs, DLAV, and vISVs then become lumenized and allow for the blood flow circulating through them once they have fully developed[143], altogether establishing the complete functional circulatory system. Furthermore, at around 27-36 hpf, ECs of the CV begin to sprout ventrally and make connections to each other, giving rise to the formation of a venous vascular network at the tail region named the caudal vein plexus (CVP), where the caudal hematopoietic tissue resides[144].

During vascular morphogenesis, another indispensable process occurring simultaneously is tubulogenesis, or vascular lumen formation, transforming an early angiogenic sprout and the vascular cord to a lumenized blood vessel that allows for blood circulation. For this, ECs engage in extensive morphological changes to form, expand, and stabilize EC-cell tight junctions on their apical surfaces where a lumen is formed[131,145]. In zebrafish, the vascular tubulogenesis first initiates in the DA at around 23 hpf, followed with which in the PCV at around 28 hpf, and other

small angiogenic vessels shortly after that[136]. Lumen formation of these vessels occurs via two primary mechanisms: cord hollowing and cell hollowing[136,146–148]. In cord hollowing, the vascular tube is formed extracellularly, in which ECs initially align to each other as a cord in a unicellular junction conformation. Subsequently, ECs rearrange to converge toward each other and form new contacts and junctions. This leads to de novo apical membrane formation at the intercellular junctions and merging of the two membrane compartments, which in turn gives rise to the formation of a continuous luminal space in-between ECs[136,146–150]. On the contrary, cell hollowing, or transcellular lumen formation, usually occurs intracellularly where cell rearrangements is initially limited. Thereby, the lumen is formed by apical membrane invagination into the cell body, along with compression of the cytoplasm and internal apical membrane fusion, to create a hollow, unicellular tube[139,145,148]. Depending highly on blood flow, the tubular network of primitive vascular plexus formed by angiogenesis is either stabilized and maintained (when experiencing constantly optimal blood flow) or remodeled through extensive EC rearrangement and vessel pruning (if receiving decreased blood flow)[139,151,152]. This process greatly involves EC nucleus migration, junction remodeling, and dynamic actin cytoskeleton remodeling, to established functionally and more refined, branched vascular network circulating proper blood flow to all tissues[152,153].

The emergence of hematopoietic stem and progenitor cells and the early development of zebrafish hematopoietic system

Hematopoiesis, a process of blood cell formation, is an intricate process which primarily involves actin-mediated and highly regulated cell proliferation, differentiation, maturation and coordinated migration, by integrating various signaling pathways influencing each step of blood

cell production from precursor cells to the differentiated blood cell types[154,155]. Hematopoietic stem and progenitor cells (HSPCs) are a rare population of blood precursor cells capable of self-renewal and multilineage differentiation to produce new mature blood cells. In zebrafish, there are two major waves of hematopoiesis: primitive and definitive waves[154,156–160] (Figures 3a and 3b). The primitive hematopoiesis is originated in the lateral plate mesoderm[161,162]. The anterior lateral plate mesoderm (ALPM) gives rise to the rostral blood island (RBI) which is the major area for primitive myelopoiesis to produce primitive myeloid cells including primitive macrophages and neutrophils (Figures 3a and 3b), while the posterior lateral plate mesoderm (PLPM) is composed primarily of erythroid precursor cells and a few myeloid precursors[157,159,160,163–168]. Importantly, the PLPM also initiates angioblasts which is a common precursor cell of ECs and definitive HSPCs[169,170]. At around 15 hpf, the PLPM cells start to migrate axially along the ventral part of the somite, forming the intermediate cell mass (ICM) at the midline where the primitive erythropoiesis mainly takes place[156,158] (Figures 3a and 3b). Simultaneously, angioblasts also migrate and arrive at the midline, generating the arterial and venous vascular cords which later develop into the DA and PCV, respectively[136].

The definitive hematopoiesis is initiated by erythromyeloid progenitors (EMPs), which emerge in the posterior blood island (PBI) at around 24-30 hpf and can differentiate into both erythroid and myeloid lineages[171] (Figures 3a and 3b). Shortly before the blood circulation begins (around 23 hpf), the specified hemogenic endothelial cells (HECs), a specialized subpopulation of ECs that reside in the ventral floor of the DA in an aorta-gonad-mesonephros (AGM) region (Figure 3a), start to develop and give rise to HSPCs through a process known as endothelial-to-hematopoietic transition (EHT). These nascent HSPCs begin to bud off from the ventral floor of the DA at around 30-54 hpf and migrate through the extracellular matrix space

between the DA and PCV to intravasate into the PCV to finally enter the blood circulation[171–173] (Figure 3b). Beginning around 48 hpf, the circulating HSPCs start to lodge in the caudal hematopoietic tissue (CHT), the vascular plexus of the CVP, which develops later at the same region as the PBI and serves as a vascular niche and transient hematopoietic organ for the HSPCs[174,175] (Figures 3a and 3b). The HSPCs then extravasate to the abluminal wall and stimulate the adjacent ECs to form a pocket like structure via a process called endothelial cuddling[174]. The dynamic interactions of the HSPCs with ECs, mesenchymal stromal cells, and immune cells within this vascular niche tightly control HSC proliferation, differentiation, and egression of the HSPCs from the CHT to the blood stream starting from 72 hpf[175–177] (Figure 3b). After entering the circulation, the HSPCs in turn colonize the thymus and the kidney, the zebrafish adult lymphopoietic- and hematopoietic organs, respectively, producing and maintaining all adult blood cells throughout life[175,178] (Figures 3a and 3b).

The development of zebrafish spinal motor nervous system

The protrusion of filopodia and lamellipodia of neurons is fundamental to axon extension and branching, dendritic branching and spine formation, synaptogenesis, and neuronal navigation and migration, which collectively establishes the highly intricate nervous system. These complex processes strictly rely on the actin filament reorganization[179,180]. In the developing central nervous system, the mature and functional neurons are differentiated from neuroectodermal epithelium-derived neural progenitor cells residing in the neural tube[181]. During development of

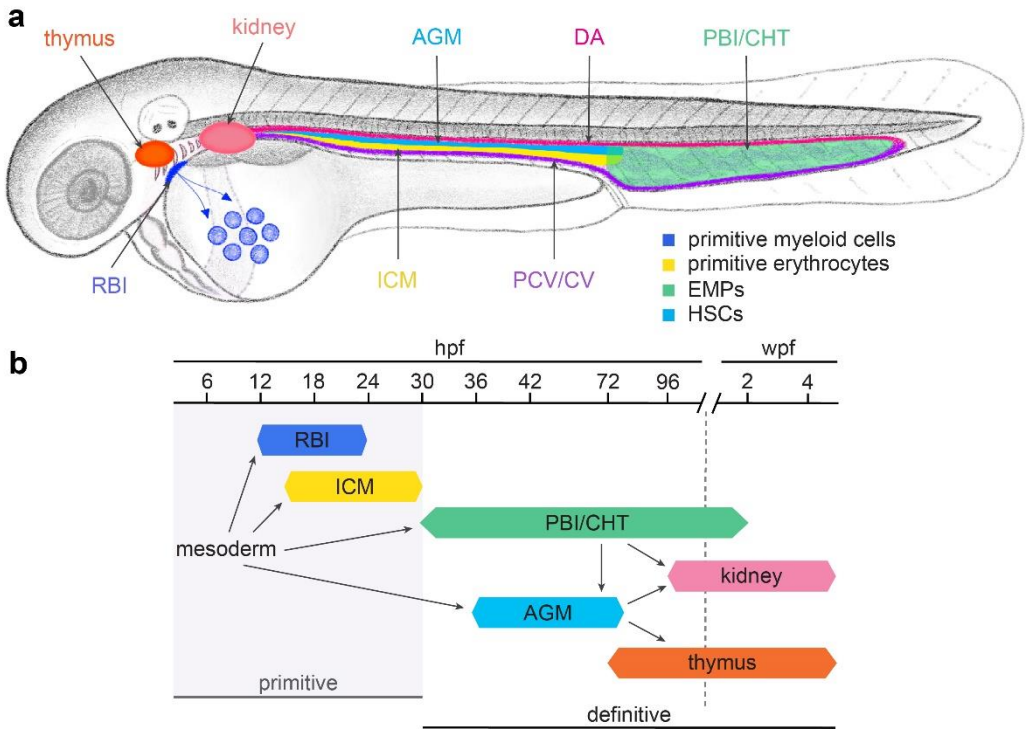

Figure 3. Illustrative drawing representing embryonic hematopoiesis in zebrafish. (**a**) Anatomical locations (lateral view) of each independent phase of primitive and definitive hematopoiesis to produce various precursor cells. First, primitive myeloid cells originate in the RBI, migrate onto the yolk ball (dark blue spots), and then spread throughout the body. Next, primitive erythrocytes develop in the ICM (yellow). The first stage of definitive hematopoiesis begins slightly later with the production of EMPs, which develop in the PBI (green). Then, HSCs emerge in the AGM region (blue), migrate to the CHT (green), and ultimately seed in the thymus and kidney (orange and pink, respectively). (**b**) Timing of zebrafish hematopoietic development during the primitive and definitive waves, which are both derived from the lateral plate mesoderm. Anatomical locations in (a) and timing of hematopoietic development in (b) are color matched. RBI: rostral blood island, AGM: aorta-gonad-mesonephros region, ICM: intermediate cell mass, PBI: posterior blood island, CHT: caudal hematopoietic tissue, EMPs: erythromyeloid progenitors, HSCs: hematopoietic stem cells, hpf: hours post fertilization, wpf: weeks post fertilization. *Note.* Adapted from "Cellular Dissection of Zebrafish Hematopoiesis" by D.L. Stachura and D. Traver, 2011, *Methods in Cell Biology*, 101, p. 75-110.

the spinal motor nervous system in zebrafish embryonic and larval stage, two major types of spinal motor neurons arise: primary motor neurons (PMNs) and secondary motor neurons (SMNs)[182–184]. PMNs normally have large cell bodies and thick axons and are localized relatively dorsally in the motor spinal column. They can be further classified into three main groups: rostral

(RoP), middle (MiP), and caudal PMNs (CaP), according to the positions of their cell bodies in the spinal cord and the trajectory of axons[182–184] (Figure 4). Additionally, a variable primary motor neuron, the fourth (minor) type of PMNs, can occasionally arise and usually innervate mostly a muscle area between RoP and MiP, however, it typically degenerates between 20-36 hpf of the development[185–187]. Unlike PMNs, the SMNs have small cell bodies and thinner axons, and typically arise 5-6 hours later than the PMNs[182]. During development, the CaP axon is the first projection that exits the spinal cord through the ventral root, followed by the MiP and, lastly, the RoP axons through the exit point where they all share in common[188]. The projection from CaP serves as a pioneer axon guiding other primary motor axons to follow its first migratory path ventrally through the middle part of the myotome to the area called choice point at the horizontal myoseptum[189] (Figure 4). Here, the CaP, MiP, and RoP axons diverge to their own highly stereotypical path to innervate their cell-specific territories of the myotome[182,184]. Generally, each somitic hemisegment of zebrafish has only one CaP, MiP, and RoP innervating each corresponding part of the myotomes (the trunk musculature) but has approximately 25-30 SMNs that have similar axonal pathfinding to the PMNs[190,191]. By bundling together, the PMNs and SMNs form two major axonal branches; dorsal and ventral branches, and one minor projection named rostral branch (Figure 4). The ventral branch extends ventrally to the middle of the myotome and curve around the ventral border of the ventral myotome where it terminates and innervates approximately the ventral two-thirds of the ventral myotomes, while the dorsal branch retracts from the choice point and continue navigating to innervate the dorsal myotome (Figure 4). And, after pausing at the choice point, the rostral branch migrates along the horizontal myoseptum into the medial myotome and the dorsal third of the ventral myotome where the axon terminals end[183,192–195] (Figure 4). Altogether, this establishes the complex network of spinal

motor circuit innervating the zebrafish trunk musculature critical for motor activity, such as swimming behavior, and movement response to environmental stimuli.

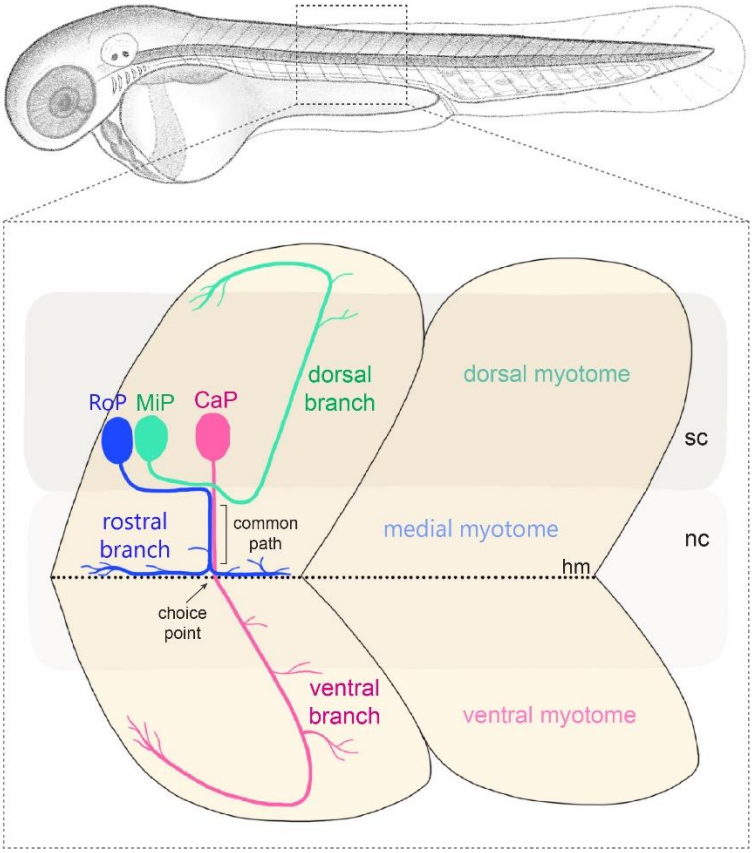

Figure 4. Schematic illustration representing axonal projection pattern of the primary spinal motor neurons in a spinal hemisegment in zebrafish (lateral view). The projections of the three major primary motor neurons: RoP, MiP, and CaP, toward their target muscle regions in the myotome are color matched in blue, green, and pink, respectively. In developing nervous system, the RoP, MiP, and CaP extend their axon along the common path to the choice point at the horizontal myoseptum (hm, dotted line). Here, the axon of RoP, MiP, and CaP diverge into their cell-specific regions in the myotome to innervate the medial, dorsal, and ventral myotome, respectively. The secondary motor neurons and their axons fasciculating with ones from the primary motor neurons to form rostral, dorsal, and ventral nerve branches are not shown in this diagram. RoP: rostral primary motor neuron, MiP: middle primary motor neuron, CaP: caudal primary motor neuron, sc: spinal cord, nc: notochord, hm: horizontal myoseptum. *Note.* Adapted from "Function of Neurolin (DM-GRASP/SC-1) in Guidance of Motor Axons during Zebrafish Development" by H. Ott, H. Diekmann, C.A.O. Stuermer and M. Bastmeyer, 2001, *Developmental Biology*, 235, p. 86-97.

Taken together, this strongly indicates the essentiality of the dynamic actin reorganization, which is required and extensively involved in several cellular functions, for instance, cell proliferation, cell differentiation, cell morphological change, cellular process extension, and especially coordinated cell migration, in order to maintain normal development and functioning of the cardiovascular and spinal motor nervous systems, as well as the emergence of hematopoietic stem and progenitor cells and early development of hematopoietic system in zebrafish.

References

1. Blanchoin L, Boujemaa-Paterski R, Sykes C, Plastino J. Actin Dynamics, Architecture, and Mechanics in Cell Motility. *Physiological Reviews*. 2014;94(1):235-263. doi:10.1152/physrev.00018.2013

2. Pollard TD, Cooper JA. Actin, a central player in cell shape and movement. *Science (1979)*. 2009;326(5957):1208-1212. doi:10.1126/science.1175862

3. Pollard TD, Borisy GG. Cellular motility driven by assembly and disassembly of actin filaments. *Cell*. 2003;112(4):453-465. doi:10.1016/S0092-8674(03)00120-X

4. Dominguez R, Holmes KC. Actin structure and function. *Annual Review of Biophysics*. 2011;40(1):169-186. doi:10.1146/annurev-biophys-042910-155359

5. Pollard TD. Nine unanswered questions about cytokinesis. *Journal of Cell Biology*. 2017;216(10):3007-3016. doi:10.1083/jcb.201612068

6. Theriot JA, Mitchison TJ. Actin microfilament dynamics in locomoting cells. *Nature*. 1991;352(6331):126-131. doi:10.1038/352126a0

7. Girao H, Geli MI, Idrissi FZ. Actin in the endocytic pathway: From yeast to mammals. *FEBS Letters*. 2008;582(14):2112-2119. doi:10.1016/j.febslet.2008.04.011

8. Khaitlina SY. Intracellular transport based on actin polymerization. *Biochemistry (Moscow)*. 2014;79(9):917-927. doi:10.1134/S0006297914090089

9. Bettinger BT, Gilbert DM, Amberg DC. Actin up in the nucleus. *Nature Reviews Molecular Cell Biology*. 2004;5(5):410-415. doi:10.1038/nrm1370

10. Miralles F, Visa N. Actin in transcription and transcription regulation. *Current Opinion in Cell Biology*. 2006;18(3):261-266. doi:10.1016/j.ceb.2006.04.009

11. Percipalle P, Visa N. Molecular functions of nuclear actin in transcription. *Journal of Cell Biology*. 2006;172(7):967-971. doi:10.1083/jcb.200512083

12. Chen M, Shen X. Nuclear actin and actin-related proteins in chromatin dynamics. *Current Opinion in Cell Biology*. 2007;19(3):326-330. doi:10.1016/j.ceb.2007.04.009

13. Hurst V, Shimada K, Gasser SM. Nuclear Actin and Actin-Binding Proteins in DNA Repair. *Trends in Cell Biology*. 2019;29(6):462-476. doi:10.1016/j.tcb.2019.02.010

14. Yamazaki D, Suetsugu S, Miki H, et al. WAVE2 is required for directed cell migration and cardiovascular development. *Nature*. 2003;424(6947):452-456. doi:10.1038/nature01770

15. Salzer E, Zoghi S, Kiss MG, et al. The cytoskeletal regulator HEM1 governs B cell development and prevents autoimmunity. *Science Immunology*. 2020;5(49). doi:10.1126/sciimmunol.abc3979

16. Qin H, Lu S, Thangaraju M, Cowell JK. Wasf3 Deficiency Reveals Involvement in Metastasis in a Mouse Model of Breast Cancer. *American Journal of Pathology*. 2019;189(12):2450-2458. doi:10.1016/j.ajpath.2019.08.012

17. Begemann A, Sticht H, Begtrup A, et al. New insights into the clinical and molecular spectrum of the novel CYFIP2-related neurodevelopmental disorder and impairment of the WRC-mediated actin dynamics. *Genetics in Medicine*. 2021;23(3):543-554. doi:10.1038/s41436-020-01011-x

18. Ogaeri T, Eto K, Otsu M, Ema H, Nakauchi H. The Actin Polymerization Regulator WAVE2 Is Required for Early Bone Marrow Repopulation by Hematopoietic Stem Cells. *Stem Cells*. 2009;27(5):1120-1129. doi:10.1002/stem.42

19. Olson TM, Michels V v., Thibodeau SN, Tai YS, Keating MT. Actin mutations in dilated cardiomyopathy, a heritable form of heart failure. *Science (1979)*. 1998;280(5364):750-752. doi:10.1126/science.280.5364.750

20. Olson TM, Doan TP, Kishimoto NY, Whitby FG, Ackerman MJ, Fananapazir L. Inherited and de novo mutations in the cardiac actin gene cause hypertrophic cardiomyopathy. *Journal of Molecular and Cellular Cardiology*. 2000;32(9):1687-1694. doi:10.1006/jmcc.2000.1204

21. Kumar A, Crawford K, Close L, et al. Rescue of cardiac α-actin-deficient mice by enteric smooth muscle γ-actin. *Proc Natl Acad Sci U S A*. 1997;94(9):4406-4411. doi:10.1073/pnas.94.9.4406

22. Klemmer P, Meredith RM, Holmgren CD, et al. Proteomics, ultrastructure, and physiology of hippocampal synapses in a fragile X syndrome mouse model reveal presynaptic phenotype. *Journal of Biological Chemistry*. 2011;286(29):25495-25504. doi:10.1074/jbc.M110.210260

23. Sousa VL, Bellani S, Giannandrea M, et al. α-Synuclein and its A30P mutant affect actin cytoskeletal structure and dynamics. *Molecular Biology of the Cell*. 2009;20(16):3725-3739. doi:10.1091/mbc.E08-03-0302

24. dos Remedios CG, Chhabra D, Kekic M, et al. Actin binding proteins: Regulation of cytoskeletal microfilaments. *Physiological Reviews*. 2003;83(2):433-473. doi:10.1152/physrev.00026.2002

25. Pollard TD. Actin and actin-binding proteins. *Cold Spring Harbor Perspectives in Biology*. 2016;8(8). doi:10.1101/cshperspect.a018226

26. Campellone KG, Welch MD. A nucleator arms race: cellular control of actin assembly. *Nat Rev Mol Cell Biol*. 2010;11(4):237-251. doi:10.1038/nrm2867

27. Foster R, Hu KQ, Lu Y, Nolan KM, Thissen J, Settleman J. Identification of a novel human Rho protein with unusual properties: GTPase deficiency and in vivo farnesylation. *Molecular and Cellular Biology*. 1996;16(6):2689-2699. doi:10.1128/mcb.16.6.2689

28. Burbelo PD, Drechsel D, Hall A. A conserved binding motif defines numerous candidate target proteins for both Cdc42 and Rac GTPases. *Journal of Biological Chemistry*. 1995;270(49):29071-29074. doi:10.1074/jbc.270.49.29071

29. Yamagishi A, Masuda M, Ohki T, Onishi H, Mochizuki N. A Novel Actin Bundling/Filopodium-forming Domain Conserved in Insulin Receptor Tyrosine Kinase Substrate p53 and Missing in Metastasis Protein. *Journal of Biological Chemistry*. 2004;279(15):14929-14936. doi:10.1074/jbc.M309408200

30. Zigmond SH. Formin-induced nucleation of actin filaments. *Current Opinion in Cell Biology*. 2004;16(1):99-105. doi:10.1016/j.ceb.2003.10.019

31. Machesky LM, Mullins RD, Higgs HN, et al. Scar, a WASp-related protein, activates nucleation of actin filaments by the Arp2/3 complex. *Proc Natl Acad Sci U S A*. 1999;96(7):3739-3744. doi:10.1073/pnas.96.7.3739

32. Stradal TEB, Rottner K, Disanza A, Confalonieri S, Innocenti M, Scita G. Regulation of actin dynamics by WASP and WAVE family proteins. *Trends in Cell Biology*. 2004;14(6):303-311. doi:10.1016/j.tcb.2004.04.007

33. Takenawa T, Suetsugu S. The WASP-WAVE protein network: Connecting the membrane to the cytoskeleton. *Nature Reviews Molecular Cell Biology*. 2007;8(1):37-48. doi:10.1038/nrm2069

34. Chen Z, Borek D, Padrick SB, et al. Structure and Control of the Actin Regulatory WAVE Complex. *Nature*. 2010;468:533-538.

35. Rottner K, Stradal TEB, Chen B. WAVE regulatory complex. *Current Biology*. 2021;31(10):R512-R517. doi:10.1016/j.cub.2021.01.086

36. Eden S, Rohatgi R, Podtelejnikov A v, Mann M, Kirschner MW. Mechanism of regulation of WAVE1-induced actin nucleation by Rac1 and Nck. *Nature*. 2002;418(6899):790-3.

37. Chen B, Chou HT, Brautigam CA, et al. Rac1 GTPase activates the WAVE regulatory complex through two distinct binding sites. *Elife*. 2017;6. doi:10.7554/eLife.29795

38. Lebensohn AM, Kirschner MW. Activation of the WAVE complex by coincident signals controls actin assembly. *Mol Cell*. 2009;36(3):512. doi:10.1016/j.molcel.2009.10.024

39. Miki H, Yamaguchi H, Suetsugu S, Takenawa T. IRSp53 is an essential intermediate between Rac and WAVE in the regulation of membrane ruffling. *Nature*. 2000;408(6813):732-5.

40. Koronakis V, Hume PJ, Humphreys D, et al. WAVE regulatory complex activation by cooperating GTPases Arf and Rac1. *Proc Natl Acad Sci U S A*. 2011;108(35):14449-14454. doi:10.1073/pnas.1107666108

41. Miki H, Suetsugu S, Takenawa T. WAVE, a novel WASP-family protein involved in actin reorganization induced by Rac. *EMBO J*. 1998;17(23):6932-41.

42. Chen B, Brinkmann K, Chen Z, et al. The WAVE regulatory complex links diverse receptors to the actin cytoskeleton. *Cell*. 2014;156(1-2):195-207. doi:10.1016/j.cell.2013.11.048

43. Chia PH, Chen B, Li P, Rosen MK, Shen K. Local F-actin network links synapse formation and axon branching. *Cell*. 2014;156(1-2):208-220. doi:10.1016/j.cell.2013.12.009

44. Squarr AJ, Brinkmann K, Chen B, et al. Fat2 acts through the WAVE regulatory complex to drive collective cell migration during tissue rotation. *The Journal of Cell Biology*. 2016;212(5):591-603. doi:10.1083/jcb.201508081

45. Lee NK, Fok KW, White A, et al. Neogenin recruitment of the WAVE regulatory complex maintains adherens junction stability and tension. *Nat Commun*. 2016;7:11082. doi:10.1038/ncomms11082

46. O'Leary CJ, Nourse CC, Lee NK, et al. Neogenin Recruitment of the WAVE Regulatory Complex to Ependymal and Radial Progenitor Adherens Junctions Prevents Hydrocephalus. *Cell Rep*. 2017;20(2):370-383. doi:10.1016/j.celrep.2017.06.051

47. Xing G, Li M, Sun Y, et al. Neurexin-Neuroligin 1 regulates synaptic morphology and functions via the WAVE regulatory complex in Drosophila neuromuscular junction. *Elife*. 2018;7. doi:10.7554/eLife.30457

48. Basquin C, Trichet M, Vihinen H, et al. Membrane protrusion powers clathrin-independent endocytosis of interleukin-2 receptor. *EMBO J*. 2015;34(16):2147-2161. doi:10.15252/embj.201490788

49. Biswas S, Emond MR, Duy PQ, Hao LT, Beattie CE, Jontes JD. Protocadherin-18b interacts with Nap1 to control motor axon growth and arborization in zebrafish. *Molecular Biology of the Cell*. 2014;25(5). doi:10.1091/mbc.E13-08-0475

50. Nakao S, Platek A, Hirano S, Takeichi M. Contact-dependent promotion of cell migration by the OL-protocadherin-Nap1 interaction. *Journal of Cell Biology*. 2008;182(2):395-410. doi:10.1083/jcb.200802069

51. Schenck A, Bardoni B, Moro A, Bagni C, Mandel JL. A highly conserved protein family interacting with the fragile X mental retardation protein (FMRP) and displaying selective interactions with FMRP-related proteins FXR1P and FXR2P. *Proc Natl Acad Sci U S A*. 2001;98(15):8844-8849. doi:10.1073/pnas.151231598

52. DeRubeis S, Pasciuto E, Li KW, et al. CYFIP1 coordinates mRNA translation and cytoskeleton remodeling to ensure proper dendritic Spine formation. *Neuron*. 2013;79(6):1169-1182. doi:10.1016/j.neuron.2013.06.039

53. Napoli I, Mercaldo V, Boyl PP, et al. The Fragile X Syndrome Protein Represses Activity-Dependent Translation through CYFIP1, a New 4E-BP. *Cell*. 2008;134(6):1042-1054. doi:10.1016/j.cell.2008.07.031

54. Pittman AJ, Gaynes JA, Chien CB. nev (cyfip2) is required for retinal lamination and axon guidance in the zebrafish retinotectal system. *Developmental Biology*. 2010;344(2):784-794. doi:10.1016/j.ydbio.2010.05.512

55. Cioni JM, Wong HHW, Bressan D, Kodama L, Harris WA, Holt CE. Axon-Axon Interactions Regulate Topographic Optic Tract Sorting via CYFIP2-Dependent WAVE Complex Function. *Neuron*. 2018;97(5). doi:10.1016/j.neuron.2018.01.027

56. Zhang Y, Kang HR, Han K. Differential cell-type-expression of CYFIP1 and CYFIP2 in the adult mouse hippocampus. *Animal Cells and Systems*. 2019;23(6):380-383. doi:10.1080/19768354.2019.1696406

57. Abekhoukh S, Bardoni B. CYFIP family proteins between autism and intellectual disability: Links with fragile X syndrome. *Frontiers in Cellular Neuroscience*. 2014;8(MAR). doi:10.3389/fncel.2014.00081

58. Nakashima M, Kato M, Aoto K, et al. De novo hotspot variants in CYFIP2 cause early-onset epileptic encephalopathy. *Annals of Neurology*. 2018;83(4):794-806. doi:10.1002/ana.25208

59. Galy A, Schenck A, Sahin HB, et al. CYFIP dependent Actin Remodeling controls specific aspects of Drosophila eye morphogenesis. *Developmental Biology*. 2011;359(1):37-46. doi:10.1016/j.ydbio.2011.08.009

60. Davenport EC, Szulc BR, Drew J, et al. Autism and Schizophrenia-Associated CYFIP1 Regulates the Balance of Synaptic Excitation and Inhibition. *Cell Reports*. 2019;26(8):2037-2051.e6. doi:10.1016/j.celrep.2019.01.092

61. Marsden KC, Jain RA, Wolman MA, et al. A Cyfip2-Dependent Excitatory Interneuron Pathway Establishes the Innate Startle Threshold. *Cell Reports*. 2018;23(3). doi:10.1016/j.celrep.2018.03.095

62. Streisinger G, Walker C, Dower N, Knauber D, Singer F. Production of clones of homozygous diploid zebra fish (Brachydanio rerio). *Nature*. 1981;291(5813):293-296. doi:10.1038/291293a0

63. Stainier DYR, Fouquet B, Chen JN, et al. Mutations affecting the formation and function of the cardiovascular system in the zebrafish embryo. *Development*. 1996;123:285-292. doi:10.1242/dev.123.1.285

64. Haffter P, Granato M, Brand M, et al. The identification of genes with unique and essential functions in the development of the zebrafish, Danio rerio. *Development*. 1996;123:1-36. doi:10.1242/dev.123.1.1

65. Driever W, Solnica-Krezel L, Schier AF, et al. A genetic screen for mutations affecting embryogenesis in zebrafish. *Development*. 1996;123:37-46. doi:10.1242/dev.123.1.37

66. Jao LE, Wente SR, Chen W. Efficient multiplex biallelic zebrafish genome editing using a CRISPR nuclease system. *Proc Natl Acad Sci U S A*. 2013;110(34):13904-13909. doi:10.1073/pnas.1308335110

67. Goldshmit Y, Sztal TE, Jusuf PR, Hall TE, Nguyen-Chi M, Currie PD. Fgf-dependent glial cell bridges facilitate spinal cord regeneration in Zebrafish. *Journal of Neuroscience*. 2012;32(22):7477-7492. doi:10.1523/JNEUROSCI.0758-12.2012

68. Lush ME, Piotrowski T. Sensory hair cell regeneration in the zebrafish lateral line. *Developmental Dynamics*. 2014;243(10):1187-1202. doi:10.1002/dvdy.24167

69. Kizil C. Mechanisms of Pathology-Induced Neural Stem Cell Plasticity and Neural Regeneration in Adult Zebrafish Brain. *Current Pathobiology Reports*. 2018;6(1):71-77. doi:10.1007/s40139-018-0158-x

70. Bhattarai P, Cosacak MI, Mashkaryan V, et al. Neuron-glia interaction through Serotonin-BDNF-NGFR axis enables regenerative neurogenesis in Alzheimer's model of adult zebrafish brain. *PLoS Biology*. 2020;18(1). doi:10.1371/journal.pbio.3000585

71. Drummond IA. Kidney development and disease in the zebrafish. *Journal of the American Society of Nephrology*. 2005;16(2):299-304. doi:10.1681/ASN.2004090754

72. Bergen DJM, Kague E, Hammond CL. Zebrafish as an emerging model for osteoporosis: A primary testing platform for screening new osteo-active compounds. *Frontiers in Endocrinology*. 2019;10(JAN). doi:10.3389/fendo.2019.00006

73. Carnovali M, Banfi G, Mariotti M. Zebrafish Models of Human Skeletal Disorders: Embryo and Adult Swimming Together. *BioMed Research International*. 2019;2019. doi:10.1155/2019/1253710

74. Martin WK, Tennant AH, Conolly RB, et al. High-Throughput Video Processing of Heart Rate Responses in Multiple Wild-type Embryonic Zebrafish per Imaging Field. *Scientific Reports*. 2019;9(1). doi:10.1038/s41598-018-35949-5

75. Teixidó E, Kießling TR, Krupp E, Quevedo C, Muriana A, Scholz S. Automated Morphological Feature Assessment for Zebrafish Embryo Developmental Toxicity Screens. *Toxicological Sciences*. 2019;167(2):438-449. doi:10.1093/toxsci/kfy250

76. Brannen KC, Panzica-Kelly JM, Danberry TL, Augustine-Rauch KA. Development of a zebrafish embryo teratogenicity assay and quantitative prediction model. *Birth Defects Research Part B - Developmental and Reproductive Toxicology*. 2010;89(1):66-77. doi:10.1002/bdrb.20223

77. Cosacak MI, Bhattarai P, Reinhardt S, et al. Single-Cell Transcriptomics Analyses of Neural Stem Cell Heterogeneity and Contextual Plasticity in a Zebrafish Brain Model of Amyloid Toxicity. *Cell Reports*. 2019;27(4):1307-1318.e3. doi:10.1016/j.celrep.2019.03.090

78. Xi Y, Noble S, Ekker M. Modeling neurodegeneration in zebrafish. *Current Neurology and Neuroscience Reports*. 2011;11(3):274-282. doi:10.1007/s11910-011-0182-2

79. Cho SJ, Park E, Baker A, Reid AY. Age Bias in Zebrafish Models of Epilepsy: What Can We Learn From Old Fish? *Frontiers in Cell and Developmental Biology*. 2020;8. doi:10.3389/fcell.2020.573303

80. Steenbergen PJ, Richardson MK, Champagne DL. The use of the zebrafish model in stress research. *Progress in Neuro-Psychopharmacology and Biological Psychiatry*. 2011;35(6):1432-1451. doi:10.1016/j.pnpbp.2010.10.010

81. Bassett DI, Currie PD. The zebrafish as a model for muscular dystrophy and congenital myopathy. *Human Molecular Genetics*. 2003;12(REV. ISS. 2). doi:10.1093/hmg/ddg279

82. Maves L. Recent advances using zebrafish animal models for muscle disease drug discovery. *Expert Opinion on Drug Discovery*. 2014;9(9):1033-1045. doi:10.1517/17460441.2014.927435

83. Machuca-Tzili LE, Buxton S, Thorpe A, et al. Zebrafish deficient for Muscleblind-like 2 exhibit features of myotonic dystrophy. *DMM Disease Models and Mechanisms*. 2011;4(3):381-392. doi:10.1242/dmm.004150

84. Liu S, Leach SD. Zebrafish models for cancer. *Annual Review of Pathology: Mechanisms of Disease*. 2011;6:71-93. doi:10.1146/annurev-pathol-011110-130330

85. van der Vaart M, Spaink HP, Meijer AH. Pathogen recognition and activation of the innate immune response in zebrafish. *Advances in Hematology*. 2012;2012. doi:10.1155/2012/159807

86. Meeker ND, Trede NS. Immunology and zebrafish: Spawning new models of human disease. *Developmental and Comparative Immunology*. 2008;32(7):745-757. doi:10.1016/j.dci.2007.11.011

87. Renshaw SA, Trede NS. A model 450 million years in the making: Zebrafish and vertebrate immunity. *DMM Disease Models and Mechanisms*. 2012;5(1):38-47. doi:10.1242/dmm.007138

88. Torraca V, Masud S, Spaink HP, Meijer AH. Macrophage-pathogen interactions in infectious diseases: New therapeutic insights from the zebrafish host model. *DMM Disease Models and Mechanisms*. 2014;7(7):785-797. doi:10.1242/dmm.015594

89. H. Meijer A, P. Spaink H. Host-Pathogen Interactions Made Transparent with the Zebrafish Model. *Current Drug Targets*. 2011;12(7):1000-1017. doi:10.2174/138945011795677809

90. Ramakrishnan L. The zebrafish guide to tuberculosis immunity and treatment. *Cold Spring Harbor Symposia on Quantitative Biology*. 2013;78(1):179-192. doi:10.1101/sqb.2013.78.023283

91. Cronan MR, Tobin DM. Fit for consumption: Zebrafish as a model for tuberculosis. *DMM Disease Models and Mechanisms*. 2014;7(7):777-784. doi:10.1242/dmm.016089

92. Zang L, Maddison LA, Chen W. Zebrafish as a model for obesity and diabetes. *Frontiers in Cell and Developmental Biology*. 2018;6(AUG). doi:10.3389/fcell.2018.00091

93. Rennekamp AJ, Peterson RT. 15 years of zebrafish chemical screening. *Current Opinion in Chemical Biology*. 2015;24:58-70. doi:10.1016/j.cbpa.2014.10.025

94. MacRae CA, Peterson RT. Zebrafish as tools for drug discovery. *Nature Reviews Drug Discovery*. 2015;14(10):721-731. doi:10.1038/nrd4627

95. Hill AJ, Teraoka H, Heideman W, Peterson RE. Zebrafish as a model vertebrate for investigating chemical toxicity. *Toxicological Sciences*. 2005;86(1):6-19. doi:10.1093/toxsci/kfi110

96. Peterson RT, Link BA, Dowling JE, Schreiber SL. Small molecule developmental screens reveal the logic and timing of vertebrate development. *Proc Natl Acad Sci U S A*. 2000;97(24):12965-12969. doi:10.1073/pnas.97.24.12965

97. Zon LI, Peterson RT. In vivo drug discovery in the zebrafish. *Nature Reviews Drug Discovery*. 2005;4(1):35-44. doi:10.1038/nrd1606

98. Dahm R. The Zebrafish Exposed: "See-through" mutants may hold the key to unraveling the mysteries of embryonic development. American Scientist, vol. 94, no. 5. Published 2006. Accessed June 9, 2022. https://www.jstor.org/stable/27858837?seq=1

99. Howe K, Clark MD, Torroja CF, et al. The zebrafish reference genome sequence and its relationship to the human genome. *Nature*. 2013;496(7446):498-503. doi:10.1038/nature12111

100. Phillips JB, Westerfield M. Zebrafish models in translational research: Tipping the scales toward advancements in human health. *DMM Disease Models and Mechanisms*. 2014;7(7):739-743. doi:10.1242/dmm.015545

101. Bradford YM, Toro S, Ramachandran S, et al. Zebrafish models of human disease: Gaining insight into human disease at ZFIN. *ILAR Journal*. 2017;58(1):4-16. doi:10.1093/ilar/ilw040

102. Bakkers J. Zebrafish as a model to study cardiac development and human cardiac disease. *Cardiovascular Research*. 2011;91(2):279-288. doi:10.1093/cvr/cvr098

103. Schuermann A, Helker CSM, Herzog W. Angiogenesis in zebrafish. *Seminars in Cell and Developmental Biology*. 2014;31:106-114. doi:10.1016/j.semcdb.2014.04.037

104. Okuda KS, Hogan BM. Endothelial Cell Dynamics in Vascular Development: Insights From Live-Imaging in Zebrafish. *Frontiers in Physiology*. 2020;11. doi:10.3389/fphys.2020.00842

105. Lawson ND, Weinstein BM. In vivo imaging of embryonic vascular development using transgenic zebrafish. *Developmental Biology*. 2002;248(2):307-318. doi:10.1006/dbio.2002.0711

106. Sonnemann KJ, Bement WM. Wound repair: Toward understanding and integration of single-cell and multicellular wound responses. *Annual Review of Cell and Developmental Biology*. 2011;27:237-263. doi:10.1146/annurev-cellbio-092910-154251

107. Weijer CJ. Collective cell migration in development. *Journal of Cell Science*. 2009;122(18):3215-3223. doi:10.1242/jcs.036517

108. Keely PJ. Cell Migration within Three-Dimensional Matrices. In: Lennarz WJ, Lane MD, eds. *Encyclopedia of Biological Chemistry*. Second Edition. Academic Press; 2013:436-445.

109. Lai FPL, Szczodrak M, Block J, et al. Arp2/3 complex interactions and actin network turnover in lamellipodia. *EMBO Journal*. 2008;27(7):982-992. doi:10.1038/emboj.2008.34

110. Insall RH, Machesky LM. Actin Dynamics at the Leading Edge: From Simple Machinery to Complex Networks. *Developmental Cell*. 2009;17(3):310-322. doi:10.1016/j.devcel.2009.08.012

111. Mitchison TJ, Cramer LP. Actin-based cell motility and cell locomotion. *Cell*. 1996;84(3):371-379. doi:10.1016/S0092-8674(00)81281-7

112. Carlier MF, Clainche C le, Wiesner S, Pantaloni D. Actin-based motility: from molecules to movement. *BioEssays*. 2003;25(4):336-345. doi:10.1002/bies.10257

113. le Clainche C, Carlier MF. Regulation of actin assembly associated with protrusion and adhesion in cell migration. *Physiological Reviews*. 2008;88(2):489-513. doi:10.1152/physrev.00021.2007

114. Ridley AJ. Life at the leading edge. *Cell*. 2011;145(7):1012-1022. doi:10.1016/j.cell.2011.06.010

115. Small JV, Stradal T, Vignal E, Rottner K. The lamellipodium: Where motility begins. *Trends in Cell Biology*. 2002;12(3):112-120. doi:10.1016/S0962-8924(01)02237-1

116. Pollard TD. Regulation of actin filament assembly by Arp2/3 complex and formins. *Annual Review of Biophysics and Biomolecular Structure*. 2007;36:451-477. doi:10.1146/annurev.biophys.35.040405.101936

117. Rouiller I, Xu XP, Amann KJ, et al. The structural basis of actin filament branching by the Arp2/3 complex. *Journal of Cell Biology*. 2008;180(5):887-895. doi:10.1083/jcb.200709092

118. Forscher P, Lin CH, Thompson C. Novel form of growth cone motility involving site-directed actin filament assembly. *Nature*. 1992;357(6378):515-518. doi:10.1038/357515a0

119. Bugyi B, Carlier MF. Control of actin filament treadmilling in cell motility. *Annual Review of Biophysics*. 2010;39(1):449-470. doi:10.1146/annurev-biophys-051309-103849

120. Lamalice L, le Boeuf F, Huot J. Endothelial cell migration during angiogenesis. *Circulation Research*. 2007;100(6):782-794. doi:10.1161/01.RES.0000259593.07661.1e

121. Stainier DYR, Lee RK, Fishman MC. Cardiovascular development in the zebrafish: I. Myocardial fate map and heart tube formation. *Development*. 1993;119(1):31-40. doi:10.1242/dev.119.1.31

122. de Pater E, Clijsters L, Marques SR, et al. Distinct phases of cardiomyocyte differentiation regulate growth of the zebrafish heart. *Development*. 2009;136(10):1633-1641. doi:10.1242/dev.030924

123. Beis D, Bartman T, Jin SW, et al. Genetic and cellular analyses of zebrafish atrioventricular cushion and valve development. *Development*. 2005;132(18):4193-4204. doi:10.1242/dev.01970

124. Scherz PJ, Huisken J, Sahai-Hernandez P, Stainier DYR. High-speed imaging of developing heart valves reveals interplay of morphogenesis and function. *Development*. 2008;135(6):1179-1187. doi:10.1242/dev.010694

125. Serluca FC. Development of the proepicardial organ in the zebrafish. *Developmental Biology*. 2008;315(1):18-27. doi:10.1016/j.ydbio.2007.10.007

126. Liu J, Stainier DYR. Tbx5 and Bmp signaling are essential for proepicardium specification in zebrafish. *Circulation Research*. 2010;106(12):1818-1828. doi:10.1161/CIRCRESAHA.110.217950

127. Smith KA, Joziasse IC, Chocron S, et al. Dominant-negative alk2 allele associates with congenital heart defects. *Circulation*. 2009;119(24):3062-3069. doi:10.1161/CIRCULATIONAHA.108.843714

128. Knöll R, Hoshijima M, Hoffman HM, et al. The cardiac mechanical stretch sensor machinery involves a Z disc complex that is defective in a subset of human dilated cardiomyopathy. *Cell*. 2002;111(7):943-955. doi:10.1016/S0092-8674(02)01226-6

129. Sehnert AJ, Huq A, Weinstein BM, Walker C, Fishman M, Stainier DYR. Cardiac troponin T is essential in sarcomere assembly and cardiac contractility. *Nature Genetics*. 2002;31(1):106-110. doi:10.1038/ng875

130. Beqqali A, Monshouwer-Kloots J, Monteiro R, et al. CHAP is a newly identified Z-disc protein essential for heart and skeletal muscle function. *Journal of Cell Science*. 2010;123(7):1141-1150. doi:10.1242/jcs.063859

131. Hogan BM, Schulte-Merker S. How to Plumb a Pisces: Understanding Vascular Development and Disease Using Zebrafish Embryos. *Developmental Cell*. 2017;42(6):567-583. doi:10.1016/j.devcel.2017.08.015

132. Coffin JD, Poole TJ. Endothelial cell origin and migration in embryonic heart and cranial blood vessel development. *The Anatomical Record*. 1991;231(3):383-395. doi:10.1002/ar.1092310312

133. Risau W, Flamme I. Vasculogenesis. *Annual Review of Cell and Developmental Biology*. 1995;11:73-91. doi:10.1146/annurev.cb.11.110195.000445

134. Weinstein BM. What guides early embryonic blood vessel formation? *Developmental Dynamics*. 1999;215(1):2-11. doi:10.1002/(SICI)1097-0177(199905)215:1<2::AID-DVDY2>3.0.CO;2-U

135. Stainier DYR, Weinstein BM, Detrich HW, Zon LI, Fishman MC. cloche, an early acting zebrafish gene, is required by both the endothelial and hematopoietic lineages. *Development*. 1995;121(10):3141-3150. doi:10.1242/dev.121.10.3141

136. Jin SW, Beis D, Mitchell T, Chen JN, Stainier DYR. Cellular and molecular analyses of vascular tube and lumen formation in zebrafish. *Development*. 2005;132(23):5199-5209. doi:10.1242/dev.02087

137. Isogai S, Horiguchi M, Weinstein BM. The vascular anatomy of the developing zebrafish: An atlas of embryonic and early larval development. *Developmental Biology*. 2001;230(2):278-301. doi:10.1006/dbio.2000.9995

138. Siekmann AF, Lawson ND. Notch signalling limits angiogenic cell behaviour in developing zebrafish arteries. *Nature*. 2007;445(7129):781-784. doi:10.1038/nature05577

139. Gebala V, Collins R, Geudens I, Phng LK, Gerhardt H. Blood flow drives lumen formation by inverse membrane blebbing during angiogenesis in vivo. *Nature Cell Biology*. 2016;18(4):443-450. doi:10.1038/ncb3320

140. Isogai S, Lawson ND, Torrealday S, Horiguchi M, Weinstein BM. Angiogenic network formation in the developing vertebrate trunk. *Development*. 2003;130(21):5281-5290. doi:10.1242/dev.00733

141. Yaniv K, Isogai S, Castranova D, Dye L, Hitomi J, Weinstein BM. Live imaging of lymphatic development in the zebrafish. *Nature Medicine*. 2006;12(6):711-716. doi:10.1038/nm1427

142. Betz C, Lenard A, Belting HG, Affolter M. Cell behaviors and dynamics during angiogenesis. *Development (Cambridge)*. 2016;143(13):2249-2260. doi:10.1242/dev.135616

143. Kamei M, Brian Saunders W, Bayless KJ, Dye L, Davis GE, Weinstein BM. Endothelial tubes assemble from intracellular vacuoles in vivo. *Nature*. 2006;442(7101):453-456. doi:10.1038/nature04923

144. Wakayama Y, Fukuhara S, Ando K, Matsuda M, Mochizuki N. Cdc42 mediates Bmp - Induced sprouting angiogenesis through Fmnl3-driven assembly of endothelial filopodia in zebrafish. *Developmental Cell*. 2015;32(1):109-122. doi:10.1016/j.devcel.2014.11.024

145. Phng LK. Endothelial Cell Dynamics during Blood Vessel Morphogenesis. In: *Zebrafish, Medaka, and Other Small Fishes*. Springer Singapore; 2018:17-35. doi:10.1007/978-981-13-1879-5_2

146. Blum Y, Belting HG, Ellertsdottir E, Herwig L, Lüders F, Affolter M. Complex cell rearrangements during intersegmental vessel sprouting and vessel fusion in the zebrafish embryo. *Developmental Biology*. 2008;316(2):312-322. doi:10.1016/j.ydbio.2008.01.038

147. Strilić B, Eglinger J, Krieg M, et al. Electrostatic cell-surface repulsion initiates lumen formation in developing blood vessels. *Current Biology*. 2010;20(22):2003-2009. doi:10.1016/j.cub.2010.09.061

148. Herwig L, Blum Y, Krudewig A, et al. Distinct cellular mechanisms of blood vessel fusion in the zebrafish embryo. *Current Biology*. 2011;21(22):1942-1948. doi:10.1016/j.cub.2011.10.016

149. Lenard A, Ellertsdottir E, Herwig L, et al. In vivo analysis reveals a highly stereotypic morphogenetic pathway of vascular anastomosis. *Developmental Cell*. 2013;25(5):492-506. doi:10.1016/j.devcel.2013.05.010

150. Pelton JC, Wright CE, Leitges M, Bautch VL. Multiple endothelial cells constitute the tip of developing blood vessels and polarize to promote lumen formation. *Development (Cambridge)*. 2014;141(21):4121-4126. doi:10.1242/dev.110296

151. Kochhan E, Lenard A, Ellertsdottir E, et al. Correction: Blood flow changes coincide with cellular rearrangements during blood vessel pruning in zebrafish embryos (PLoS ONE). *PLoS ONE*. 2014;9(1). doi:10.1371/annotation/9e16dd10-9d37-4d4f-85b2-0811852b15f0

152. Wen L, Zhang T, Wang J, et al. The blood flow-klf6a-tagln2 axis drives vessel pruning in zebrafish by regulating endothelial cell rearrangement and actin cytoskeleton dynamics. *PLoS Genetics*. 2021;17(7). doi:10.1371/journal.pgen.1009690

153. Lenard A, Daetwyler S, Betz C, et al. Endothelial Cell Self-fusion during Vascular Pruning. Hogan BLM, ed. *PLOS Biology*. 2015;13(4):e1002126. doi:10.1371/journal.pbio.1002126

154. Paik EJ, Zon LI. Hematopoietic development in the zebrafish. *International Journal of Developmental Biology*. 2010;54(6-7):1127-1137. doi:10.1387/ijdb.093042ep

155. Gore A v., Pillay LM, Venero Galanternik M, Weinstein BM. The zebrafish: A fintastic model for hematopoietic development and disease. *Wiley Interdisciplinary Reviews: Developmental Biology*. 2018;7(3). doi:10.1002/wdev.312

156. Davidson AJ, Zon LI. The “definitive” (and ’primitive’) guide to zebrafish hematopoiesis. *Oncogene*. 2004;23(43 REV. ISS. 6):7233-7246. doi:10.1038/sj.onc.1207943

157. Galloway JL, Zon LI. 3 Ontogeny of hematopoiesis: Examining the emergence of hematopoietic cells in the vertebrate embryo. *Current Topics in Developmental Biology*. 2003;53:139-158. doi:10.1016/s0070-2153(03)53004-6

158. de Jong JLO, Zon LI. Use of the zebrafish system to study primitive and definitive hematopoiesis. *Annual Review of Genetics*. 2005;39:481-501. doi:10.1146/annurev.genet.39.073003.095931

159. Bertrand JY, Kim AD, Violette EP, Stachura DL, Cisson JL, Traver D. Definitive hematopoiesis initiates through a committed erythromyeloid progenitor in the zebrafish embryo. *Development*. 2007;134(23):4147-4156. doi:10.1242/dev.012385

160. Ciau-Uitz A, Patient R. The embryonic origins and genetic programming of emerging haematopoietic stem cells. *FEBS Letters*. 2016;590(22):4002-4015. doi:10.1002/1873-3468.12363

161. Liao EC, Paw BH, Oates AC, Pratt SJ, Postlethwait JH, Zon LI. SCL/Tal-1 transcription factor acts downstream of cloche to specify hematopoietic and vascular progenitors in zebrafish. *Genes and Development*. 1998;12(5):621-626. doi:10.1101/gad.12.5.621

162. Thompson MA, Ransom DG, Pratt SJ, et al. The Cloche and Spadetail Genes Differentially Affect Hematopoiesis and Vasculogenesis. *Developmental Biology*. 1998;197(2):248-269. doi:10.1006/dbio.1998.8887

163. Detrich HW, Kieran MW, Chan FY, et al. Intraembryonic hematopoietic cell migration during vertebrate development. *Proc Natl Acad Sci U S A*. 1995;92(23):10713-10717. doi:10.1073/pnas.92.23.10713

164. Warga RM, Kane DA, Ho RK. Fate Mapping Embryonic Blood in Zebrafish: Multi- and Unipotential Lineages Are Segregated at Gastrulation. *Developmental Cell*. 2009;16(5):744-755. doi:10.1016/j.devcel.2009.04.007

165. Forrester AM, Berman JN, Payne EM. Myelopoiesis and myeloid leukaemogenesis in the zebrafish. *Advances in Hematology*. 2012;2012. doi:10.1155/2012/358518

166. Li L, Jin H, Xu J, Shi Y, Wen Z. Irf8 regulates macrophage versus neutrophil fate during zebrafish primitive myelopoiesis. *Blood*. 2011;117(4):1359-1369. doi:10.1182/blood-2010-06-290700

167. le Guyader D, Redd MJ, Colucci-Guyon E, et al. Origins and unconventional behavior of neutrophils in developing zebrafish. *Blood*. 2008;111(1):132-141. doi:10.1182/blood-2007-06-095398

168. Lieschke GJ, Oates AC, Crowhurst MO, Ward AC, Layton JE. Morphologic and functional characterization of granulocytes and macrophages in embryonic and adult zebrafish. *Blood*. 2001;98(10):3087-3096. doi:10.1182/blood.V98.10.3087

169. Dooley KA, Davidson AJ, Zon LI. Zebrafish scl functions independently in hematopoietic and endothelial development. *Developmental Biology*. 2005;277(2):522-536. doi:10.1016/j.ydbio.2004.09.004

170. Patterson LJ, Gering M, Patient R. Scl is required for dorsal aorta as well as blood formation in zebrafish embryos. *Blood*. 2005;105(9):3502-3511. doi:10.1182/blood-2004-09-3547

171. Bertrand JY, Chi NC, Santoso B, Teng S, Stainier DYR, Traver D. Haematopoietic stem cells derive directly from aortic endothelium during development. *Nature*. 2010;464(7285):108-111. doi:10.1038/nature08738

172. Kissa K, Herbomel P. Blood stem cells emerge from aortic endothelium by a novel type of cell transition. *Nature*. 2010;464(7285):112-115. doi:10.1038/nature08761

173. Wilkinson RN, Pouget C, Gering M, et al. Hedgehog and Bmp Polarize Hematopoietic Stem Cell Emergence in the Zebrafish Dorsal Aorta. *Developmental Cell*. 2009;16(6):909-916. doi:10.1016/j.devcel.2009.04.014

174. Tamplin OJ, Durand EM, Carr LA, et al. Hematopoietic stem cell arrival triggers dynamic remodeling of the perivascular niche. *Cell*. 2015;160(1-2):241-252. doi:10.1016/j.cell.2014.12.032

175. Murayama E, Kissa K, Zapata A, et al. Tracing Hematopoietic Precursor Migration to Successive Hematopoietic Organs during Zebrafish Development. *Immunity*. 2006;25(6):963-975. doi:10.1016/j.immuni.2006.10.015

176. Theodore LN, Hagedorn EJ, Cortes M, et al. Distinct Roles for Matrix Metalloproteinases 2 and 9 in Embryonic Hematopoietic Stem Cell Emergence, Migration, and Niche Colonization. *Stem Cell Reports*. 2017;8(5):1226-1241. doi:10.1016/j.stemcr.2017.03.016

177. Blaser BW, Moore JL, Hagedorn EJ, et al. CXCR1 remodels the vascular niche to promote hematopoietic stem and progenitor cell engraftment. *Journal of Experimental Medicine*. 2017;214(4):1011-1027. doi:10.1084/jem.20161616

178. Kissa K, Murayama E, Zapata A, et al. Live imaging of emerging hematopoietic stem cells and early thymus colonization. *Blood*. 2008;111(3):1147-1156. doi:10.1182/blood-2007-07-099499

179. Kevenaar JT, Hoogenraad CC. The axonal cytoskeleton: From organization to function. *Frontiers in Molecular Neuroscience*. 2015;8(AUGUST):44. doi:10.3389/fnmol.2015.00044

180. Marín O, Valiente M, Ge X, Tsai LH. Guiding neuronal cell migrations. *Cold Spring Harb Perspect Biol*. 2010;2(2). doi:10.1101/cshperspect.a001834

181. Schmidt R, Strähle U, Scholpp S. Neurogenesis in zebrafish - from embryo to adult. *Neural Development*. 2013;8(1). doi:10.1186/1749-8104-8-3

182. Myers PZ, Eisen JS, Westerfield M. Development and axonal outgrowth of identified motoneurons in the zebrafish. *Journal of Neuroscience*. 1986;6(8):2278-2289. doi:10.1523/jneurosci.06-08-02278.1986

183. Westerfield M, McMurray J v., Eisen JS. Identified motoneurons and their innervation of axial muscles in the zebrafish. *Journal of Neuroscience*. 1986;6(8):2267-2277. doi:10.1523/jneurosci.06-08-02267.1986

184. Eisen JS, Myers PZ, Westerfield M. Pathway selection by growth cones of identified motoneurones in live zebra fish embryos. *Nature*. 1986;320(6059):269-271. doi:10.1038/320269a0

185. Eisen JS, Pike SH, Debu B. The growth cones of identified motoneurons in embryonic zebrafish select appropriate pathways in the absence of specific cellular interactions. *Neuron*. 1989;2(1):1097-1104. doi:10.1016/0896-6273(89)90234-1

186. Eisen JS, Pike SH, Romancier B. An identified motoneuron with variable fates in embryonic zebrafish. *Journal of Neuroscience*. 1990;10(1):34-43. doi:10.1523/jneurosci.10-01-00034.1990

187. Eisen JS, Melancon E. Interactions with identified muscle cells break motoneuron equivalence in embryonic zebrafish. *Nature Neuroscience*. 2001;4(11):1065-1070. doi:10.1038/nn742

188. Eisen JS. Development of motoneuronal phenotype. *Annual Review of Neuroscience*. 1994;17:1-30. doi:10.1146/annurev.ne.17.030194.000245

189. Melançon E, Liu DWC, Westerfield M, Eisen JS. Pathfinding by identified zebrafish motoneurons in the absence of muscle pioneers. *Journal of Neuroscience*. 1997;17(20):7796-7804. doi:10.1523/jneurosci.17-20-07796.1997

190. Beattie CE. Control of motor axon guidance in the zebrafish embryo. *Brain Research Bulletin*. 2000;53(5):489-500. doi:10.1016/S0361-9230(00)00382-8

191. Zelenchuk TA, Brusés JL. In Vivo labeling of zebrafish motor neurons using an mnx1 enhancer and Gal4/UAS. *Genesis*. 2011;49(7):546-554. doi:10.1002/dvg.20766

192. Zeller J, Schneider V, Malayaman S, et al. Migration of zebrafish spinal motor nerves into the periphery requires multiple myotome-derived cues. *Developmental Biology*. 2002;252(2):241-256. doi:10.1006/dbio.2002.0852

193. Gong J, Wang X, Zhu C, et al. Insm1a regulates motor neuron development in zebrafish. *Frontiers in Molecular Neuroscience*. 2017;10. doi:10.3389/fnmol.2017.00274

194. Issa FA, Mock AF, Sagasti A, Papazian DM. Spinocerebellar ataxia type 13 mutation that is associated with disease onset in infancy disrupts axonal pathfinding during neuronal development. *DMM Disease Models and Mechanisms*. 2012;5(6):921-929. doi:10.1242/dmm.010157

195. Ott H, Diekmann H, Stuermer CAO, Bastmeyer M. Function of neurolin (DM-GRASP/SC-1) in guidance of motor axons during zebrafish development. *Developmental Biology*. 2001;235(1):86-97. doi:10.1006/dbio.2001.0278

CHAPTER 2. CHARACTERIZING THE IN VIVO FUNCTIONS OF CYFIP1 IN THE DEVELOPMENT OF CARDIOVASCULAR, HEMATOPOIETIC, AND NERVOUS SYSTEMS BY PRECISE TARGETED GENOME EDITING IN ZEBRAFISH

Pongrat Jaisil[1,2,3], Jeffrey J. Essner[2,*], Baoyu Chen[1,*]

[1] Department of Biochemistry, Biophysics and Molecular Biology, Iowa State University, Ames, IA 50011, USA

[2] Department of Genetics, Development, and Cell Biology, Iowa State University, Ames, IA 50011, USA

[3] Neuroscience Interdepartmental Program, Iowa State University, Ames, IA 50011, USA

[*] Corresponding authors: stone@iastate.edu and jessner@iastate.edu

Modified from a manuscript to be submitted to *eLife*

Abstract

Actin cytoskeleton is the most abundant and crucial protein in most eukaryotic cells, involving a broad range of essential cellular processes. The major regulator for actin dynamics is the WAVE regulatory complex (WRC). The activation and function of the WRC is governed through its own subunit called Cyfip. In vertebrates, there are two Cyfip isoforms, Cyfip1 and Cyfip2, which have been shown to have different expression patterns and distinct functions in various biological systems. However, there is a limited understanding of the *in vivo* functions of Cyfip proteins in animals, especially in vertebrates. With the development of CRISPR/Cas9-based gene editing technologies and zebrafish as a vertebrate model organism, we have established cyfip1 and cyfip2 knockout mutant in zebrafish using a newly developed and efficient CRISPR/Cas9-based short homology targeted integration strategy named GeneWeld.

Together with a novel gene inactivation method called pPRISM-Stop vector, we explored the *in vivo* functions of each Cyfip isoform in various biological systems, including cardiovascular, hematopoietic, retinotectal, and spinal motor nervous systems. With the high efficiency of the GeneWeld method for precise targeted integration of pPRISM-Stop cassette into each cyfip locus, we were able to recover cyfip1 and cyfip2 germline transmitting adults with on-target integration with frequencies at 13% for both cyfip loci (3/24 for cyfip1 and 2/16 for cyfip2). Despite an unexpected integration of the vector backbone into cyfip2 locus uncovered later, we were able to successfully establish stable lines of true cyfip1 knockout mutant to investigate the phenotypes from its homozygous deletion. Intriguingly, we discovered that cyfip1 abolishment during early stage of development led to mismigration or stalled development of endothelial cells and stenotic vessels accompanied by disrupted blood circulation, substantial reduction of the HSPCs in various hematopoietic tissues, as well as aberrant axon branching and abnormal axon terminals. Taken together, our study demonstrated efficient targeted integration at zebrafish cyfip1 locus using CRISPR/Cas9 short homology targeted GeneWeld strategy and pPRISM-Stop-mediated gene inactivation method to establish, for the first time, stable cyfip1 knockout mutant zebrafish lines to analyze cyfip1 knockout phenotypes and characterize the *in vivo* functions of cyfip1 in cardiovascular, hematopoietic, retinotectal and spinal motor nervous systems. Although additional samples and further analysis is necessary to make final conclusions, the pronounced morphological and microscopic phenotypes discovered in this study suggested the promising essential *in vivo* functions of cyfip1 in the development of cardiovascular, hematopoietic, retinotectal, and spinal motor nervous systems, which worth investigating more profoundly to fully characterize the *in vivo* functions and identify molecular mechanisms of cyfip1, and the WRC-mediated actin remodeling, in these physiological systems.

Introduction

Actin cytoskeleton is one of the most fascinating cellular components, as well as the most abundant protein in most eukaryotic cells. It is highly conserved through evolution and is involved in more protein-protein interactions than any other known protein. Actin dynamics contribute to many essential cellular processes, ranging from cell shape integrity, cell proliferation, cell migration, cell adhesion and fusion, endocytosis and vesicle trafficking, chromatin remodeling, DNA repair and regulation of transcription[1–13]. The actin cytoskeleton has been studied for several decades and many relevant aspects have been partially uncovered[14], for example, actin structure and its cellular functions, actin binding proteins, and actin molecular machinery. However, several questions about the detailed structure of actin cytoskeleton and its dynamics, as well as how these define its functions, both *in vitro* and *in vivo*, and its regulation controlling dynamic actin remodeling still remain unclear[15].

Actin is critically important for cell motility and migration[4], which are indispensable processes for morphogenesis and structural and organ development in various physiological systems during vertebrate embryogenesis. In motile cells, their membrane leading edge consists primarily of lamellipodia, which are thin sheet-like membrane protrusions enriched by branched actin filament networks underneath the cell membrane. The formation of these branched F-actin networks is initiated by a major Y-branching actin nucleator named the Arp2/3 complex. The Arp2/3 complex can be activated by its binding to actin nucleation promoting factors (NPFs), in which one of the key NPFs and actin remodeling regulators controlling Arp2/3-mediated F-actin branching is the WAVE protein. In nature, the WAVE protein exists in a form of cytosolic protein complex called the WAVE regulatory complex (WRC)[16]. This heteropentameric protein complex consists of five conserved protein subunits: Cyfip (cytoplasmic FMR1-interacting

protein), Nap (Nck-associated protein), Abi (Abelson-interacting protein), HSPC300 (hematopoietic stem progenitor cell 300), and WAVE (Wiskott-Aldrich syndrome protein family verprolin-homologous protein)[17–19]. Normally, the WRC is auto-inhibited in a basal state. It is mainly activated by binding to its ubiquitous regulator Rac1 GTPases[20–25], and is recruited to the plasma membrane by interacting with various specific ligands containing a short peptide motif named WIRS (WRC interacting receptor sequence)[26–34]. Intriguingly, these two signaling pathways and their corresponding binding pockets converge on the Cyfip subunit of the WRC, implicating the Cyfip subunit as central to the mechanisms behind the WRC regulation and, ultimately, the dynamic actin remodeling.

In vertebrates, there are two Cyfip isoforms, Cyfip1 and Cyfip2. These two Cyfip proteins are highly conserved among vertebrates, in which human Cyfip1 shares 98.7% and 93% with their mouse and zebrafish orthologues, respectively. Human Cyfip2 shares 99.9% and 98% with their mouse and zebrafish orthologues, respectively[35,36]. Despite high sequence homology between Cyfip1 and Cyfip2 (for example, 86% between the two zebrafish Cyfip isoforms[35,36]), differential expression patterns and non-redundant functions of the two isoforms are observed[37–40], suggesting distinct roles of each Cyfip isoform in different tissue and different developmental stages. There is limited research investigating *in vivo* functions of Cyfip in animals, especially in vertebrates. Most studies have primarily been focused on defects in the nervous system in invertebrates, where there is only one form of Cyfip, and identified abnormalities in dendritic spine morphogenesis and axon pathfinding[39,41–43]. In addition, knocking out single subunit of the WRC in mice, which essentially resembles deletion of Cyfip subunit or the whole WRC due to protein complex disassembly, led to impaired hematopoietic cell development, as well as defective directed cell migration and severe gross lesions in the cardiovascular system and

hemorrhages, which eventually resulted in embryonic death[44–47]. Altogether, these findings suggested potential roles of each Cyfip isoform in, at least, the cardiovascular, hematopoietic, and nervous systems in vertebrates. Therefore, this poses a critical need for investigating *in vivo* functions of the Cyfip proteins in these biological systems and its detailed underlying mechanisms. Lack of this knowledge has hindered the understanding of physiological roles and functional differences between the two Cyfip isoforms involving the WRC signaling-mediated actin reorganization in various biological systems.

CRISPR/Cas9-mediated genome engineering to create targeted transgene knock-in and precise genome modification with high efficiency and specificity allows assessment of the *in vivo* functions of Cyfip isoforms[48–50]. Key to studying a molecular mechanism in animals is to obtain a stable line of the mutant and a strong, quantifiable phenotype for the gene of interest, which have not been pursued in any biological systems for Cyfip. To achieve this, we utilized zebrafish, a robust and ideal model vertebrate for forward and reverse genetic studies[51], together with a novel CRISPR/Cas9-based short homology targeted integration strategy named GeneWeld[52,53], and a newly developed gene inactivation tool called pPRISM-Stop vector (plasmids for PRecise Integration with Secondary Markers) to generate either *cyfip1* or *cyfip2* stable knockout mutant in various transgenic zebrafish to investigate *in vivo* functions of each Cyfip isoform in several biological systems. With high efficiency of the GeneWeld method for precise targeted integration of pPRISM-Stop cassette into each *cyfip* loci, we observed high frequencies of somatic reporter expression in the injected embryos for *cyfip1* and *cyfip2* loci of 86% and 69%, respectively. In addition, high germline transmission rates of *cyfip1* and *cyfip2* knockout alleles were also obtained, at 46% (11/24) and 38% (6/16) for *cyfip1* and *cyfip2* loci, respectively. Among these, we were able to recover *cyfip1* and *cyfip2* germline transmitting

adults with precise targeted integration with frequencies at 13% for both *cyfip* loci (3/24 for *cyfip1*, and 2/16 for *cyfip2*). A functional pPRISM-Stop cassette was precisely integrated, and *cyfip1* knockout homozygotes expressing blue fluorescent protein (BFP) secondary marker (corresponding to approximately 25% of the population in each mating) displayed marked morphological phenotypes which included defects in the retinotectal, cardiovascular, hematopoietic, and spinal motor nervous systems. Their genotypes were confirmed by 5' and 3' genome/vector junction PCR analysis, which revealed precise 5' integration, likely mediated by homology mediated end joining (HMEJ) DNA repair mechanism. The 3' end of the pPRISM-Stop repair template was also incorporated correctly into the desired locus, however, the duplication of 3' short homologous sequence was observed, which is likely generated by microhomology-mediated end joining (MMEJ) or classic non-homologous end joining (cNHEJ) pathways. No part of pPRISM-Stop donor vector backbone was detected in either 5' or 3' genome/vector junction. In contrast, inconsistent microscopic phenotypes in the retinotectal system were observed in *cyfip2* knockout mutant. This phenotypic inconsistency was determined to be due to an integration of the donor vector backbone along with the repair donor template, with duplicated 5' homologous sequence at the 5' junction, although the 3' junction was precise and had no sequence duplication. This unexpected incorporation of the donor vector backbone at 5' junction was hypothesized to be mediated by cNHEJ repair mechanism, or cNHEJ together with MMEJ pathways, which could cause genomic compensation resulting in possible incomplete gene inactivating functionality of the pPRISM-Stop cassette, leading to inconsistent phenotypes found in *cyfip2* knockout homozygotes. Taken together, our study demonstrated efficient targeted integration at zebrafish *cyfip1* locus using CRISPR/Cas9 short homology targeted GeneWeld strategy and pPRISM-Stop-mediated gene inactivation. The pronounced

phenotypes uncovered in this study suggested the essential *in vivo* functions of *cyfip1* in the development of cardiovascular, hematopoietic, retinotectal, and spinal motor nervous systems. This is worth examining further to fully characterize the *in vivo* functions and identify the molecular mechanisms of *cyfip1*. Our study also suggested other possible DNA repair pathway choices in CRISPR/Cas-mediated genome editing, including cNHEJ and MMEJ, which we should also take into consideration when performing homology-based targeted integration at other gene loci to achieve high efficiency and precise genome editing outcome.

Results

The recently published short homology CRISPR/Cas9 knock in strategy, named GeneWeld, uses 24 or 48 base pairs of homologies to induce precise targeted integration of an exogenous DNA cassette to the sgRNA cleavage site through HDR[52,53]. The pPRISM-Stop repair donor vector was designed in accordance with the method described in GeneWeld strategy[52,53]. The pPRISM-Stop expression cassette contains two key functional units (Figure 1a). The first unit contains multiple stop codons serving to inactivate gene expression. The stop codons are right at the beginning of the pPRISM-Stop cassette (downstream to the flanking 5' homology arm sequence), followed by an ocean pout terminator and polyadenylation sequence. The second part is a secondary fluorescent marker expression cassette, consisting of a gamma crystallin (γ-cry) promoter, a mini-intron (for enhancing the expression of a secondary marker), a blue fluorescent protein (BFP) secondary reporter with a nuclear localization signal, and a bovine growth hormone and two SV40 polyadenylation/transcriptional termination sequences. The γ-cry promoter in the cassette drives lens-specific expression of BFP, which facilitates identification of mutant fishes by following their blue fluorescent eye lens. At each end of the pPRISM-Stop

cassette, there are type IIS restriction enzyme sites for cloning the 5’ and 3’ homology arms into the pPRISM-Stop targeting vector, which are BfuAI and BspQI, respectively. Flanking the 5’ and 3’ homology sequences, there are UsgRNA sequences for inducing DSBs of the repair donor vector (Figure 1a), liberating the homology arm *in vivo* and inducing the targeted integration of the repair pPRISM-Stop cassette through HMEJ pathway.

CRISPR/Cas9-Based GeneWeld Strategy Efficiently Generates *cyfip1*- and *cyfip2-pPRISM-Stop* Mutant Zebrafishes

To create pPRISM-Stop donor vector to generate either *cyfip1* or *cyfip2* knockout mutant zebrafish, we design ed a single guide RNA (sgRNA) targeting the first coding exon (exon 2) of either zebrafish *cyfip1* or *cyfip2* gene. The sgRNAs were verified via sgRNA mutagenesis efficiency test by injecting each of the sgRNA into one-cell zebrafish embryos along with Cas9 mRNA. The injected embryos were then analyzed to be checked for formation of insertions and deletions (indels) by gel electrophoresis of PCR amplification over the targeted exon. Next, according to the GeneWeld strategy for CRISPR/Cas9-based precise targeted integration, the repair templates to incorporate the pPRISM-Stop cassette into each targeted genome were designed and created by cloning the 24-base pair (bp) or 48-bp homology sequences (for *cyfip1* and *cyfip2*, respectively) flanking each verified sgRNA cleavage site into the pPRISM-Stop vector[52–54] (Figure 1a). These short homology arms flank the targeting pPRISM-Stop cassette and were used to induce integration of the repair template into the targeted genome through HMEJ mechanism of DNA double-strand break (DSB) repair[52–54] (Figure 1b). In addition to multiple stop codons residing in the pPRISM-Stop vector to mediate inactivation of the targeted gene, it also contains a BFP secondary marker expression cassette driven by an exogenous γ-cry

promotor. This secondary fluorescence served as a tracking marker for conveniently identifying the desired mutant alleles by following BFP expression specifically in the lens of developing zebrafish larvae (Figure 1b-d).

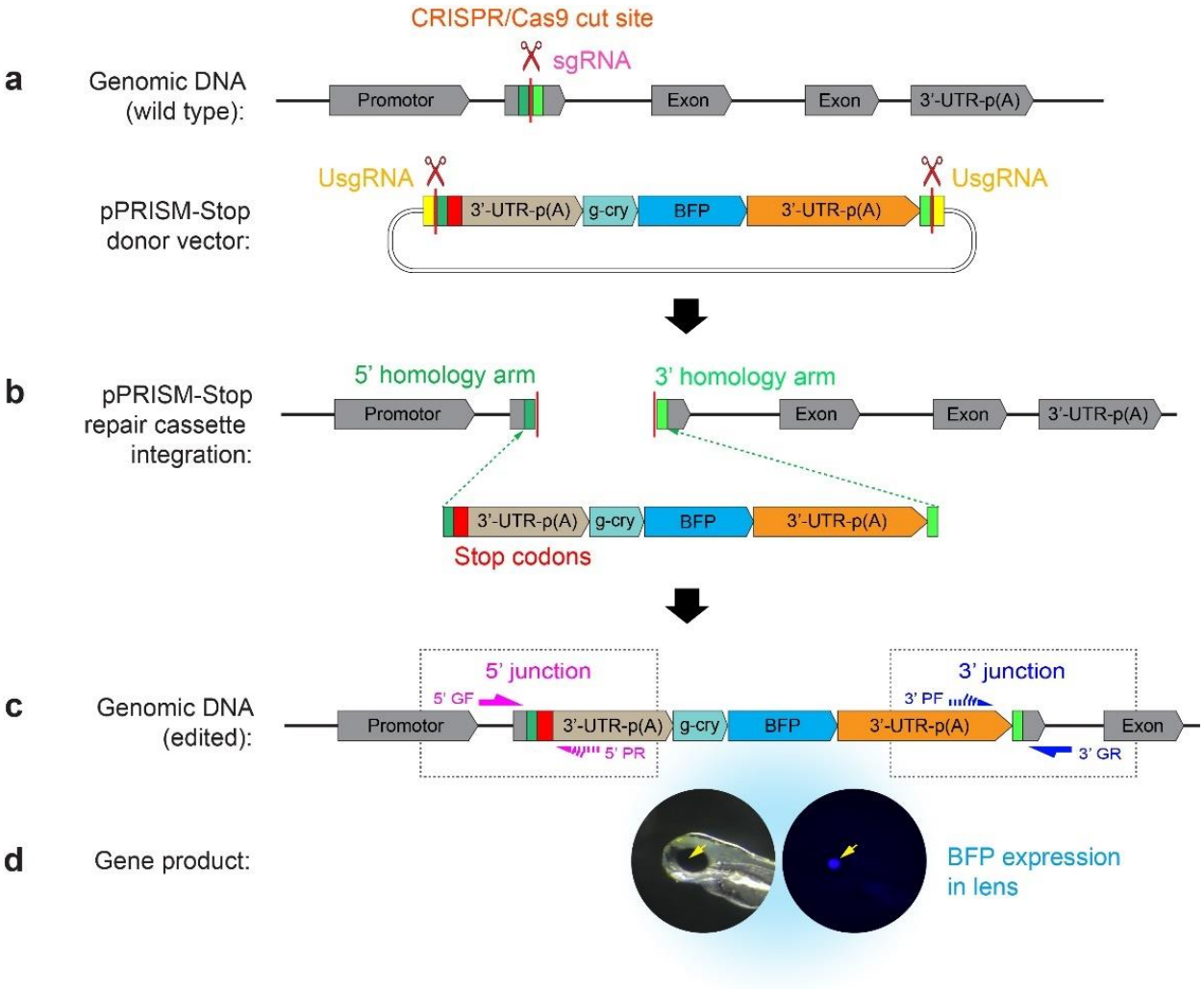

Figure 1. Schematic diagram of the GeneWeld strategy together with pPRISM-Stop method for targeted gene inactivation. (**a**) The genomic sgRNA (sgRNA) duplexed with Cas9 protein derived from mRNA (not shown here) induces a DSB of the targeted genomic DNA (red lines). Simultaneously, the Universal sgRNA (UsgRNA) also cleaves the pPRISM-Stop donor vector (2 cut sites) liberating the pPRISM-Stop cassette flanked with 24-bp or 48-bp 5' and 3' homology arms (dark and light green bars) which then are used to promote the pPRISM-Stop cassette integration into the genomic DSB site through HMEJ mechanism (b). (**b**) The major functional unit of the pPRISM-Stop repair cassette contains the stop codons followed by 3'-UTR-poly(A) sequence, a gamma-crystallin promotor, Tag BFP, and 3'-UTR-poly(A) sequence, which is flanked with 5' and 3' homology arms carrying DNA sequence

complementary to the genomic DNA sequence flanking the genomic sgRNA cleavage site. The pPRISM-Stop cassette serves to mediate gene inactivation and drive BFP expression specific in the eye lens. (**c**) Representative edited genomic DNA resulted from precise integration of pPRISM-Stop repair cassette into the targeted genomic DSB cleaved by the sgRNA designed, which ultimately gives rise to gene knockout with lens specific expression of BFP and no final gene-specific protein produced (d). The dotted box regions show the boundaries of 5' and 3' genome/vector junction for junction PCR analysis of the mutant. The 5' junction fragment PCR uses one 5' gene-specific forward primer (5' GF, magenta solid half-arrow) paired with one 5' pPRISM-specific reverse primer (5' PR, magenta striped half-arrow), and vice versa for the 3' junction fragment PCR. (**d**) An example of BFP expression in the lens (yellow arrow) of a *cyfip1* mutant zebrafish larva as a secondary marker arising from an integration of pPRISM-Stop cassette into the genome.

To establish *cyfip1* or *cyfip2* knockout mutant zebrafish, we performed microinjections of a solution containing the targeted sgRNA, universal sgRNA (UsgRNA), Cas9 mRNA, and the donor pPRISM-Stop vector carrying the 24- or 48-bp homology arms (for *cyfip1* and *cyfip2,* respectively), into one-cell zebrafish embryos. Cas9 mRNA is translated into Cas9 protein in the embryo and duplexes with either the UsgRNA or the targeted genomic sgRNA and induces DSBs at the UsgRNA site flanking the pPRISM-Stop donor vector and at the targeted genomic locus, respectively. The liberated repair template flanked by the short homology arms was integrated into the targeted genomic DNA at the double-strand break[52–54].

To identify the first generation of either cyfip1 or cyfip2 knockout mutant zebrafish, which was called F0 generation, we screened for the lens specific BFP secondary marker in the injected embryos starting at 3 days post fertilization (3 dpf). Due to the different degree of mosaicism in each lens, which possibly led to false-negative misinterpretation of the BFP expression especially at early embryonic stage, we rechecked the BFP expression in either lens at 4 to 5 dpf. The frequencies of somatic expression of BFP in the lens of cyfip1 and cyfip2 targeted F0s was at 86% and 69%, respectively (Table 1).

Table 1. Efficient recovery of *cyfip1* and *cyfip2* knockout mutant lines by CRISPR/Cas9- and GeneWeld-based pPRISM-Stop targeted integration

Genomic target	*cyfip1*	*cyfip2*
Targeted exon	2	2
Homology arm length (5'/3' HA; bp)	24/24	48/48
F0 larvae expressing secondary marker	86% (189/221)	69% (127/184)
F0 adults transmitting secondary marker	46% (11/24)	38% (6/16)
F0 adults transmitting on-target integration	13% (3/24)	13% (2/16)

The BFP-positive F0 larvae were then selected and raised to adulthood to be checked for germline transmission. At adult stage, each individual F0 was outcrossed to wild type WIK strain to test whether the animal was carrying cyfip allele through germline and transmitting it to their offspring, by using BFP expression at the lens after 2 dpf as an indicator to screen for (Figure 1b). We found that the frequencies of germline transmission of cyfip1 and cyfip2 were at 46% (11/24) and 38% (6/16), respectively (Table 1). The BFP-positive F1 larvae were then collected for PCR to be checked for precise integration at the targeted genomic cyfip loci by amplification over the 5' and 3' boundaries between the targeted genome and pPRISM-Stop cassette, as well as for DNA sequencing of the purified amplicons. This 5' and 3' junction fragment analysis was carried out by utilizing primer pairs that combine one primer located in the genome, upstream or downstream to the sgRNA cut site (for 5' or 3' junction, respectively) and outside the homology arms, and the other primer located within either end of the pPRISM-Stop cassette (Figures 1c). We found that the germline transmission rates of on-target integration were 13% for both *cyfip1*

(3/24) and *cyfip2* (2/16) loci (Table 1). Several BFP-positive F1 larvae from single F0 showing precise integration from PCR for junction analysis were selected and raised to adulthood.

Next, individual adult F1s were fin clipped for genotyping via junction fragment analysis to identify an F1 allele carrying precise pPRISM-Stop cassette integration. Once confirmed, the verified F1 allele for either *cyfip* was then used to outcross to various transgenic lines to establish either *cyfip1* or *cyfip2* knockout stable F2 generations with different transgenic background fluorescently marking specific cell populations in various biological systems. These transgenic zebrafish lines used for outcrossing included *Tg(ath5:GFP)* (retinotectal system)[73–75], *Tg(mnx1:GFP)* (spinal motor nervous system)[76–79], *Tg(fli1:EGFP)^{y1}; Tg(gata1:DsRed)^{sd}* (cardiovascular system)[80–82], and *Tg(cd41:GFP)* (hematopoietic stem and progenitor cells)[83-88]. Of note, since the complete abolishment of either *cyfip* is embryonically lethal, *cyfip1* and *cyfip2* F2 transgenes, as well as all F1 generations, were raised as heterozygotes. Taken together, these results demonstrated an efficient strategy for precise targeted integration of pPRISM-Stop cassette by CRISPR/Cas9- and the short homology-mediated GeneWeld method to establish *cyfip1* and *cyfip2* knockout mutants in zebrafish.

Precise Targeted Integration of pPRISM-Stop Donor Cassette into *cyfip1* Locus Results in Phenotypes in the Zebrafish Retinotectal System

To characterize *cyfip1* loss-of-function phenotypes resulting from integration of the pPRISM-Stop cassette at *cyfip1* locus, we incrossed *cyfip1* F2 heterozygous adults carrying the transgenic *Tg(ath5:GFP)*[73–75] to investigate the phenotypes in retinal ganglion cells (RGCs) and their projections which were fluorescently labeled with GFP. We noticed the proportion of lens specific BFP-expressed F3 larvae as approximately 75%. More intriguingly, around one third of

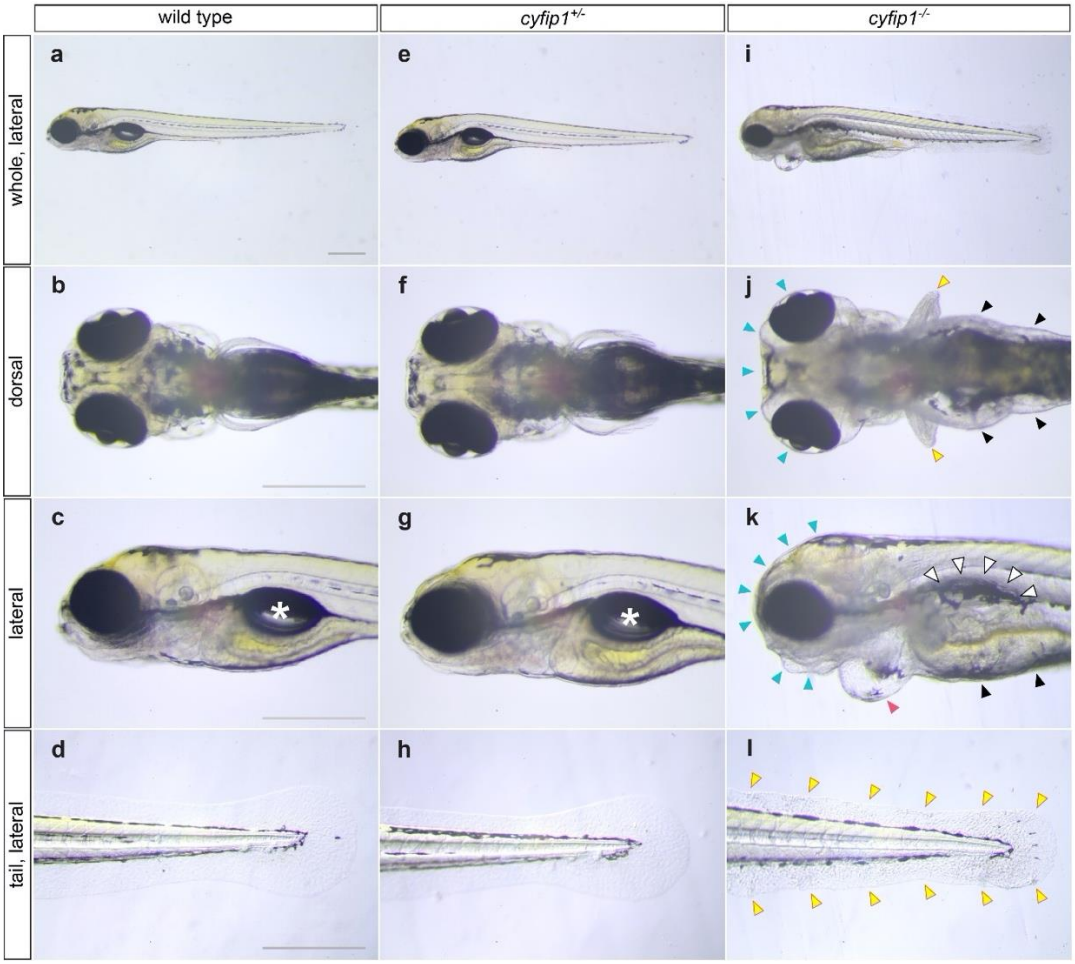

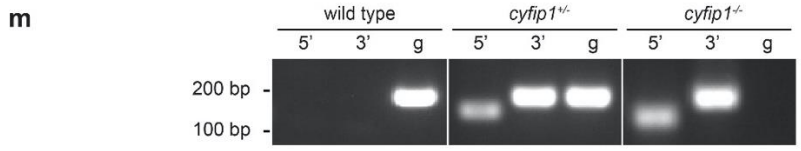

n

5′ junctions

	cyfip1 — 5' homology arm — vector
Precise junction	GGAGGAGCTGCCACTTCCAGATCAGCAGCCCTGCCTTCTATAAT
F0#8, F1#2	GGAGGAGCTGCCACTTCCAGATCAGCAGCCCTGCCTTCTATAAT
F0#8, F1#7	GGAGGAGCTGCCACTTCCAGATCAGCAGCCCTGCCTTCTATAAT
F0#8, F1#9	GGAGGAGCTGCCACTTCCAGATCAGCAGCCCTGCCTTCTATAAT

3′ junctions

	vector — 3′ homology arm — cyfip1
Precise junction	AGCAAGGAAGATCGAGCCTCTGCCCTCCTCACTCATTTACCAGG
F0#8, F1#2	AGCAAGGAAGATCGAGCCTCTGCCCTCCTCACTCGAGCCTCTGCCCTCCTCACTCATTTACCAGG
F0#8, F1#7	AGCAAGGAAGATCGAGCCTCTGCCCTCCTCACTCGAGCCTCTGCCCTCCTCACTCATTTACCAGG
F0#8, F1#9	AGCAAGGAAGATCGAGCCTCTGCCCTCCTCACTCGAGCCTCTGCCCTCCTCACTCATTTACCAGG

Figure 2. Morphological phenotypes and genotypic analysis of *cyfip1* knockout mutants. (**a-l**) Bright field images in dorsal and lateral views of wild type (**a-d**), *cyfip1* knockout heterozygous (**e-h**), and *cyfip1*

knockout homozygous (**i-l**) F3 larvae at 5 dpf. (**e-h**) *cyfip1*$^{+/-}$ mutant showed similar morphology to wild type. (**i-l**) *cyfip1*$^{-/-}$ mutant exhibited several gross phenotypes, consisting of abnormalities of the head (including an enlarged head with edema, distant eyes, and irregular mouth and jaw shape, as indicated with cyan arrow heads; in j and k), rough-surfaced pectoral and tail fins (yellow arrow heads; in j and l), enlarged heart (pink arrow head; in k), abdominal distention (black arrow head; in j and k), and loss of swim bladder (white arrow head; in k). Normal swim bladders were present in wild type and *cyfip1*$^{+/-}$ larvae (white asterisk; in c and g). Scale bar = 500 um. (**m**) Genotypic analysis of *cyfip1* mutant by PCR amplification over 5' junction (5'), 3' junction (3'), and original non-edited genomic DNA (g), with the expected PCR amplicons to be 139 bp, 183 bp, and 184 bp, respectively. (**n**) Sanger sequencing of 5' and 3' junction fragments of *cyfip1*$^{+/-}$ F1s from the founder F0#8, aligned to the expected precise junctions from pPRISM-Stop cassette integration, to select for an F1 to outcross with various transgenic lines.

those BFP-expressing larvae, or approximately 25% of the population, exhibited several apparent gross morphological phenotypes. These consisted of an enlarged head with edema, distant eyes, abnormal mouth and jaw shape, irregular (rough-surfaced) pectoral and tail fins, enlarged heart with slow or weak heartbeat, disrupted circulation in multiple blood vessels (including dorsal artery, posterior cardinal vein, caudal vein, and intersegmental vessels), abdominal distention, loss of swim bladder, and delayed or less pigmentation. (Figure 2a-l). These potential homozygotes displaying morphological defects were usually unable to survive after 4 to 5 dpf. Mutant larvae were confirmed to be homozygous for the *cyfip1* allele by junction fragment analysis, although there was a duplication of short homologous sequence at 3' junction (Figure 2m-n), which was likely mediated by MMEJ DSB repair. With these consistent, reproducible, and obvious gross phenotypes, we then used these phenotypic abnormalities to preliminarily segregate the *cyfip1* knockout homozygous mutants from the heterozygous and the wild type animals.

Next, we explored phenotypes of *cyfip1* homozygous mutant larvae carrying the transgenic *Tg(ath5:GFP)*[73–75] which labels the RGCs with GFP by using live confocal imaging. Normally, most RGC axons project to the contralateral optic tectum, which is the primary visual

center in fish[55–57]. The RGCs differentiate in the basal-most cell layer of the retina and grow an axon from their basal pole[58]. The RGC axons project to the optic nerve head in central retina and exit the eye. They then fasciculate to form the optic nerve stalk (which becomes the optic nerve later) and grow toward the midline. There, they cross the ventral midline of the forebrain at the optic chiasm and become the optic tract. They then turn dorsocaudally and project toward the contralateral optic tectum in the dorsal midbrain, where they branch extensively terminating topographically at their synaptic targets according to their original location in the retina[55–57,59].

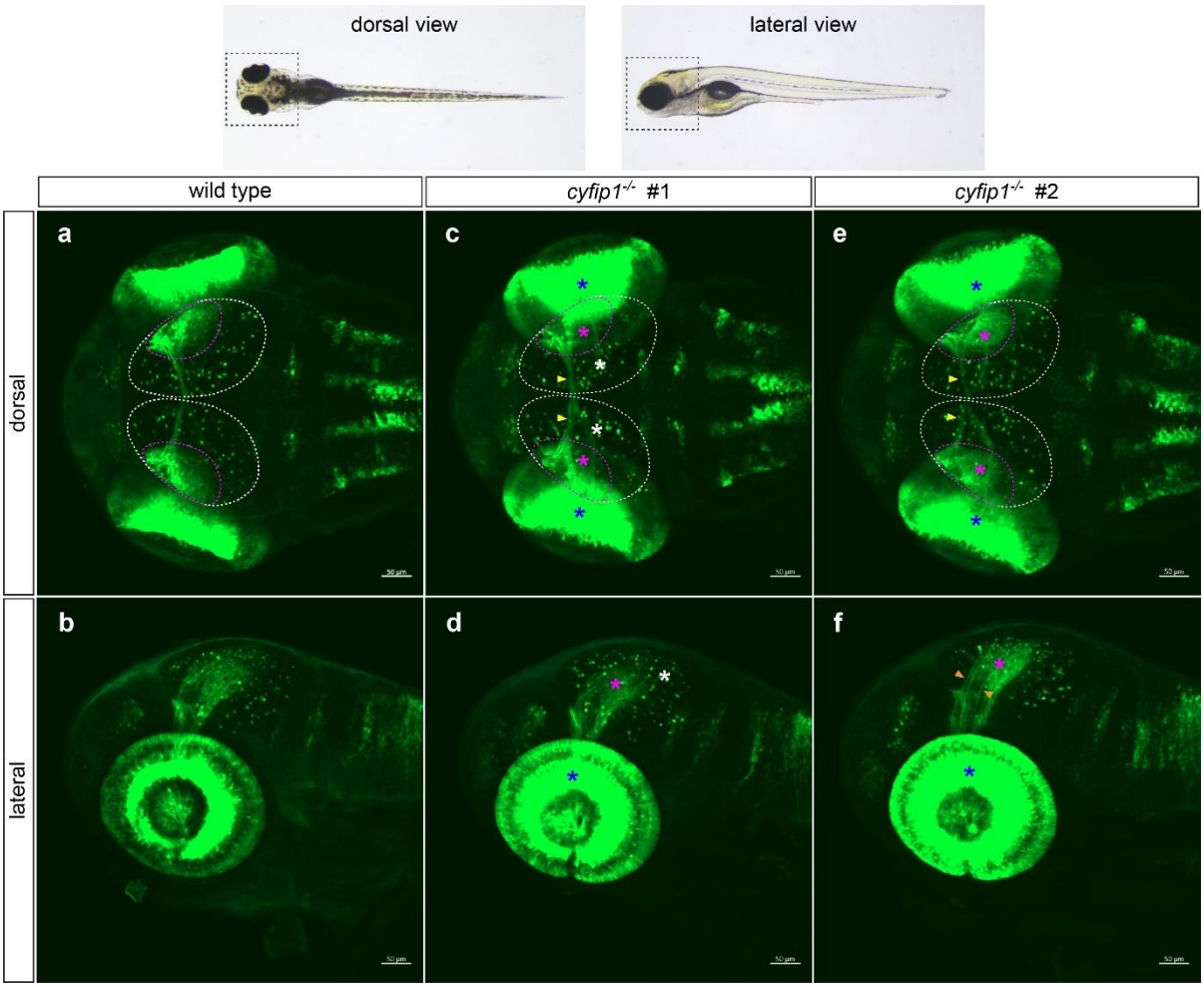

Figure 3. Microscopic phenotypes in the retinotectal system of *cyfip1* knockout mutants at 3 dpf. Bright field images on the top panel show the dotted boxes indicating the areas where the confocal images

were taken in the dorsal and lateral views. (**a-f**) Confocal images in dorsal and lateral views of wild type (**a,b**) and two *cyfip1* knockout homozygous (**c-f**) F3 larvae in transgenic *Tg(ath5:GFP)* line primarily marking RGCs with GFP. In the dorsal view (a, c, e), the areas in magenta dotted circle represent left and right optic tecta. White dotted lines encircle the areas where GFP-positive periventricular interneurons reside in. (**c-f**) *cyfip1*$^{-/-}$ mutant exhibited several abnormal phenotypes, including increased GFP-positive area and increased GFP intensity of both retinae (as indicated with blue asterisks), less organized fasciculation of the optic tracts (yellow arrow heads in c and e), reduced size of tectal neuropil (the area inside magenta dotted circles which is marked with magenta asterisks in c-f), reduced number of periventricular interneurons surrounding each tectal neuropil (in the areas marked white asterisks in c and d), and aberrant retinotectal axon branching (orange arrow heads in f). Scale bar = 50 um.

Our results showed that *cyfip1*$^{-/-}$ mutants exhibited multiple phenotypes at 3 dpf, including increased number of GFP-positive RGCs (increased GFP-positive area and probably increased GFP intensity) of both retinae, aberrant retinotectal axon branching and less organized fasciculation of the optic tracts. Interestingly, we also noticed a reduced size or volume of retinotectal neuropil and reduced number of periventricular interneurons surrounding the neuropil of each optic tectum (Figure 3a-f).

Unexpected Integration of pPRISM Stop Donor Vector Backbone in Zebrafish Targeted *cyfip2* Gene Locus with the Resulting Inconsistent Phenotypes

In parallel with *cyfip1* gene, we also tested the functionality of pPRISM-Stop vector, as well as investigated whether the pPRISM-Stop cassette was incorporated effectively and precisely into another targeted gene locus, *cyfip2*, using similar methods. Again, we incrossed *cyfip2* F2 heterozygous adults carrying the transgenic *Tg(ath5:GFP)*[73–75] to examine the phenotypes in the retinotectal system. In addition to this, while we raised the transgenic *cyfip2*$^{+/-}$ F2s to adulthood, we mated the verified *cyfip2*$^{+/-}$ F1s to begin exploring morphological defects and phenotypes in RGC axonal tracts of *cyfip2* mutant F2 larvae by immunostaining the whole larvae with anti-acetylated tubulin antibodies.

Intriguingly, in contrast to *cyfip1*$^{-/-}$ knockout mutants, the *cyfip2*$^{-/-}$ knockout mutants exhibited subtle gross defects. The *cyfip2*$^{-/-}$ mutant appeared relatively normal compared to the wild type siblings, except that they lacked the swim bladder, even after 6 to 7 dpf when the swim bladder should have fully developed (Figure 4a-d). Despite of such mild morphological

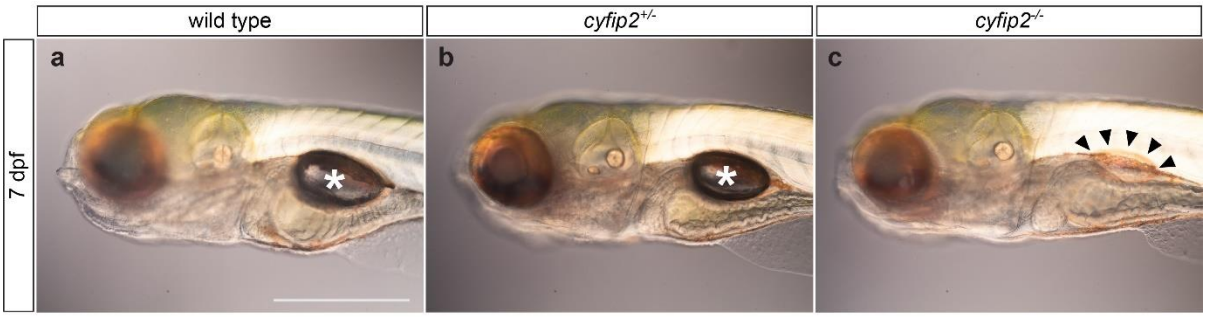

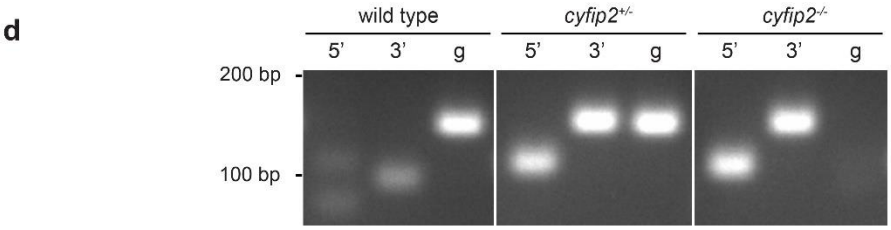

e

5′ junctions

	cyfip2 — 5′ homology arm — vector
Precise junction	AGTGAACCTGTGTCGCCATGACAACCCACGTGACCCTGGAGGATGCGCTGTCCAatCTTCTA
F0#5, F1#9	AGTGAACCTGTGTCGCCATGACAACCCACGTGACCCTGGAGGATGCGCTGTCCAatCTTCTA
F0#6, F1#6	AGTGAACCTGTGTCGCCATGACAACCCACGTGACCCTGGAGGATGCGCTGTCCAatCTTCTA

3′ junctions

	vector — 3′ homology arm — cyfip2
Precise junction	AGGAAGATGTGGACCTGCTGGAGGAGCTTCCTCTCCCAGACCAGCAGCCATGCATCGAGC
F0#5, F1#9	AGGAAGATGTGGACCTGCTGGAGGAGCTTCCTCTCCCAGACCAGCAGCCATGCATCGAGC
F0#6, F1#6	AGGAAGATGTGGACCTGCTGGAGGAGCTTCCTCTCCCAGACCAGCAGCCATGCATCGAGC

Figure 4. Morphological phenotypes and genotypic analysis of *cyfip2* knockout mutants. (**a-c**) Differential Interference Contrast (DIC) microscopic images in lateral views of wild type (**a**), *cyfip2* knockout heterozygous (**b**), and *cyfip2* knockout homozygous (**c**) F2 larvae at 7 dpf. The swim bladders are indicated with white asterisks, in which is absent in *cyfip2*$^{-/-}$ (area indicated with black arrow heads in c). Scale bar = 500 um. (**d**) Genotypic analysis of *cyfip2* mutant by PCR amplification over 5' junction (5'), 3' junction (3'), and original non-edited genomic DNA (g), with the expected PCR amplicons to be 117 bp, 152 bp, and 150 bp, respectively. (**e**) Sanger sequencing of 5' and 3' junction fragments of

cyfip2$^{+/-}$ F1s from two different founder F0#5 and F0#6, aligned to the expected precise junctions from pPRISM-Stop cassette integration, to select for an F1 to outcross with various transgenic lines.

phenotype found, inspiringly, our preliminary results showed multiple very interesting microscopic defects in the retinotectal system of *cyfip2*$^{-/-}$ mutant starting at 2 dpf, including decreased number of GFP-positive RGCs (decreased GFP-positive area) of both retinae, aberrant retinotectal axon branching, as well as thinner and less dense fasciculation of the optic nerves and tracts (Figure 5a and 5f). In addition, there appeared to be reduced size or volume of retinotectal neuropils and reduced number of cells in various brain regions, including olfactory bulbs, habenulae, retinae, tectal periventricular interneurons surrounding the neuropil, cerebellum, and medulla oblongata (Figure 5a and 5f). Along with these, at 4 dpf, there were likely to be decreased number of intertectal fascicles and commissures, tectal projections, cerebellar fibers, and medulla oblongata fibers (Figure 5c and 5h). Nevertheless, the *cyfip2*$^{+/-}$ mutants appeared to be relatively normal both morphologically and microscopically compared to their wild type siblings, at least in the retinotectal system we have explored (Figure 5b-e). We, thus, did not attempt to further investigate or quantify any additional abnormalities of those *cyfip2* heterozygotes in this biological system.

More fascinatingly, we uncovered unique phenotypes of one of the *cyfip2*$^{-/-}$ mutants at 3 dpf showing a smaller head and incorrect axon branching and pathfinding of the optic tracts (Figure 5b and 5g). Instead of projecting dorsocaudally to terminate at their retinotopographic targets in the contralateral optic tectal hemispheres, each affected optic tract projected craniodorsally in the opposite direction toward its contralateral habenula. This phenotype was

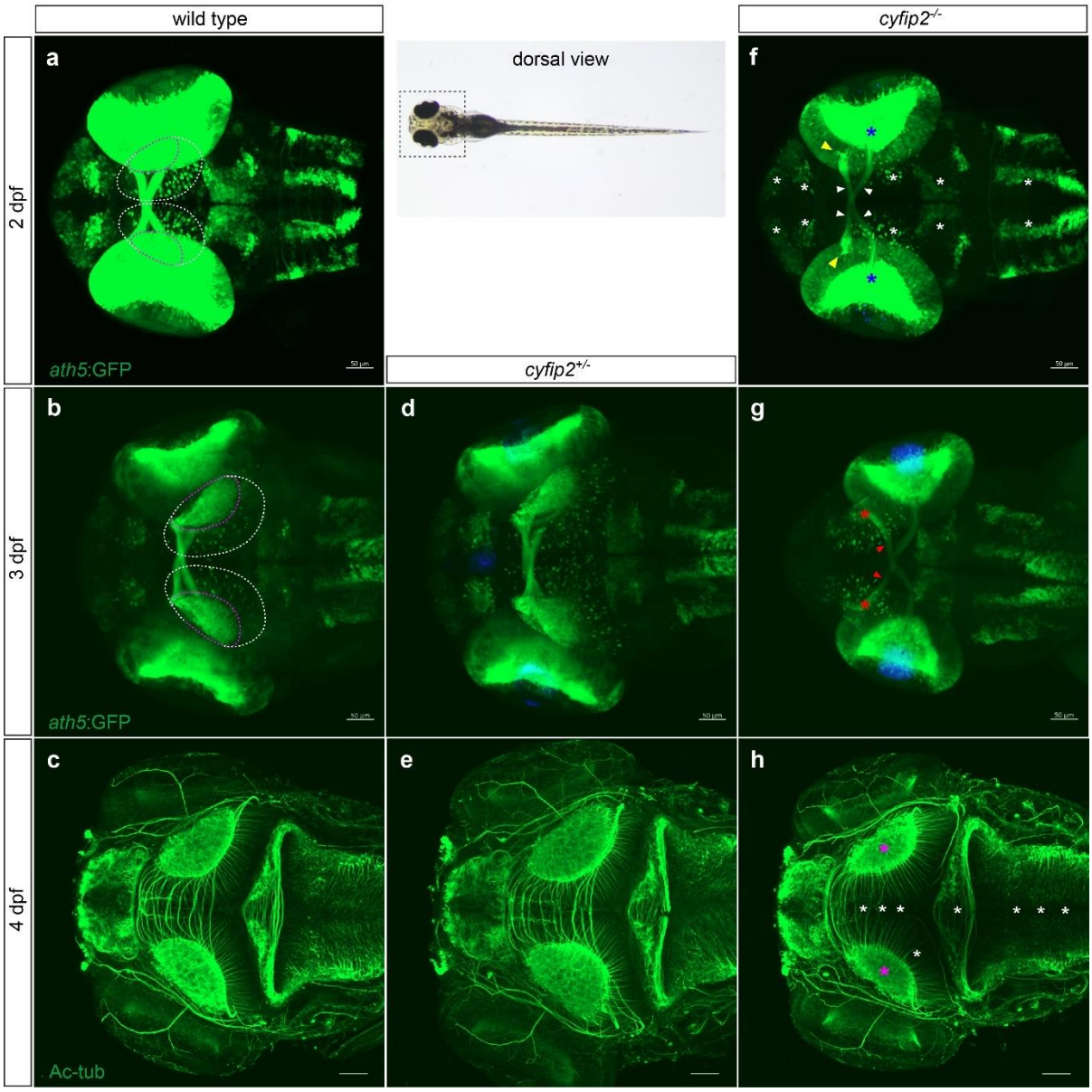

Figure 5. Microscopic phenotypes in the retinotectal system of *cyfip2* knockout mutants at three different stages. A bright field image on the top middle panel shows the dotted boxes indicating the area where the confocal images were taken in the dorsal view. The confocal images were taken at 2 dpf, 3 dpf, and 4 dpf in wild type (**a-c**), *cyfip2* knockout heterozygous (**d, e**), and *cyfip2* knockout homozygous (**g-h**) larvae carrying the transgenic *Tg(ath5:GFP)* primarily marking RGCs with GFP, and in larvae with axonal tracts immunostained with anti-acetylated tubulin antibodies (Ac-tub; at 4 dpf in c, e, h). The areas in magenta dotted circle (a, b) represent left and right optic tecta. White dotted lines encircle the areas where GFP-positive periventricular interneurons reside in. (**d,e**) *cyfip2*$^{+/-}$ mutant at 3 dpf and 4 dpf showed relatively similar phenotypes compared to the wild type (*cyfip2*$^{+/-}$ mutant at 2 dpf is not shown here). (**f-h**) *cyfip2*$^{-/-}$ mutant exhibited several defective phenotypes. (**f**) At 2 dpf, there were decreased GFP-positive area of both retinae (blue asterisk), aberrant retinotectal axon branching (yellow arrow heads), thinner and less dense fasciculation of the optic nerves and tracts (white arrow heads), and

reduced number of cells in various brain regions, including olfactory bulbs, habenulae, retinae, tectal periventricular interneurons surrounding the neuropil, cerebellum, and medulla oblongata (white asterisks). (**g**) At 3 dpf, one *cyfip2*$^{-/-}$ mutant displayed defects, which included a smaller head and incorrect axon branching and pathfinding of the optic tracts which mismigrate craniodorsally toward its contralateral habenula (red arrow heads and asterisks). (**h**) At 4 dpf, the *cyfip2*$^{-/-}$ mutant showed reduced size of tectal neuropils (magenta asterisks), likely decreased number of intertectal fascicles and commissures, tectal projections, cerebellar fibers, and medulla oblongata fibers (white asterisks). Scale bar = 50 um.

one of the most attractive defects we discovered. However, we were not able to reproduce the *cyfip2*$^{-/-}$ mutants with this type of defects again at any developmental stages. Additionally, we noticed inconsistency in the degree of severity of the phenotypes in the retinotectal system among all *cyfip2*$^{-/-}$ mutants we have studied (Figure 6a-f). We, therefore, attempted to find the reason behind the inconsistent phenotypes, including optimizing the PCR protocol and primers for junction fragment analysis using several different methods, and re-analyze the genotype of the *cyfip2*$^{+/-}$ F1 and F2 alleles we obtained. We uncovered that the *cyfip2*$^{+/-}$ F1s and F2s from two different F0 founders, which we used to outcross to establish transgenic *cyfip2*$^{+/-}$ F2s to study, carried not only the desired pPRISM-Stop cassette serving to inactivate the gene function through premature stop codons, but also the pPRISM-Stop vector backbone along with partial duplication of the 5' homology arm at 5' genome/vector junction (Figure 6i-k). Although the 3' vector/genome junction was as expected and the integration occurred at the targeted *cyfip2* locus (Figure 6i-k), the incorporation of the pPRISM-Stop vector backbone into the genome could cause genomic compensation resulting in possible incomplete functioning of the pPRISM-Stop cassette, as well as the inconsistent phenotypes displayed in *cyfip2*$^{-/-}$ mutants. Taken together, these results suggested possible variation in the alleles obtained using homology-based DSB repair mechanisms induced by CRISPR/Cas9 system for zebrafish genome editing.

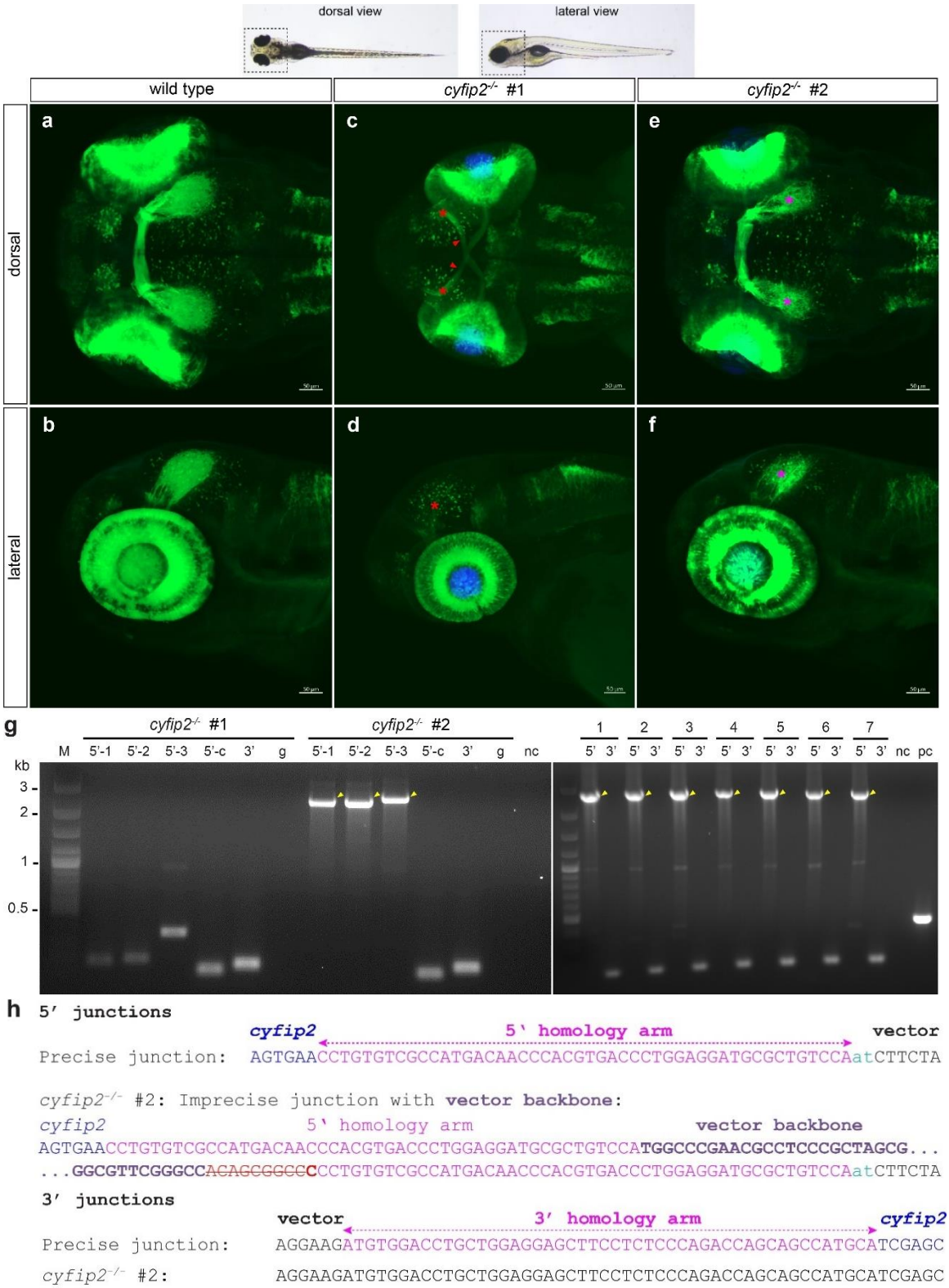

Figure 6. Inconsistent phenotypes of in the retinotectal system of *cyfip2* knockout mutants at 3 dpf and their genotypic analysis revealed imprecise integration of pPRISM-Stop vector backbone

incorporated. Bright field images on the top panel show the dotted boxes indicating the areas where the confocal images were taken in the dorsal and lateral views. The confocal images were taken at 2 dpf in wild type (**a, b**), *cyfip2*$^{-/-}$ mutant #1 (**c, d**), and *cyfip2*$^{-/-}$ mutant #2 (**e, f**) carrying the transgenic *Tg(ath5:GFP)* primarily marking RGCs with GFP. (**c, d**) The unique axon branching and pathfinding phenotypes of *cyfip2*$^{-/-}$ mutant #1 was shown earlier in Figure 5g (red arrow heads and asterisks). (**e, f**) *cyfip2*$^{-/-}$ mutant #2 and the majority of other *cyfip2*$^{-/-}$ mutants exhibited milder defects or relatively similar phenotypes to the wild type. (**g**) Left agarose gel image showed large PCR amplicons at approximately 2.5 kb from 3 different primer pair for amplifying 5' junction fragment (yellow arrow heads) in *cyfip2*$^{-/-}$ mutant #2, but not in mutant #1. The right agarose gel image showed 5' and 3' junction PCR from seven different F2 adults (1 to 7) whose 5' junctions also contained similarly large PCR bands. 5'-1 to 5'-c: four different primer pairs (including one control primer pair) to verify 5' junction fragment (the expected length for the four 5' junction primer pairs are 165, 178, 343, and 117 bp, respectively), 3': a primer pair used to amplify 3' junction fragment (152 bp), g: primer pair for amplifying the original non-edited genomic DNA sequence (150 bp), nc: negative control, pc: positive control, kb: kilobases, M: DNA reference marker. (**h**) Sanger sequencing of 5' and 3' junction fragments of *cyfip2*$^{-/-}$ mutant #2, aligned to the expected precise junctions from pPRISM-Stop cassette integration. The sequencing result revealed unexpected integration of pPRISM-Stop vector backbone at 5' junction. The unexpected integration of vector backbone is represented in purple letters. Lower case letters in green indicate additional nucleotides added to make the homology sequence of the repair template in-frame with the coding sequence. Upper case crossed letters in red represent the missing nucleotides after DSB repair. Upper case bold letter in red (one C letter) represents the extra nucleotide inserted.

Homozygous Mutants of *cyfip1* Have Defective Phenotypes in the Cardiovascular System, Hematopoietic Stem and Progenitor Cells, and Spinal Motor Nervous System in Zebrafish

Due to the imprecise integration of pPRISM-Stop cassette along with its vector backbone into *cyfip2* targeted locus, which likely gave rise to variable penetrance and incomplete gene inactivating functionality of pPRISM-Stop cassette resulting in inconsistent and non-reproducible phenotypes, we focused on characterizing the phenotypes of *cyfip1* loss-of-function mutant during zebrafish embryogenesis in three systems: the cardiovascular, hematopoietic, and spinal motor nervous systems.

To analyze the phenotypes of *cyfip1*$^{-/-}$ mutants in the cardiovascular system, we incrossed *cyfip1* F2 heterozygous adults carrying the transgenic *Tg(fli1:EGFP)*^{y1}*; Tg(gata1:DsRed)*^{sd} in the background[80–82] to examine the patterning of endothelial cells and circulation of red blood cells. Based on the marked morphological phenotypes we observed before, we segregated the potential

cyfip1$^{-/-}$ mutants based on phenotype before validating their genotypes by 5' and 3' junction fragment analysis. Morphologically, the *cyfip1*$^{-/-}$ mutants exhibited several abnormalities in the cardiovascular system, consisting of an enlarged heart with a slow or weak heartbeat, disrupted circulation in multiple blood vessels including dorsal aorta (DA), posterior cardinal vein (PCV), caudal vein (CV), and intersegmental vessels (ISVs). We also investigated the phenotypes via confocal live imaging. Normally, by 3 dpf, the zebrafish embryo develops a complete and functional blood circulatory loop starting from the regularly beating heart, along with fully lumenized DA, PCV, CV, DLAV, and ISVs (interconnecting and transferring blood between DA and DLAV), to distribute blood throughout the body (Figure 7a). Intriguingly, at 4 dpf, the *cyfip1*$^{-/-}$ mutants exhibited several marked abnormalities (Figure d-e, yellow arrow heads), consisting of stenotic or collapsed ISVs and DLAV with disrupted and reduced blood flow inside their lumen, delayed or stalled development of ISVs, mismigration of endothelial cells lining some ISVs, reduced diameter of DA, less organized or unsmoothed vascular wall of PCV, as well as reduced caudal vein plexus (CVP; Figure 7d, blue asterisks) and decreased area of caudal hematopoietic tissue (CHT) between DA and CV (Figure 7e, magenta asterisks).

We explored the consequences from *cyfip1* homozygous deletion in the hematopoietic system, particularly in the emergence and early development of Hematopoietic Stem and Progenitor Cells (HSPCs). We incrossed *cyfip1* F2 heterozygous adults carrying the transgenic *Tg(cd41:GFP)*[83-88] to generate *cyfip1* knockout homozygotes. Based on the marked morphological phenotypes we observed before of *cyfip1*$^{-/-}$ gross phenotypes, we segregated the potential *cyfip1*$^{-/-}$ mutants for further investigation and live confocal imaging prior to confirming their genotypes by junction fragment analysis. Normally, at around 30-36 hpf, the HSPCs start

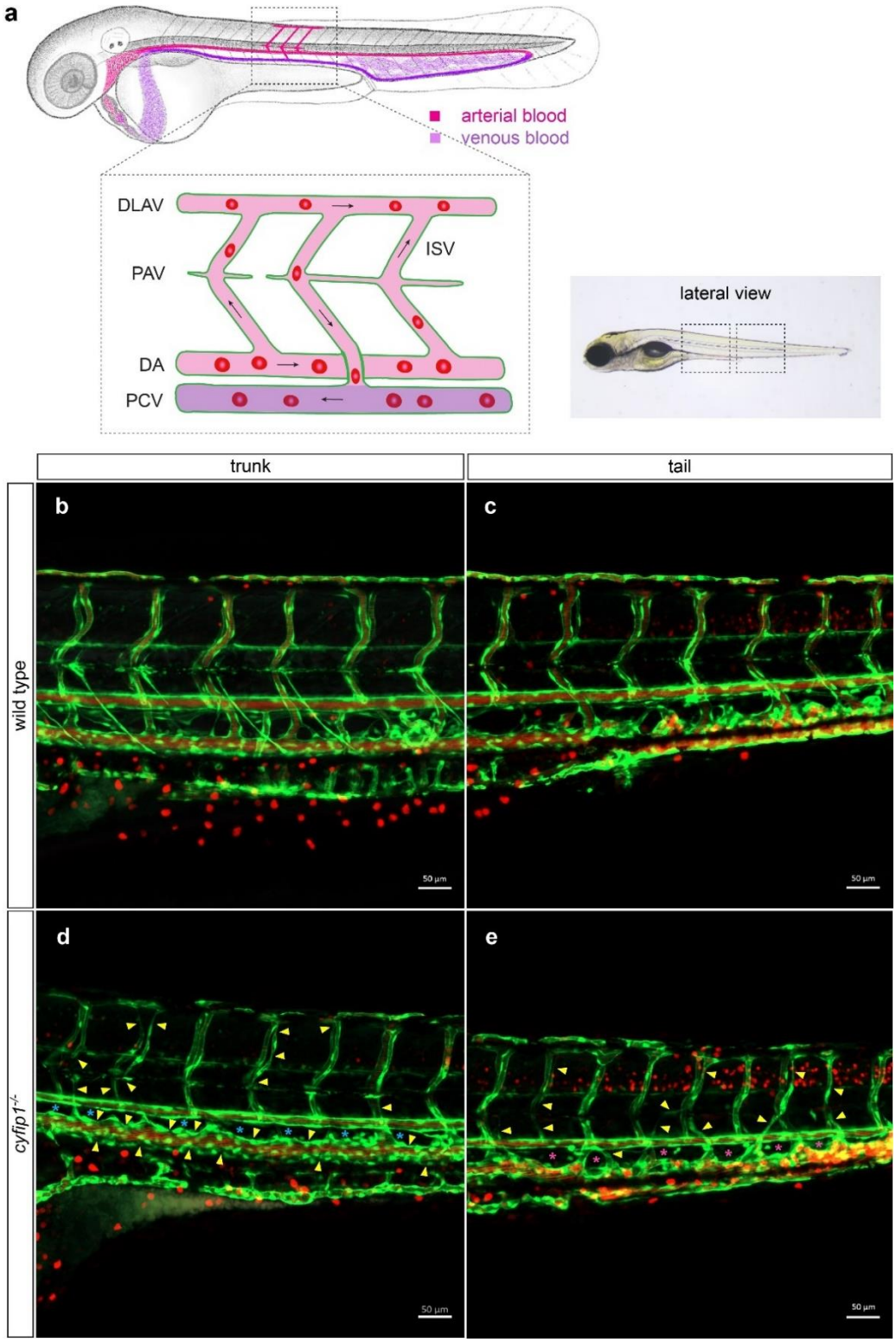

Figure 7. *cyfip1* knockout homozygous mutants display cardiovascular defects at 4 dpf. A bright field image on the top right shows the dotted boxes indicating the areas where the confocal images were

taken in lateral view of the trunk and tail sections. (**a**) Schematic illustration showing the normal complete cardiovascular system in developing zebrafish embryo. The diagram focuses only on the main blood vessels in trunk area (lateral view), as indicated in the dotted box. Arterial and venous blood circulation are represented in pink and purple color, respectively, with red blood cells circulating inside. The direction of blood flow is indicated by the arrows. DLAV: dorsal longitudinal anastomotic vessel, PAV: parachordal vessels, DA: dorsal aorta, PCV: posterior cardinal vein, ISV: intersegmental vessel. (**b-e**) Confocal images in lateral view of the trunk and tail areas in wild type (**b, c**) and *cyfip1*$^{-/-}$ mutant larva (**d, e**) in transgenic *Tg(fli1:EGFP)*^{y1}*; Tg(gata1:DsRed)*^{sd} lines, marking vascular endothelial cells in green and red blood cells in red. (**d, e**) The abnormal phenotypes of *cyfip1*$^{-/-}$ mutant are indicated with yellow arrow heads, including stenotic or collapsed ISVs, disrupted and reduced blood flow in ISVs, delayed or stalled development of ISVs, mismigration of ISV endothelial cells, smaller diameter of DA, less organized PCV vascular wall, reduced caudal vein plexus (CVP), as well as decreased area of an aorta-gonad-mesonephros (AGM) region and caudal hematopoietic tissue (CHT) underneath DA (blue and magenta asterisks in d and e, respectively). Scale bar = 50 um.

emerging in the AGM region (Figure 8a-b). They then migrate to the CHT and eventually seed in the thymus and kidney after 3-4 dpf. Interestingly, at 5 dpf, the *cyfip1*$^{-/-}$ mutants exhibited multiple defects, including loss of, or delay in HSPC homing in thymus and kidney (Figure 8h), as well as a reduction in number of HSPCs in AGM (Figure 8j, blue arrow heads) and CHT (Figure 8k-l, yellow arrow heads).

Lastly, we investigated the phenotypes of *cyfip1*$^{-/-}$ mutants in the spinal motor neurons in the nervous system, specifically the three major spinal nerve branches which are the rostral, dorsal, and ventral branches. We incrossed *cyfip1* F2 heterozygous adults carrying the transgenic *Tg(mnx1:GFP)*[76–79], and identified the potential *cyfip1*$^{-/-}$ mutants to study before validating their genotypes by junction fragment analysis. Normally, in the developing zebrafish embryo, there are three major primary motor neuron projections arising from the rostral (RoP), middle (MiP), and caudal (CaP) primary motor neurons residing in the spinal cord: rostral, dorsal, and ventral nerve branches, respectively. These three major nerve branches project toward their target to innervate the medial, dorsal, and ventral myotome, respectively (Figure 9a). At 4 dpf, *cyfip1*$^{-/-}$

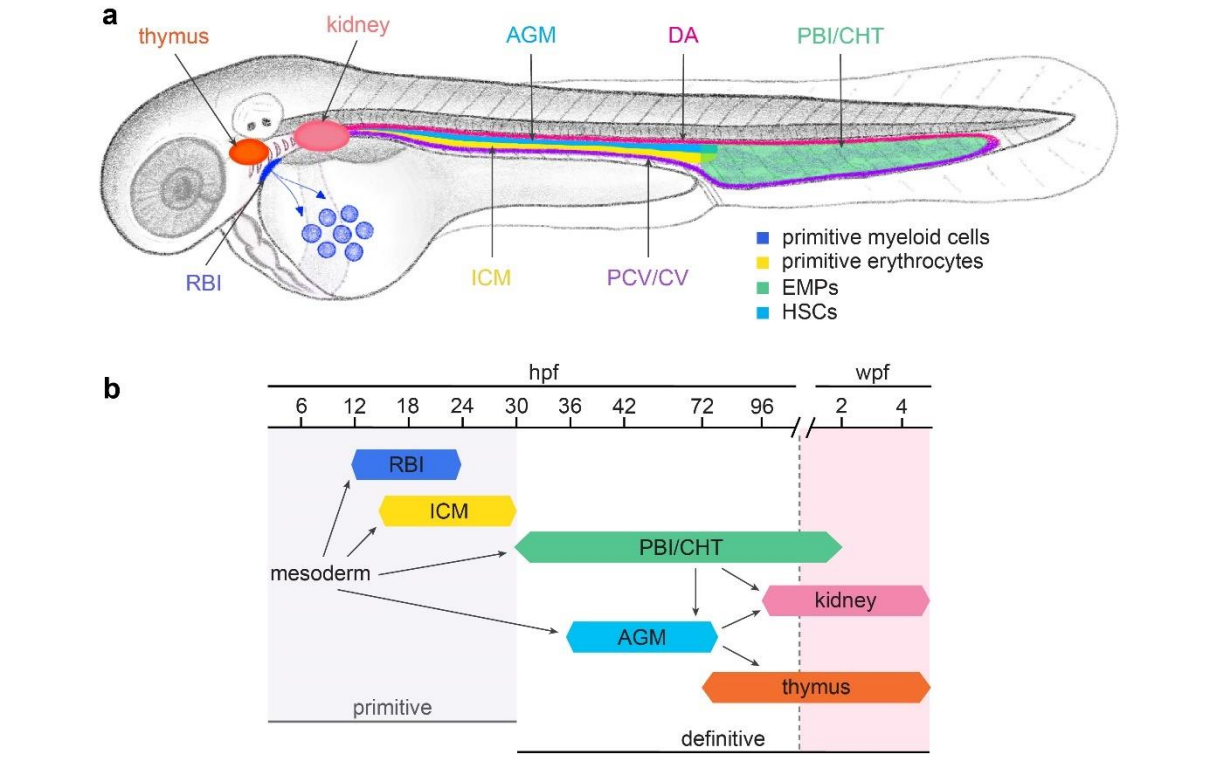

Figure 8. Phenotypes in early development of hematopoietic system and Hematopoietic Stem and Progenitor Cells (HSPCs) of *cyfip1* knockout homozygous mutants at 5 dpf. (**a, b**) Illustrative drawing and diagram representing embryonic hematopoiesis in zebrafish. (**a**) Anatomical locations (lateral view) of each independent phase of primitive and definitive hematopoiesis to produce various precursor cells. First, primitive myeloid cells originate in the RBI, migrate onto the yolk ball (dark blue spots), and then spread throughout the body. Next, primitive erythrocytes develop in the ICM (yellow). The first stage of definitive hematopoiesis begins slightly later with the production of EMPs, which develop in the PBI (green). Then, HSCs emerge in the AGM region (blue), migrate to the CHT (green),

and ultimately seed in the thymus and kidney (orange and pink, respectively). (**b**) Timing of zebrafish hematopoietic development during the primitive and definitive waves, which are both derived from the lateral plate mesoderm. Anatomical locations in (a) and timing of hematopoietic development in (b) are color matched. RBI: rostral blood island, AGM: aorta-gonad-mesonephros region, ICM: intermediate cell mass, PBI: posterior blood island, CHT: caudal hematopoietic tissue, EMPs: erythromyeloid progenitors, HSCs: hematopoietic stem cells, hpf: hours post fertilization, wpf: weeks post fertilization. (**c-l**) Confocal images in lateral view of each compartment from head to tail in wild type (**c-g**) and *cyfip1*$^{-/-}$ mutant larva (**h-l**) carrying the transgenic *Tg(cd41:GFP)* marking HSPCs with GFP in green. Orange and pink dotted circles in c and h represent the areas where the thymus and kidney are located. (**h-l**) *cyfip1*$^{-/-}$ mutant exhibited several defective phenotypes, including loss of, or delayed in lodging of, HSPCs in thymus and kidney, and reduced number of HSPCs in AGM (blue arrow heads in j) and CHT (yellow arrow heads in k and l). Scale bar = 50 um.

mutants exhibited several pronounced defects, including aberrant CaP axon branching with increased number of axon terminals, and a shortened length of the CaP axon projections (Figure 9 d-e, pink arrow heads). Missing CaP axon ventral projection is indicated with pink asterisk (Figure 9e). *cyfip1*$^{-/-}$ mutant also displayed aberrant branching (Figure 9d-e, blue arrow heads), missing of rostral projection of RoP (Figure 9d-e, blue asterisks), aberrant branching with abnormal axon terminals (Figure 9d-e, yellow arrow heads), and missing dorsal projections of MiP (Figure 9d-e, yellow asterisks).

Discussion

Actin is the most abundant and indispensable protein in most eukaryotic cells, involving in a broad range of essential cellular processes[1–13], in which its dynamics is driven by its major regulator, the WAVE regulatory complex (WRC). Intriguingly, the activation and membrane recruitment signaling pathways of this heteropentameric protein complex is communicated solely through its own subunit called Cyfip[20–22,24,26,28–31]. In vertebrates, there are two Cyfip isoforms, Cyfip1 and Cyfip2. The differential expression pattern, together with non-redundant and distinct functions of the two isoforms has been evidenced[37–40], however, there have been very limited

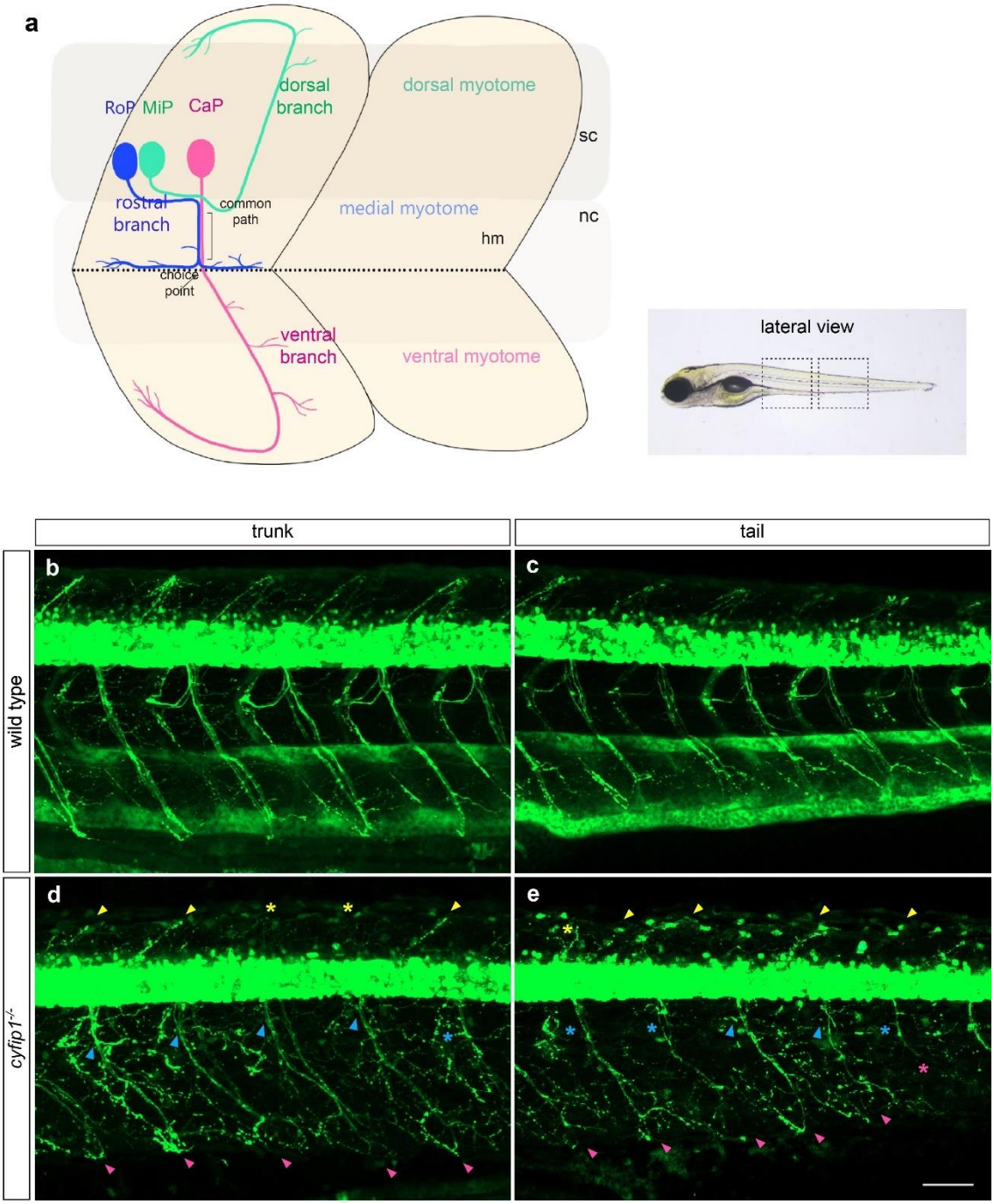

Figure 9. Phenotypes in spinal motor neurons in the nervous system of *cyfip1* knockout homozygous mutants at 4 dpf. A bright field image on the top right shows the dotted boxes indicating the areas where the confocal images were taken in lateral view of the trunk and tail sections. (**a**) Schematic illustration representing axonal projection pattern of the primary spinal motor neurons in a spinal hemisegment of zebrafish (lateral view). The projections of the three major primary motor neurons: RoP, MiP, and CaP, toward their target muscle regions in the myotome are color matched in blue, green, and pink, respectively. In developing nervous system, the RoP, MiP, and CaP extend their axon along the common

path to the choice point at the horizontal myoseptum (hm, dotted line). Here, the axon of RoP, MiP, and CaP diverge into their cell-specific regions in the myotome to innervate the medial, dorsal, and ventral myotome, respectively. The secondary motor neurons and their axons fasciculating with ones from the primary motor neurons to form rostral, dorsal, and ventral nerve branches are not shown in this diagram. RoP: rostral primary motor neuron, MiP: middle primary motor neuron, CaP: caudal primary motor neuron, sc: spinal cord, nc: notochord, hm: horizontal myoseptum. (**b-e**) Confocal images in lateral view of the trunk and tail areas in wild type (**b, c**) and *cyfip1*$^{-/-}$ mutant larva (**d, e**) carrying the transgenic *Tg(mnx1:GFP)* marking motor neurons and their projections with GFP. (**d, e**) *cyfip1*$^{-/-}$ mutant exhibited marked abnormal phenotypes, including aberrant CaP axon branching with increased number of axon terminals, and likely shorten length of CaP axon projections (pink arrow heads in d and e). Missing CaP axon ventral projection is indicated with pink asterisk (e). *cyfip1*$^{-/-}$ mutant also displayed aberrant branching and missing of rostral projection of RoP, as marked with blue arrow heads and blue asterisks, respectively. Aberrant branching with abnormal axon terminals and missing dorsal projections of MiP at the trunk and tail parts were also noticed (yellow arrow heads and yellow asterisks, respectively). Scale bar = 50 um.

studies examining *in vivo* functions of both Cyfip proteins in animals, especially in vertebrates. In addition, generating stable line of either *cyfip1* or *cyfip2* mutant, which is key to studying function and molecular mechanism of the gene of interest in animals, has not been achieved.

Here, we have established stable lines of *cyfip1* and *cyfip2* knockout mutant in zebrafish using a newly developed efficient CRISPR/Cas9-based short homology targeted integration strategy called GeneWeld[52–54]. This method was used in combination with a novel gene inactivation tool called pPRISM-Stop vector that contains the lens specific BFP secondary marker for aiding in identifying the mutant animals, to investigate *in vivo* functions of each Cyfip isoform. With the high efficiency of the GeneWeld method for precise targeted integration of pPRISM-Stop cassette into each *cyfip* loci, we were able to obtain high somatic reporter expression rates at 86% and 69% in the injected embryos for *cyfip1* and *cyfip2* loci, respectively. In addition, high frequencies of germline transmission of *cyfip1* and *cyfip2* knockout alleles were also carried out, at 46% (11/24) and 38% (6/16), respectively. Furthermore, we were able to recover *cyfip1* and *cyfip2* germline transmitting adults with on-target integration with frequencies

at 13% for both *cyfip* loci (3/24 for *cyfip1* and 2/16 for *cyfip2*). Due to on-target integration of the functional pPRISM-Stop cassette, *cyfip1* knockout homozygotes with a BFP secondary reporter exhibited marked morphological phenotypes, including the retinotectal system during early stage of development. By 5' and 3' genome/vector junction PCR analysis, the genotype of *cyfip1*$^{-/-}$ mutant was confirmed to carry precise 5' integration presumably mediated by HMEJ DNA repair mechanism. The 3' end of the pPRISM-Stop repair template was also incorporated correctly into the desired locus, however, the duplication of 3' short homologous sequence was observed, which could possibly be generated by MMEJ or cNHEJ repair pathways[48–50]. No part of pPRISM-Stop donor vector backbone was detected in either 5' or 3' genome/vector junction of *cyfip1* mutant. *cyfip2* knockout mutant showed inconsistent microscopic phenotypes in the retinotectal system, which were later determined to be resulted from an integration of the donor vector backbone along with the repair donor template at the 5' junction. The 3' junction was precise and had no sequence duplication. This unexpected incorporation of the pPRISM-Stop donor vector backbone at 5' junction was hypothesized to be mediated by cNHEJ repair mechanism, or cNHEJ together with MMEJ pathways[48–50], which could possibly give rise to genomic compensation and incomplete gene inactivating functionality of the pPRISM-Stop cassette, leading to inconsistent phenotypes observed in *cyfip2* knockout homozygotes.

Systematically characterizing *in vivo* functions of Cyfip1 and Cyfip2 in animals requires precise genome editing with high frequency and specificity at the targeted genomic loci to establish stable lines of each *cyfip* mutant. To accomplish this, we utilized a newly developed pPRISM-Stop cargo that contains stop codons right at the beginning of the cassette to mediate either *cyfip1* or *cyfip2* gene inactivation after being integrated into the genome. Additionally, the pPRISM-Stop cassette contains secondary reporter that drives lens specific expression of BFP,

which facilitates identification of mutant larval fishes by following their blue fluorescent lens and without necessitation for genotyping by junction PCR analysis.

Along with the pPRISM-Stop vector, we used GeneWeld method, which has recently been developed and shown to successfully design the homology arms to knock-in an exogenous DNA into the zebrafish genome[52–54], to mediate the integration of pPRISM-Stop cassette into the targeted *cyfip1* and *cyfip2* loci. Different from a knockout resulting from nonsense or frameshift mutations caused by cNHEJ, which often undergo gene compensation[60], the GeneWeld strategy uses 24 or 48 bp of homology flanking the desired sgRNA cut site to disrupt the targeted gene by inserting an exogenous cassette into the cleavage site through homology-directed repair (HDR), possibly creating alleles which do not induce compensation. This method is highly efficient, achieving an average of approximately 50% germline transmission rates across several zebrafish loci[52–54]. The result from what we attempted was very exciting since, for the first time, stable lines of *cyfip1* and *cyfip2* knockout mutants in zebrafish have been established to systematically investigate *in vivo* functions of each Cyfip protein in several biological systems, in which phenotypes were identified in both *cyfip1* and *cyfip2* knockout zebrafish mutants. One limitation to the pPRISM-Stop strategy is the constitutive gene knockout which could lead to pleiotropic effects of homozygous mutation of the gene of interest, especially in case of a targeted gene that is expressed ubiquitously, like *cyfip1* and *cyfip2*. In such case, these pleiotropic effects could severely impair physiological functions of several biological systems simultaneously, leading to severely defective phenotypes which could eventually result in embryonic lethality. This was observed in *cyfip1*$^{-/-}$ and *cyfip2*$^{-/-}$ mutants that usually died approximately within 7 dpf. Although these early-staged embryos contained rich information about the development in various biological systems, they were not able to allow for phenotypic analyses of later stages of

development. In addition, phenotypic analyses may also be complicated by disturbance of other vital systems, such as the cardiovascular and nervous systems where Cyfip1 and Cyfip2 potentially play critical roles. This limitation could be addressed by creating conditional knockout mutants in which *cyfip1* or *cyfip2* is deleted only in a particular system[48,50]. The possible strategy that we could utilize is a novel method named UFlip which combines the GeneWeld method with the established Cre-Lox recombination technology[61]. This type of study will distinguish the role and location of each Cyfip isoform through different stages of development in a specific biological system, which will allow for analyses of spatiotemporal functions of Cyfip, and ultimately the WRC signaling and WRC-mediated dynamic actin remodeling, in regulation of various single specific biological system.

Our preliminary phenotypic analysis of *cyfip1* knockout homozygous mutants in four different biological systems showed morphological abnormalities. Unquestionably, the actin cytoskeleton is a crucial component for cell migration[44,62–68]. Abolishing *cyfip1*, which is one of the key members of the actin remodeling major regulator WRC, led to various abnormal phenotypes relating to membrane protrusion and cell migration. First, the defects identified in the cardiovascular system, including mismigration or stalled development of endothelial cells, as well as stenosis or vascular collapse, and disrupted circulation, suggested defective directed cell migration or cell adhesion. Similarly, homozygous deletion of *cyfip1* resulted in substantial reduction of the HSPCs in various hematopoietic tissues, which could relate to the emergence and migration of the HSPCs from one hematopoietic tissue to another location during the development. This is critical for the HSPCs to become mature and capable of maintaining blood components throughout life. In addition, loss of HSPCs during early stage of the development of hematopoietic system could also suggest defects in stem cell differentiation, mobilization, and

proliferation, due to disruption of the WRC-mediated dynamic actin polymerization[69,70]. Interestingly, when analyzing the *cyfip1* knockout phenotypes in the cardiovascular system within the transgenic *Tg(fli1:EGFP)*^{y1}*; Tg(gata1:DsRed)*^{sd} zebrafish line, we observed a possible alteration in the AGM region and the CHT, where the HSPCs emerge and reside in, suggesting that malfunctioning actin remodeling could give rise to changes in vascular niche essential for HSPC emergence and development. Lastly, the overall phenotypes resulting from *cyfip1* abolishment in both retinotectal and spinal motor nervous systems showed aberrant axon branching and abnormal axon terminals with extensive distal branching. Actin filaments are a required cytoskeletal component in the dendritic spine, where the local assembly of actin filaments initiates synaptogenesis and axon branching[27,71,72]. Together, this suggested important roles of *cyfip1* in axon branching and synaptogenesis, and probably also synaptic pruning, through WRC-mediated dynamic actin reorganization.

Taken together, our study demonstrated efficient targeted integration at zebrafish *cyfip1* locus using CRISPR/Cas9 short homology targeted GeneWeld strategy and pPRISM-Stop-mediated gene inactivation method to establish stable *cyfip1* knockout mutant zebrafish lines to analyze *cyfip1* loss-of-function phenotypes and characterize the *in vivo* functions of *cyfip1* in various biological systems, including the cardiovascular, hematopoietic, retinotectal and spinal motor nervous systems. Although additional samples and further analysis will be needed to finally conclude our findings, the pronounced morphological and microscopic phenotypes discovered in this study suggested essential *in vivo* functions of *cyfip1* in the development of cardiovascular, hematopoietic, retinotectal, and spinal motor nervous systems. Further characterization is now enabled to examine the *in vivo* functions and identification of molecular mechanisms of *cyfip1*.

Materials and Methods

cyfip1 Targeted sgRNA Selection and Homology Arm Design

The genomic CRISPR sgRNA target sites in the coding sequence were designed to target the first coding exon (exon 2) of either zebrafish *cyfip1* or *cyfip2* gene (Table 2). The designed sgRNAs were verified via a sgRNA mutagenesis efficiency test by injecting each of the sgRNA into one-cell zebrafish embryos along with Cas9 mRNA. The injected embryos were then analyzed to check the heteroduplex (indel) formation by gel electrophoresis of PCR amplification over the targeted exon before the most efficient sgRNAs for *cyfip1* and *cyfip1* targeted loci were selected. According to the GeneWeld strategy[52,53], the homology arms containing 24-bp (for *cyfip1*) or 48-bp (for *cyfip2*) homology sequences flanking each sgRNA cut site were designed (Table 2). The repair templates to incorporate the pPRISM-Stop repair cassette into each targeted genome were then created by cloning the 24-bp or 48-bp homology arms (for *cyfip1* and *cyfip2*, respectively) into the pPRISM-Stop vector. Although 24-bp and 48-bp homology sequences were equally efficient at targeted integration[52,53], the 24-bp homology arms were used for *cyfip1* to avoid the repetitive or non-specific sequence in the intronic region, which could lead to imprecise integration of the repair template.

Table 2. CRISPR sgRNA target sites and vector homology arm sequences

Gene	Genomic sgRNA with PAM	5' Homology arm	3' Homology arm
cyfip1	CCCTGCATCGAGCCTCTGCCCTC	CCACTTCCAGATCAGCAGCCCTGC	ATCGAGCCTCTGCCCTCCTCACTC
cyfip2	GGAGGATGCGCTGTCCAATGTGG	CCTGTGTCGCCATGACAACCCACGTGACCCTGGAGGATGCGCTGTCCA	ATGTGGACCTGCTGGAGGAGCTTCCTCTCCCAGACCAGCAGCCATGCA

Zebrafish Strains and Maintenance

Zebrafish (Danio rerio) were maintained on an Aquatic Habitats (Pentair) or Aquaneering aquaculture system at 27ºC on a 14-hour light/10-hour dark cycle. The wild type strain WIK was used to generate all mutant lines and was obtained from the Zebrafish International Resource Center. All zebrafish experiments were conducted in accordance with approved protocols from Iowa State University Animal Care and Use Committee Log#11-06-6252, complying with American Veterinary Medical Association and NIH guidelines for the humane use of animals in research.

Zebrafish Embryo Microinjection

The injection solution containing genomic sgRNA, UsgRNA, pPRISM-Stop repair donor vector, and Cas9 mRNA was prepared as previously described in Wierson et al. (2020)[52,53]. Zebrafish embryos at the 1-cell stage were injected with 2 nl of the injection mixture containing 150 pg of mRNA, 25 pg of genomic sgRNA, 25 pg of UsgRNA, and 12.5 pg of pPRISM-Stop donor vector diluted in RNase-free ddH_2O. The injected embryos were screened for fluorescent secondary marker (lens specific BFP) expression at 3 dpf. The BFP expression in either lens was rechecked again at 4 to 5 dpf to include any possibly misinterpreted false negative BFP expression due to mosaicism in each eye lens. All injected embryos showing lens specific BFP expression were selected and raised to adulthood.

Identification of Zebrafish F0 Founders, Genome/Vector Junction Fragment Analysis (Genotyping) of the *cyfip1* Targeted Integration, and Recovery of Germline Transmitted F1 Alleles

We used the selected sgRNAs to introduce the genomic cleavage and used a pPRISM-Stop repair template to induce HDR. The injected embryos were screened for lens specific BFP secondary marker expression on a Zeiss Discovery dissection microscope at 3 dpf. The BFP expression in either lens was rechecked again at 4 to 5 dpf to include any possibly misinterpreted false negative BFP expression due to mosaicism or weak BFP expression in each eye lens. All injected F0 embryos showing lens specific BFP were selected and raised to adulthood.

To identify the founders, the F0 adult fish expressing BFP positive were outcrossed to the wild type strain WIK. For each F0 fish, at least 120 embryos were screened for lens specific BFP in order to find a possible germline transmitted founder. Once a founder was identified, its F1 BFP positive embryos were collected for genome/vector junction analysis. Genomic DNA was extracted by digestion of single embryo in 50 mM NaOH (20 ul per individual embryo) at 95ºC for 30 minutes and neutralized by adding 1/10th volume 1M Tris-HCl pH 7.5. Both 5' and 3' junction fragments were amplified by PCR using the primers in combination of gene-specific and pPRISM-Stop-specific primers (Table 3). The PCR products were then purified and sent for sequencing, by Sanger sequencing at the Iowa State University DNA Facility. After the F0 founder transmitting precise integration events was determined and confirmed based on the sequencing result, its F1 offspring expressing lens specific BFP were selected and raised. Once the F1s become adults, they were fin-clipped for PCR genotyping (junction analysis) and sent for sequencing again to validate the inherited precise targeted pPRISM-Stop cassette integration. The confirmed F1 mutants were then outcrossed to various transgenic fish lines to establish *cyfip1* and *cyfip2* heterozygous knockout F2 mutants in different transgenic backgrounds. *cyfip1*

and *cyfip2* F2 mutant adults in each transgenic line were used for incross to generate the homozygous knockout mutants to study.

Imaging

Zebrafish embryos used in this study were treated with 1-phenyl 2-thiourea (PTU) within 24 hours post fertilization to prevent pigmentation. At the stage specified in each experiment, the PTU treated embryos were anesthetized with 160 ug/ml tricaine methanesulfonate and mounted on slides in 1.2% low-melting agarose. Confocal images were then captured on a Zeiss LSM 800 laser scanning confocal microscope.

Table 3. Primer sequences

Primer name	Sequence	Purpose
cyfip1F	GACTCTGGAAGATGCTCTGTCC	*cyfip1* sgRNA target mutagenesis analysis
cyfip1R	GCAGATACAGAAGAAGGGTTGCTC	cyfip1 sgRNA target mutagenesis analysis
cyfip2F	GTGAACCTGTGTCGCCATGA	*cyfip2* sgRNA target mutagenesis analysis
cyfip2R	TGCATTAGGACGTGTACCTGG	*cyfip2* sgRNA target mutagenesis analysis
cyfip1jxn5'F#1	ATGTGGACTTGCTGGAGGAG	*cyfip1* genome/vector 5' junction analysis
cyfip1jxn5'F#2	GACTCTGGAAGATGCTCTGTCC	*cyfip1* genome/vector 5' junction analysis
cyfip1jxn5'F#3	TAGAGCAATGGCGTCCACAG	*cyfip1* genome/vector 5' junction analysis
cyfip1jxn5'F#4	TGGGAAATTGGGACATCCCTAG	*cyfip1* genome/vector 5' junction analysis
cyfip1jxn5'F#5	GCTACCTCACAGAAGTGCTCTG	*cyfip1* genome/vector 5' junction analysis
cyfip1jxn5'F#6	CGAGTATGTCTGCGGTCTGG	*cyfip1* genome/vector 5' junction analysis

Table 3. Continued

Primer name	Sequence	Purpose
cyfip1jxn5'F#7	GAGACGCTATTGGGTAAATGCTGG	*cyfip1* genome/vector 5' junction analysis
cyfip1jxn5'F#8	CCAGATCCGATCACGTGATCG	*cyfip1* genome/vector 5' junction analysis
cyfip1jxn5'F#9	CTCTGTCCAATGTGGACTTGC	*cyfip1* genome/vector 5' junction analysis
cyfip1jxn5'F#10	TCTGGAAGATGCTCTGTCCAATG	*cyfip1* genome/vector 5' junction analysis
cyfip1jxn5'F#11	CCACAGTGACTCTGGAAGATGC	*cyfip1* genome/vector 5' junction analysis
cyfip1jxn5'F#12	ATGGCGTCCACAGTGACTC	*cyfip1* genome/vector 5' junction analysis
cyfip1jxn5'F#13	AGTCTTGCATGCCATGTCTCA	*cyfip1* genome/vector 5' junction analysis
cyfip1jxn3'R#1	AGAAGGGTTGCTCTTGCCTG	*cyfip1* genome/vector 3' junction analysis
cyfip1jxn3'R#2	GCAGATACAGAAGAAGGGTTGCTC	*cyfip1* genome/vector 3' junction analysis
cyfip1jxn3'R#3	AACGATATATAGTGCAGCCCTAGTG	*cyfip1* genome/vector 3' junction analysis
cyfip1jxn3'R#4	TGCGGTCCTCAAAGTTGGTG	*cyfip1* genome/vector 3' junction analysis
cyfip2jxn5'F#1	GTGAACCTGTGTCGCCATGA	*cyfip2* genome/vector 5' junction analysis
cyfip2jxn5'F#2	TGAACCTGACCATTTCTGTTTTGTG	*cyfip2* genome/vector 5' junction analysis
cyfip2jxn5'F#3	TGTCTCATGGTATTGAACCTGACC	*cyfip2* genome/vector 5' junction analysis
cyfip2jxn5'F#4	ATTTGCTGGCAGCCACTTCA	*cyfip2* genome/vector 5' junction analysis
cyfip2jxn3'R	TGCATTAGGACGTGTACCTGG	*cyfip2* genome/vector 3' junction analysis
PRISMjxn5'R	ACGGTGGCTGAGACTTAATTACTA	Genome/vector 5' junction analysis
PRISMjxn3'F	CTCACCCGGGCTAGCGAT	Genome/vector 3' junction analysis

References

1. Blanchoin L, Boujemaa-Paterski R, Sykes C, Plastino J. Actin Dynamics, Architecture, and Mechanics in Cell Motility. *Physiological Reviews*. 2014;94(1):235-263. doi:10.1152/physrev.00018.2013

2. Pollard TD, Cooper JA. Actin, a central player in cell shape and movement. *Science (1979)*. 2009;326(5957):1208-1212. doi:10.1126/science.1175862

3. Pollard TD, Borisy GG. Cellular motility driven by assembly and disassembly of actin filaments. *Cell*. 2003;112(4):453-465. doi:10.1016/S0092-8674(03)00120-X

4. Dominguez R, Holmes KC. Actin structure and function. *Annual Review of Biophysics*. 2011;40(1):169-186. doi:10.1146/annurev-biophys-042910-155359

5. Pollard TD. Nine unanswered questions about cytokinesis. *Journal of Cell Biology*. 2017;216(10):3007-3016. doi:10.1083/jcb.201612068

6. Theriot JA, Mitchison TJ. Actin microfilament dynamics in locomoting cells. *Nature*. 1991;352(6331):126-131. doi:10.1038/352126a0

7. Girao H, Geli MI, Idrissi FZ. Actin in the endocytic pathway: From yeast to mammals. *FEBS Letters*. 2008;582(14):2112-2119. doi:10.1016/j.febslet.2008.04.011

8. Khaitlina SY. Intracellular transport based on actin polymerization. *Biochemistry (Moscow)*. 2014;79(9):917-927. doi:10.1134/S0006297914090089

9. Bettinger BT, Gilbert DM, Amberg DC. Actin up in the nucleus. *Nature Reviews Molecular Cell Biology*. 2004;5(5):410-415. doi:10.1038/nrm1370

10. Miralles F, Visa N. Actin in transcription and transcription regulation. *Current Opinion in Cell Biology*. 2006;18(3):261-266. doi:10.1016/j.ceb.2006.04.009

11. Percipalle P, Visa N. Molecular functions of nuclear actin in transcription. *Journal of Cell Biology*. 2006;172(7):967-971. doi:10.1083/jcb.200512083

12. Chen M, Shen X. Nuclear actin and actin-related proteins in chromatin dynamics. *Current Opinion in Cell Biology*. 2007;19(3):326-330. doi:10.1016/j.ceb.2007.04.009

13. Hurst V, Shimada K, Gasser SM. Nuclear Actin and Actin-Binding Proteins in DNA Repair. *Trends in Cell Biology*. 2019;29(6):462-476. doi:10.1016/j.tcb.2019.02.010

14. Feuer G, Molnar F, Pettko E, Straub FB. Studies on the composition and polymerization of actin. *Hung Acta Physiol*. 1948;1(4-5):150-163. Accessed June 21, 2022. http://www.ncbi.nlm.nih.gov/pubmed/18911922

15. Reisler E, Egelman EH. Actin structure and function: What we still do not understand. *Journal of Biological Chemistry*. 2007;282(50):36133-36137. doi:10.1074/jbc.R700030200

16. Stradal TEB, Rottner K, Disanza A, Confalonieri S, Innocenti M, Scita G. Regulation of actin dynamics by WASP and WAVE family proteins. *Trends in Cell Biology*. 2004;14(6):303-311. doi:10.1016/j.tcb.2004.04.007

17. Takenawa T, Suetsugu S. The WASP-WAVE protein network: Connecting the membrane to the cytoskeleton. *Nature Reviews Molecular Cell Biology*. 2007;8(1):37-48. doi:10.1038/nrm2069

18. Chen Z, Borek D, Padrick SB, et al. Structure and Control of the Actin Regulatory WAVE Complex. *Nature*. 2010;468:533-538.

19. Rottner K, Stradal TEB, Chen B. WAVE regulatory complex. *Current Biology*. 2021;31(10):R512-R517. doi:10.1016/j.cub.2021.01.086

20. Eden S, Rohatgi R, Podtelejnikov A v, Mann M, Kirschner MW. Mechanism of regulation of WAVE1-induced actin nucleation by Rac1 and Nck. *Nature*. 2002;418(6899):790-3.

21. Chen B, Chou HT, Brautigam CA, et al. Rac1 GTPase activates the WAVE regulatory complex through two distinct binding sites. *Elife*. 2017;6. doi:10.7554/eLife.29795

22. Lebensohn AM, Kirschner MW. Activation of the WAVE complex by coincident signals controls actin assembly. *Mol Cell*. 2009;36(3):512. doi:10.1016/j.molcel.2009.10.024

23. Miki H, Yamaguchi H, Suetsugu S, Takenawa T. IRSp53 is an essential intermediate between Rac and WAVE in the regulation of membrane ruffling. *Nature*. 2000;408(6813):732-5.

24. Koronakis V, Hume PJ, Humphreys D, et al. WAVE regulatory complex activation by cooperating GTPases Arf and Rac1. *Proc Natl Acad Sci U S A*. 2011;108(35):14449-14454. doi:10.1073/pnas.1107666108

25. Miki H, Suetsugu S, Takenawa T. WAVE, a novel WASP-family protein involved in actin reorganization induced by Rac. *EMBO J*. 1998;17(23):6932-41.

26. Chen B, Brinkmann K, Chen Z, et al. The WAVE regulatory complex links diverse receptors to the actin cytoskeleton. *Cell*. 2014;156(1-2):195-207. doi:10.1016/j.cell.2013.11.048

27. Chia PH, Chen B, Li P, Rosen MK, Shen K. Local F-actin network links synapse formation and axon branching. *Cell*. 2014;156(1-2):208-220. doi:10.1016/j.cell.2013.12.009

28. Squarr AJ, Brinkmann K, Chen B, et al. Fat2 acts through the WAVE regulatory complex to drive collective cell migration during tissue rotation. *The Journal of Cell Biology*. 2016;212(5):591-603. doi:10.1083/jcb.201508081

29. Lee NK, Fok KW, White A, et al. Neogenin recruitment of the WAVE regulatory complex maintains adherens junction stability and tension. *Nat Commun*. 2016;7:11082. doi:10.1038/ncomms11082

30. O'Leary CJ, Nourse CC, Lee NK, et al. Neogenin Recruitment of the WAVE Regulatory Complex to Ependymal and Radial Progenitor Adherens Junctions Prevents Hydrocephalus. *Cell Rep*. 2017;20(2):370-383. doi:10.1016/j.celrep.2017.06.051

31. Xing G, Li M, Sun Y, et al. Neurexin-Neuroligin 1 regulates synaptic morphology and functions via the WAVE regulatory complex in Drosophila neuromuscular junction. *Elife*. 2018;7. doi:10.7554/eLife.30457

32. Basquin C, Trichet M, Vihinen H, et al. Membrane protrusion powers clathrin-independent endocytosis of interleukin-2 receptor. *EMBO J*. 2015;34(16):2147-2161. doi:10.15252/embj.201490788

33. Biswas S, Emond MR, Duy PQ, Hao LT, Beattie CE, Jontes JD. Protocadherin-18b interacts with Nap1 to control motor axon growth and arborization in zebrafish. *Molecular Biology of the Cell*. 2014;25(5). doi:10.1091/mbc.E13-08-0475

34. Nakao S, Platek A, Hirano S, Takeichi M. Contact-dependent promotion of cell migration by the OL-protocadherin-Nap1 interaction. *Journal of Cell Biology*. 2008;182(2):395-410. doi:10.1083/jcb.200802069

35. Schenck A, Bardoni B, Moro A, Bagni C, Mandel JL. A highly conserved protein family interacting with the fragile X mental retardation protein (FMRP) and displaying selective interactions with FMRP-related proteins FXR1P and FXR2P. *Proc Natl Acad Sci U S A*. 2001;98(15):8844-8849. doi:10.1073/pnas.151231598

36. Pittman AJ, Gaynes JA, Chien CB. nev (cyfip2) is required for retinal lamination and axon guidance in the zebrafish retinotectal system. *Developmental Biology*. 2010;344(2):784-794. doi:10.1016/j.ydbio.2010.05.512

37. Cioni JM, Wong HHW, Bressan D, Kodama L, Harris WA, Holt CE. Axon-Axon Interactions Regulate Topographic Optic Tract Sorting via CYFIP2-Dependent WAVE Complex Function. *Neuron*. 2018;97(5). doi:10.1016/j.neuron.2018.01.027

38. Zhang Y, Kang HR, Han K. Differential cell-type-expression of CYFIP1 and CYFIP2 in the adult mouse hippocampus. *Animal Cells and Systems*. 2019;23(6):380-383. doi:10.1080/19768354.2019.1696406

39. Pathania M, Davenport EC, Muir J, Sheehan DF, López-Doménech G, Kittler JT. The autism and schizophrenia associated gene CYFIP1 is critical for the maintenance of dendritic complexity and the stabilization of mature spines. *Translational Psychiatry*. 2014;4. doi:10.1038/tp.2014.16

40. Marsden KC, Jain RA, Wolman MA, et al. A Cyfip2-Dependent Excitatory Interneuron Pathway Establishes the Innate Startle Threshold. *Cell Reports*. 2018;23(3). doi:10.1016/j.celrep.2018.03.095

41. Schenck A, Bardoni B, Langmann C, Harden N, Mandel JL, Giangrande A. CYFIP/Sra-1 controls neuronal connectivity in Drosophila and links the Rac1 GTPase pathway to the fragile X protein. *Neuron*. 2003;38(6):887-898. doi:10.1016/S0896-6273(03)00354-4

42. Galy A, Schenck A, Sahin HB, et al. CYFIP dependent Actin Remodeling controls specific aspects of Drosophila eye morphogenesis. *Developmental Biology*. 2011;359(1):37-46. doi:10.1016/j.ydbio.2011.08.009

43. Davenport EC, Szulc BR, Drew J, et al. Autism and Schizophrenia-Associated CYFIP1 Regulates the Balance of Synaptic Excitation and Inhibition. *Cell Reports*. 2019;26(8):2037-2051.e6. doi:10.1016/j.celrep.2019.01.092

44. Yamazaki D, Suetsugu S, Miki H, et al. WAVE2 is required for directed cell migration and cardiovascular development. *Nature*. 2003;424(6947):452-456. doi:10.1038/nature01770

45. Dubielecka PM, Ladwein KI, Xiong X, et al. Essential role for Abi1 in embryonic survival and WAVE2 complex integrity. *Proc Natl Acad Sci U S A*. 2011;108(17):7022-7027. doi:10.1073/pnas.1016811108

46. Ring C, Ginsberg MH, Haling J, Pendergast AM. Abl-interactor-1 (Abi1) has a role in cardiovascular and placental development and is a binding partner of the α4 integrin. *Proc Natl Acad Sci U S A*. 2011;108(1):149-154. doi:10.1073/pnas.1012316108

47. Park H, Staehling-Hampton K, Appleby MW, et al. A point mutation in the murine Hem1 gene reveals an essential role for Hematopoietic protein 1 in lymphopoiesis and innate immunity. *J Exp Med*. 2008;205(12):2899-2913. doi:10.1084/jem.20080340

48. Lau CH, Tin C, Suh Y. CRISPR-based strategies for targeted transgene knock-in and gene correction. *Faculty Reviews*. 2020;9. doi:10.12703/r/9-20

49. Xue C, Greene EC. DNA Repair Pathway Choices in CRISPR-Cas9-Mediated Genome Editing. *Trends Genet*. 2021;37(7):639-656. doi:10.1016/j.tig.2021.02.008

50. Zhang X, Li T, Ou J, Huang J, Liang P. Homology-based repair induced by CRISPR-Cas nucleases in mammalian embryo genome editing. *Protein Cell*. 2022;13(5):316-335. doi:10.1007/s13238-021-00838-7

51. Hisano Y, Ota S, Kawahara A. Genome editing using artificial site-specific nucleases in zebrafish. *Development Growth and Differentiation*. 2014;56(1):26-33. doi:10.1111/dgd.12094

52. Welker JM, Wierson WA, Almeida MP, et al. GeneWeld: Efficient targeted integration directed by short homology in Zebrafish. *Bio Protoc*. 2021;11(14). doi:10.21769/BioProtoc.4100

53. Wierson WA, Welker JM, Almeida MP, et al. Efficient targeted integration directed by short homology in zebrafish and mammalian cells. *Elife*. 2020;9:1-25. doi:10.7554/eLife.53968

54. Almeida MP, Welker JM, Siddiqui S, et al. Endogenous zebrafish proneural Cre drivers generated by CRISPR/Cas9 short homology directed targeted integration. *Scientific Reports*. 2021;11(1). doi:10.1038/s41598-021-81239-y

55. Stuermer CAO. Retinotopic organization of the developing retinotectal projection in the zebrafish embryo. *Journal of Neuroscience*. 1988;8(12):4513-4530. doi:10.1523/jneurosci.08-12-04513.1988

56. Burrill JD, Easter SS. Development of the retinofugal projections in the embryonic and larval zebrafish (Brachydanio rerio). *Journal of Comparative Neurology*. 1994;346(4):583-600. doi:10.1002/cne.903460410

57. Hutson LD, Chien C bin. Wiring the zebrafish: Axon guidance and synaptogenesis. *Current Opinion in Neurobiology*. 2002;12(1):87-92. doi:10.1016/S0959-4388(02)00294-5

58. Zolessi FR, Poggi L, Wilkinson CJ, Chien CB, Harris WA. Polarization and orientation of retinal ganglion cells in vivo. *Neural Dev*. 2006;1(1):2. doi:10.1186/1749-8104-1-2

59. Davison C, Zolessi FR. Slit2 is necessary for optic axon organization in the zebrafish ventral midline. *Cells & Development*. 2021;166:203677. doi:10.1016/j.cdev.2021.203677

60. El-Brolosy MA, Stainier DYR. Genetic compensation: A phenomenon in search of mechanisms. *PLoS Genetics*. 2017;13(7):e1006780. doi:10.1371/journal.pgen.1006780

61. Liu F, Kambakam S, Almeida MP, et al. Cre/lox regulated conditional rescue and inactivation with zebrafish UFlip alleles generated by CRISPR-Cas9 targeted integration. *Elife*. 2022;11. doi:10.7554/elife.71478

62. Krause M, Gautreau A. Steering cell migration: Lamellipodium dynamics and the regulation of directional persistence. *Nature Reviews Molecular Cell Biology*. 2014;15(9). doi:10.1038/nrm3861

63. Lamalice L, le Boeuf F, Huot J. Endothelial cell migration during angiogenesis. *Circulation Research*. 2007;100(6):782-794. doi:10.1161/01.RES.0000259593.07661.1e

64. Weijer CJ. Collective cell migration in development. *Journal of Cell Science*. 2009;122(18):3215-3223. doi:10.1242/jcs.036517

65. le Clainche C, Carlier MF. Regulation of actin assembly associated with protrusion and adhesion in cell migration. *Physiological Reviews*. 2008;88(2):489-513. doi:10.1152/physrev.00021.2007

66. Coffin JD, Poole TJ. Endothelial cell origin and migration in embryonic heart and cranial blood vessel development. *The Anatomical Record*. 1991;231(3):383-395. doi:10.1002/ar.1092310312

67. Cao J, Ehling M, März S, et al. Polarized actin and VE-cadherin dynamics regulate junctional remodelling and cell migration during sprouting angiogenesis. *Nature Communications*. 2017;8(1). doi:10.1038/s41467-017-02373-8

68. Zeller J, Schneider V, Malayaman S, et al. Migration of zebrafish spinal motor nerves into the periphery requires multiple myotome-derived cues. *Developmental Biology*. 2002;252(2):241-256. doi:10.1006/dbio.2002.0852

69. Ogaeri T, Eto K, Otsu M, Ema H, Nakauchi H. The Actin Polymerization Regulator WAVE2 Is Required for Early Bone Marrow Repopulation by Hematopoietic Stem Cells. *Stem Cells*. 2009;27(5):1120-1129. doi:10.1002/stem.42

70. Sen B, Uzer G, Samsonraj RM, et al. Intranuclear Actin Structure Modulates Mesenchymal Stem Cell Differentiation. *Stem Cells*. 2017;35(6):1624-1635. doi:10.1002/stem.2617

71. Spence EF, Soderling SH. Actin out: Regulation of the synaptic cytoskeleton. *Journal of Biological Chemistry*. 2015;290(48):28613-28622. doi:10.1074/jbc.R115.655118

72. Lamprecht R. Actin Cytoskeleton Role in the Maintenance of Neuronal Morphology and Long-Term Memory. *Cells*. 2021;10(7):1795. doi:10.3390/cells10071795

73. Kay JN, Link BA, Baier H. Staggered cell-intrinsic timing of ath5 expression underlies the wave of ganglion cell neurogenesis in the zebrafish retina. *Development*. 2005;132(11): 2573–2585. doi:10.1242/dev.01831

74. Janssens E, Gaublomme D, Groef LD, Darras VM, Arckens L, Delorme N, Claes F, Hove IV, Moons L. Matrix Metalloproteinase 14 in the Zebrafish: An Eye on Retinal and Retinotectal Development. *PLOS ONE*. 2013;8(1):e52915. doi:10.1371/journal.pone.0052915

75. Weaver CJ, Terzi A, Roeder H, Gurol T, Deng Q, Leung YF, Suter DM. nox2/cybb deficiency affects zebrafish retinotectal connectivity. *Journal of Neuroscience*. 2018; 1483-1516. doi:10.1523/JNEUROSCI.1483-16.2018

76. Dong Z, Wu S, Zhu C, Wang X, Li Y, Chen X, Liu D, Qiang L, Baas PW, Liu M. Clustered Regularly Interspaced Short Palindromic Repeats (CRISPR)/Cas9-mediated kif15 mutations accelerate axonal outgrowth during neuronal development and regeneration in zebrafish. *Traffic*. 2019;20(1):71-81. doi:10.1111/tra.12621

77. Nagar D, Carrington B, Burgess SM, Ghose A. Development of motor neurons and motor activity in zebrafish requires F-actin nucleation by Fmn2b. *bioRxiv.* 2021.08.10.455777. doi:10.1101/2021.08.10.455777

78. Xing L, Chai R, Wang J, Lin J, Li H, Wang Y, Lai B, Sun J, Chen G. Expression of myelin transcription factor 1 and lamin B receptor mediate neural progenitor fate transition in the zebrafish spinal cord pMN domain. *J Biol Chem*. 2022;298(10):102452. doi:10.1016/j.jbc.2022.102452

79. Zheng Y, Suo G, Liu D, Li H, Wu Y, Ni H. Nexmifa Regulates Axon Morphogenesis in Motor Neurons in Zebrafish. *Frontiers in Molecular Neuroscience*. 2021. doi:10.3389/fnmol.2022.848257

80. Eisa-Beygi S, Benslimane FM, El-Rass S, Prabhudesai S, Abdelrasoul MKA, Simpson PM, Yalcin HC, Burrows PE, Ramchandran R. Characterization of Endothelial Cilia Distribution During Cerebral-Vascular Development in Zebrafish (Danio rerio). *Arterioscler Thromb Vasc Biol*. 2018;38(12):2806-2818. doi:10.1161/ATVBAHA.118.311231

81. Kotini MP, Bachmann F, Spickermann J, McSheehy PM, Affolter M. Probing the Effects of the FGFR-Inhibitor Derazantinib on Vascular Development in Zebrafish Embryos. *Pharmaceuticals*. 2021;14(1):25. doi:10.3390/ph14010025

82. Li W, Tran V, Shaked I, Xue B, Moore T, Lightle R, Kleinfeld D, Awad IA, Ginsberg MH. Abortive intussusceptive angiogenesis causes multi-cavernous vascular malformations. *Elife*. 2021;10:e62155. doi:10.7554/eLife.62155

83. Ma D, Zhang J, Lin HF, Italiano J, Handin RI. The identification and characterization of zebrafish hematopoietic stem cells. *Blood*. 2011;118(2):289-297. doi:10.1182/blood-2010-12-327403

84. Anderson H, Patch TC, Reddy NG, Hagedorn EJ., Kim PG, Solti KA, Chen MJ, Tamplin, OJ, Frye M, MacLean GA, Hübner K, Bauer DE, Kanki JP, Vogin G, Huston NC, Nguyen M, Fujiwara Y, Paw BH, Vestweber D, Zon LI, Orkin SH, Daley GQ, Shah DI. Hematopoietic stem cells develop in the absence of endothelial cadherin 5 expression. *Blood*. 2015;126(26):2811-2820. doi:10.1182/blood-2015-07-659276

85. Bertrand JY, Kim AD, Teng S, Traver D; CD41+ cmyb+ precursors colonize the zebrafish pronephros by a novel migration route to initiate adult hematopoiesis. *Development.* 2008; 135(10):1853–1862. doi:10.1242/dev.015297

86. Martin CS, Moriyama A, Zon LI. Hematopoietic stem cells, hematopoiesis and disease: lessons from the zebrafish model. *Genome Med.* 2011;3(12):83. doi:10.1186/gm299

87. Li Y, Esain V, Teng L, Xu J, Kwan W, Frost IM, Yzaguirre AD, Cai X, Cortes M, Maijenburg MW, Tober J, Dzierzak E, Orkin SH, Tan K, North TE, Speck NA. Inflammatory signaling regulates embryonic hematopoietic stem and progenitor cell production. *Genes Dev*. 2014;28(23):2597-2612. doi:10.1101/gad.253302.114

88. Eckfeldt CE, Mendenhall EM, Flynn CM, Wang TF, Pickart MA, Grindle SM, Ekker SC, Verfailli CM. Functional Analysis of Human Hematopoietic Stem Cell Gene Expression Using Zebrafish. *PLOS Biology*. 2005;3(8): e254. doi:10.1371/journal.pbio.0030254

CHAPTER 3. GENERAL CONCLUSION

Summary and Future Directions

Actin cytoskeleton is one of the most fascinating cellular components, and actin is the most abundant protein in most eukaryotic cells. It is highly conserved through evolution, in which its dynamics contributes to many essential cellular processes, ranging from cell shape integrity, cell proliferation, cell migration, cell adhesion and fusion, endocytosis and vesicle trafficking, chromatin remodeling, DNA repair and regulation of transcription[1–13]. Even though the actin has been studied for decades, several questions about the detailed structure of actin cytoskeleton and its dynamics, as well as how these define its functions, both *in vitro* and *in vivo*, still remain unclear. Dynamic actin reorganization is governed by its major regulator, the WAVE regulatory complex (WRC). Intriguingly, the activation and membrane recruitment signaling pathways of the WRC is mediated solely through its own subunit called Cyfip[14–22]. In vertebrates, there are two isoforms of Cyfip, Cyfip1 and Cyfip2. Although the two isoforms share high sequence homology[23,24], the differential expression patterns and distinct functions of Cyfip1 and Cyfip2 have been evidenced[25–28]. However, there have been very limited studies investigating *in vivo* functions of both Cyfip proteins in animals, especially in vertebrates. In addition, key to characterizing function and molecular mechanism of the gene of interest in animals is to obtain a stable line of the mutant and a strong, quantifiable phenotype for the gene of interest. Therefore, this poses a critical need for determining *in vivo* functions of the Cyfip proteins and their detailed underlying mechanisms.

To accomplish this, in chapter 2, we demonstrated that we have established stable lines of *cyfip1* and *cyfip2* knockout mutant in zebrafish using a newly developed efficient CRISPR/Cas9-

based short homology targeted integration strategy namely GeneWeld[29–31], in combination with a novel gene inactivation tool called pPRISM-Stop vector (plasmids for PRecise Integration with Secondary Markers) that contains the lens specific BFP secondary marker for facilitating visually identification of the mutant animals to investigate *in vivo* functions of each Cyfip isoform in four different biological systems, including cardiovascular, hematopoietic, retinotectal and spinal motor nervous systems. With high efficiency of the GeneWeld strategy for precise targeted integration of pPRISM-Stop cassette into each *cyfip* locus, we were able to recover *cyfip1* and *cyfip2* germline transmitting adults with on-target integration with frequencies at 13% for both *cyfip* loci (3/24 for *cyfip1* and 2/16 for *cyfip2*). Despite an unexpected vector backbone integration into *cyfip2* locus we identified in subsequent generations, we were able to successfully establish stable lines of true *cyfip1* knockout mutant to study further. Intriguingly, it was notable that *cyfip1* homozygous deletion during early stage of development resulted in mismigration and delayed, or stalled, development of endothelial cells along with stenotic and disrupted blood circulation, a reduction of the HSPCs in different hematopoietic tissues, as well as aberrant axon branching and abnormal axon terminals. Taken together, our study demonstrated efficient targeted integration at zebrafish *cyfip1* locus via CRISPR/Cas9 short homology targeted GeneWeld strategy and pPRISM-Stop-mediated gene inactivation. We generated stable *cyfip1* knockout mutant zebrafish lines to analyze *cyfip1* knockout phenotypes and characterize the *in vivo* functions of *cyfip1* in cardiovascular, hematopoietic, retinotectal and spinal motor nervous systems. Although additional samples and further analysis is necessary to make final conclusions, the pronounced phenotypes discovered in this study suggested the essential *in vivo* functions of *cyfip1* in the development of cardiovascular, hematopoietic, retinotectal, and spinal motor nervous systems. This is worth investigating further to fully

characterize the *in vivo* functions and identify molecular mechanisms of *cyfip1*, and the WRC-mediated actin remodeling, in these physiological systems. Accomplishing this work will establish the functional essentiality of *cyfip1* in these four biological systems, as well as create a phenotypic framework for studying distinctive *in vivo* functions of *cyfip2*, WRC signaling and actin regulation in zebrafish.

Of note, although the pPRISM-Stop strategy provides great advantages to generate gene inactivation, there is one caveat: gene function analysis could be limited due to pleiotropic effects of homozygous deletion of the gene of interest resulting from constitutive gene knockout, especially in case when the targeted gene can be expressed ubiquitously, like *cyfip1* and *cyfip2*. In such case, these pleiotropic effects could severely impair physiological functions of several biological systems simultaneously, leading to severely defective phenotypes which could ultimately result in embryonic lethality, as observed in *cyfip1*$^{-/-}$ and *cyfip2*$^{-/-}$ mutants that usually died approximately within 7 dpf. Although these early-staged embryos were extensively informative about the development in various biological systems, they were not able to allow for phenotypic analyses of later stages of development. In addition, phenotypic analyses may also be complicated by disturbance of other vital systems, such as the cardiovascular and nervous systems where Cyfip1 and Cyfip2 potentially play critical roles. This limitation could be overcome by creating conditional knockout mutants in which *cyfip1* or *cyfip2* is deleted only in a specific biological system or tissue type, and at a particular time point[32,33]. The possible strategy that we could utilize is a novel method named UFlip which is an advancement of the GeneWeld method with the established Cre-Lox recombination technology[34]. This type of study will distinguish the role and location of each Cyfip isoform through different stages of development in a specific biological system, which will allow for analyses of spatiotemporal functions of

Cyfip, and ultimately the WRC signaling and WRC-mediated dynamic actin remodeling, in regulation of various single specific biological system or tissue type.

References

1. Blanchoin L, Boujemaa-Paterski R, Sykes C, Plastino J. Actin Dynamics, Architecture, and Mechanics in Cell Motility. *Physiological Reviews*. 2014;94(1):235-263. doi:10.1152/physrev.00018.2013

2. Pollard TD. Nine unanswered questions about cytokinesis. *Journal of Cell Biology*. 2017;216(10):3007-3016. doi:10.1083/jcb.201612068

3. Pollard TD, Borisy GG. Cellular motility driven by assembly and disassembly of actin filaments. *Cell*. 2003;112(4):453-465. doi:10.1016/S0092-8674(03)00120-X

4. Pollard TD, Cooper JA. Actin, a central player in cell shape and movement. *Science (1979)*. 2009;326(5957):1208-1212. doi:10.1126/science.1175862

5. Dominguez R, Holmes KC. Actin structure and function. *Annual Review of Biophysics*. 2011;40(1):169-186. doi:10.1146/annurev-biophys-042910-155359

6. Theriot JA, Mitchison TJ. Actin microfilament dynamics in locomoting cells. *Nature*. 1991;352(6331):126-131. doi:10.1038/352126a0

7. Girao H, Geli MI, Idrissi FZ. Actin in the endocytic pathway: From yeast to mammals. *FEBS Letters*. 2008;582(14):2112-2119. doi:10.1016/j.febslet.2008.04.011

8. Khaitlina SY. Intracellular transport based on actin polymerization. *Biochemistry (Moscow)*. 2014;79(9):917-927. doi:10.1134/S0006297914090089

9. Bettinger BT, Gilbert DM, Amberg DC. Actin up in the nucleus. *Nature Reviews Molecular Cell Biology*. 2004;5(5):410-415. doi:10.1038/nrm1370

10. Miralles F, Visa N. Actin in transcription and transcription regulation. *Current Opinion in Cell Biology*. 2006;18(3):261-266. doi:10.1016/j.ceb.2006.04.009

11. Percipalle P, Visa N. Molecular functions of nuclear actin in transcription. *Journal of Cell Biology*. 2006;172(7):967-971. doi:10.1083/jcb.200512083

12. Chen M, Shen X. Nuclear actin and actin-related proteins in chromatin dynamics. *Current Opinion in Cell Biology*. 2007;19(3):326-330. doi:10.1016/j.ceb.2007.04.009

13. Hurst V, Shimada K, Gasser SM. Nuclear Actin and Actin-Binding Proteins in DNA Repair. *Trends in Cell Biology*. 2019;29(6):462-476. doi:10.1016/j.tcb.2019.02.010

14. Eden S, Rohatgi R, Podtelejnikov A v, Mann M, Kirschner MW. Mechanism of regulation of WAVE1-induced actin nucleation by Rac1 and Nck. *Nature*. 2002;418(6899):790-3.

15. Chen B, Chou HT, Brautigam CA, et al. Rac1 GTPase activates the WAVE regulatory complex through two distinct binding sites. *Elife*. 2017;6. doi:10.7554/eLife.29795

16. Lebensohn AM, Kirschner MW. Activation of the WAVE complex by coincident signals controls actin assembly. *Mol Cell*. 2009;36(3):512. doi:10.1016/j.molcel.2009.10.024

17. Koronakis V, Hume PJ, Humphreys D, et al. WAVE regulatory complex activation by cooperating GTPases Arf and Rac1. *Proc Natl Acad Sci U S A*. 2011;108(35):14449-14454. doi:10.1073/pnas.1107666108

18. Squarr AJ, Brinkmann K, Chen B, et al. Fat2 acts through the WAVE regulatory complex to drive collective cell migration during tissue rotation. *The Journal of Cell Biology*. 2016;212(5):591-603. doi:10.1083/jcb.201508081

19. Chen B, Brinkmann K, Chen Z, et al. The WAVE regulatory complex links diverse receptors to the actin cytoskeleton. *Cell*. 2014;156(1-2):195-207. doi:10.1016/j.cell.2013.11.048

20. Lee NK, Fok KW, White A, et al. Neogenin recruitment of the WAVE regulatory complex maintains adherens junction stability and tension. *Nat Commun*. 2016;7:11082. doi:10.1038/ncomms11082

21. O'Leary CJ, Nourse CC, Lee NK, et al. Neogenin Recruitment of the WAVE Regulatory Complex to Ependymal and Radial Progenitor Adherens Junctions Prevents Hydrocephalus. *Cell Rep*. 2017;20(2):370-383. doi:10.1016/j.celrep.2017.06.051

22. Xing G, Li M, Sun Y, et al. Neurexin-Neuroligin 1 regulates synaptic morphology and functions via the WAVE regulatory complex in Drosophila neuromuscular junction. *Elife*. 2018;7. doi:10.7554/eLife.30457

23. Pittman AJ, Gaynes JA, Chien CB. nev (cyfip2) is required for retinal lamination and axon guidance in the zebrafish retinotectal system. *Developmental Biology*. 2010;344(2):784-794. doi:10.1016/j.ydbio.2010.05.512

24. Schenck A, Bardoni B, Moro A, Bagni C, Mandel JL. A highly conserved protein family interacting with the fragile X mental retardation protein (FMRP) and displaying selective interactions with FMRP-related proteins FXR1P and FXR2P. *Proc Natl Acad Sci U S A*. 2001;98(15):8844-8849. doi:10.1073/pnas.151231598

25. Cioni JM, Wong HHW, Bressan D, Kodama L, Harris WA, Holt CE. Axon-Axon Interactions Regulate Topographic Optic Tract Sorting via CYFIP2-Dependent WAVE Complex Function. *Neuron*. 2018;97(5). doi:10.1016/j.neuron.2018.01.027

26. Zhang Y, Kang HR, Han K. Differential cell-type-expression of CYFIP1 and CYFIP2 in the adult mouse hippocampus. *Animal Cells and Systems*. 2019;23(6):380-383. doi:10.1080/19768354.2019.1696406

27. Pathania M, Davenport EC, Muir J, Sheehan DF, López-Doménech G, Kittler JT. The autism and schizophrenia associated gene CYFIP1 is critical for the maintenance of dendritic complexity and the stabilization of mature spines. *Translational Psychiatry*. 2014;4. doi:10.1038/tp.2014.16

28. Marsden KC, Jain RA, Wolman MA, et al. A Cyfip2-Dependent Excitatory Interneuron Pathway Establishes the Innate Startle Threshold. *Cell Reports*. 2018;23(3). doi:10.1016/j.celrep.2018.03.095

29. Welker JM, Wierson WA, Almeida MP, et al. GeneWeld: Efficient targeted integration directed by short homology in Zebrafish. *Bio Protoc*. 2021;11(14). doi:10.21769/BioProtoc.4100

30. Wierson WA, Welker JM, Almeida MP, et al. Efficient targeted integration directed by short homology in zebrafish and mammalian cells. *Elife*. 2020;9:1-25. doi:10.7554/eLife.53968

31. Almeida MP, Welker JM, Siddiqui S, et al. Endogenous zebrafish proneural Cre drivers generated by CRISPR/Cas9 short homology directed targeted integration. *Scientific Reports*. 2021;11(1). doi:10.1038/s41598-021-81239-y

32. Zhang X, Li T, Ou J, Huang J, Liang P. Homology-based repair induced by CRISPR-Cas nucleases in mammalian embryo genome editing. *Protein Cell*. 2022;13(5):316-335. doi:10.1007/s13238-021-00838-7

33. Lau CH, Tin C, Suh Y. CRISPR-based strategies for targeted transgene knock-in and gene correction. *Faculty Reviews*. 2020;9. doi:10.12703/r/9-20

34. Liu F, Kambakam S, Almeida MP, et al. Cre/lox regulated conditional rescue and inactivation with zebrafish UFlip alleles generated by CRISPR-Cas9 targeted integration. *Elife*. 2022;11. doi:10.7554/elife.71478